In lovely memory

of my grandmother Nice

SAPIENZA
UNIVERSITÀ DI ROMA

PhD Thesis

Materials Science

Department of Basic and Applied Sciences for Engineering

Department of Chemistry

SYNTHESIS, CHARACTERIZATION AND FUNCTIONALIZATION OF PEDOT CONDUCTING SYSTEMS ON ETHYLENE VINYL ALCOHOL COPOLYMER SUPPORTS AND DERIVATIVES

Advisor:

Prof. Andrea Martinelli

Candidate:

Dr. Elisa Pizzi

Cycle XXVI

A. Y. 2012/2013

Ithaka

As you set out for Ithaka
hope the voyage is a long one,
full of adventure, full of discovery.
Laistrygonians and Cyclops,
angry Poseidon - don't be afraid of them:
you'll never find things like that on your way
as long as you keep your thoughts raised high,
as long as a rare excitement
stirs your spirit and your body.
Laistrygonians and Cyclops,
wild Poseidon - you won't encounter them
unless you bring them along inside your soul,
unless your soul sets them up in front of you.

Hope the voyage is a long one.
May there be many a summer morning when,
with what pleasure, what joy,
you come into harbors seen for the first time;
may you stop at Phoenician trading stations
to buy fine things,
mother of pearl and coral, amber and ebony,
sensual perfume of every kind -
as many sensual perfumes as you can;
and may you visit many Egyptian cities
to gather stores of knowledge from their scholars.

Keep Ithaka always in your mind.
Arriving there is what you are destined for.
But do not hurry the journey at all.
Better if it lasts for years,
so you are old by the time you reach the island,
wealthy with all you have gained on the way,
not expecting Ithaka to make you rich.

Ithaka gave you the marvelous journey.
Without her you would not have set out.
She has nothing left to give you now.

And if you find her poor, Ithaka won't have fooled you.
Wise as you will have become, so full of experience,
you will have understood by then what these Ithakas
mean.

(Constantine P. Cavafy, *Collected Poems.*
Translated by Edmund Keeley and Philip Sherrard.
Edited by George Savidis. Revised Edition.
Princeton University Press, 1992)

ACKNOWLEDGEMENTS

We could realize everything, but its importance in our consciousness arises from every person who sustained and helped us in all possible ways.

First of all, my deepest thanks and gratitude goes to my advisor Prof. Andrea Martinelli, who really guided me with great patience in every professional aspect of this research activity. His bright ideas and his dynamic approach, never ordinary, have been fundamental for my personal grown.

I would like to thank greatly Prof. Lucio d'Ilario who allowed me to become part of his research group, while sustaining me with valid counsels and precious encouragement.

Endless thanks go to Prof. Antonella Piozzi and Dr. Iolanda Francolini for their continuous availability and collaboration.

Moreover, I desire to thank Prof. Daniela Zane for her kind help specially in EIS analysis.

Thanks to Dr. Francesco Mura of CNIS Laboratories of Sapienza and thanks to Dr. Daniela Ferro for their help in SEM characterizations.

I want to thank also Dr. Fernanda Crisante and Dr. Vincenzo Taresco for their daily friendship and support. And special thanks go to my lab-friend Mr. Matteo Cara for his fruitful experimental collaboration.

Finally, about my research period abroad at the Danish Technical University (DTU), my particular and notable acknowledgements are addressed to Prof. Søren Hvilsted and Dr. Anders Egede Daugaard of Danish Polymer Centre (DPC) at Department of Biochemical and Chemical Engineering. They have welcomed me into their research group with great attention and kindness, giving me the possibility to take advantage of their enlightening guidance and significant contribution. Thanks to all collaborators of DPC. Thanks to Miss Adele Faralli and all collaborators of Nanotech Department at DTU, for their help in experimental characterization. Thanks obviously to all my DPC colleagues and friends who helped and accompanied me during that engaging period!

And so on... Really thanks to all the lab friends I've met during this important time of my life!

Thanks to my family, to all my dear ones who have fed my roots.

I hope that I have not forget to mention anyone...

TABLE OF CONTENTS

AIM OF THE RESEARCH

The research work described in this PhD thesis focuses essentially on methods and strategies of employing a polymer substrate for poly(3,4-ethylenedioxythiophene) (PEDOT) synthesis.

For the purpose an ethylene vinyl alcohol copolymer (EVAL) was chosen. It offers many potentialities. Serving as mechanical support and/or functionalizable phase, it can be differently combined with PEDOT to give conductive systems or it can be modified to obtain electro-active materials.

Aim of the work is to show how, starting from the same base, it is possible to introduce functionalities into supported conductive systems both through the substrate and through the conducting phase, and all the strategies that were adopted.

Hope of the work is that some applications lie ahead!

1
BACKGROUND

1.1 INTRINSICALLY CONDUCTING POLYMERS (ICP)

The fundamental discovery in the field of intrinsically conducting polymers (ICP) was the synthesis of polyacetylene published in 1977 by H. Shirakawa, A. G. McDiarmind and A. J. Heeger and honored by Nobel Prize in 2000.[1,2] The *trans*-polyacetylene films, prepared some years before by Shirakawa, originally showed a resistivity of about 10^4 Ω cm, behaving as semiconductors.[3] Cis-polyacetylene films exhibited a remarkably higher resistivity of about 2.4 x 10^8 Ω cm. In this context the fundamental breakthrough was the discovery that PA could be partially oxidized by halogens or arsenic pentafluoride (process known as "doping"). Nowadays, the resulting doped PA still represents as the conductive polymer with highest specific conductivity: 10^5 S cm^{-1}.[4]

Some intrinsic obstacles have contained the commercialization of polyacetylene (PA). Because of its remarkable degradability on air and absence of processability, a large amount of attempts were made to establish new ICP combining all properties necessary to commercialization: high conductivity, processability and long term stability under application conditions. The most important candidates are polyaniline (PAni), polypyrrole (PPy) and polythiophene (PT). Some of these ICP classes have found special commercial use.

1.2 POLYTHIOPHENE (PT) AND DERIVATIVES (PTs)

Polythiophenes (PTs) represent one prominent class of ICP presently in the market. Although PT is relatively stable compared with other conducting polymers, the decrease of its conductivity over a long period limits its industrial applications. The stability of PT may be improved by decreasing its oxidizing potential. This can be achieved by introducing an alkoxyl group (such as ether group) which has electron-donating character. Substituted thiophene can be polymerized at a lower potential than thiophene and the resulting polymers

are more stable in the anion-doped state especially when the side chain is not too long. For this reason, an important progress in polythiophene chemistry was achieved by the mono- and dialkoxy substituted derivatives (3-alkoxy, 3,4-alkoxy and 3,4-(crown ether) thiophenes), introduced by Daoust and Leclerc[5] and industrial scientists at Hoechst AG.[6-8]

However, study of PTs have shown that the introduction of long side chain on the aromatic ring can bring about a distortion of the polymer backbone leading to a reduction of the electron conjugation and, hence, electrical conduction. Therefore a shorter chain dialkoxy substituted thiophene, in the form of a 3,4-(crown ether) thiophene, has attracted great attention. In the PTs chemistry, the real breakthrough was the synthesis of polymers of the bicyclic ethylenedioxythiophene and its derivatives. They were first electrochemically polymerized by Heinze *et al.* and chemically polymerized by Jonas *et al.* in the Bayer Corporate Research laboratories.[9,10] These poly-ethylenedioxythiophenes formally belongs to the subgroup of the poly-dialkoxythiophenes, but, differently from other PTs sister polymers, showed different properties. Poly(3,4-ethylenedioxythiophene), also known as PEDOT or PEDT, is a "low band gap polymer" characterized by high stability and conductivity (Fig. 1.1). For these main features, its use as technical material and consequent commercialization followed soon.

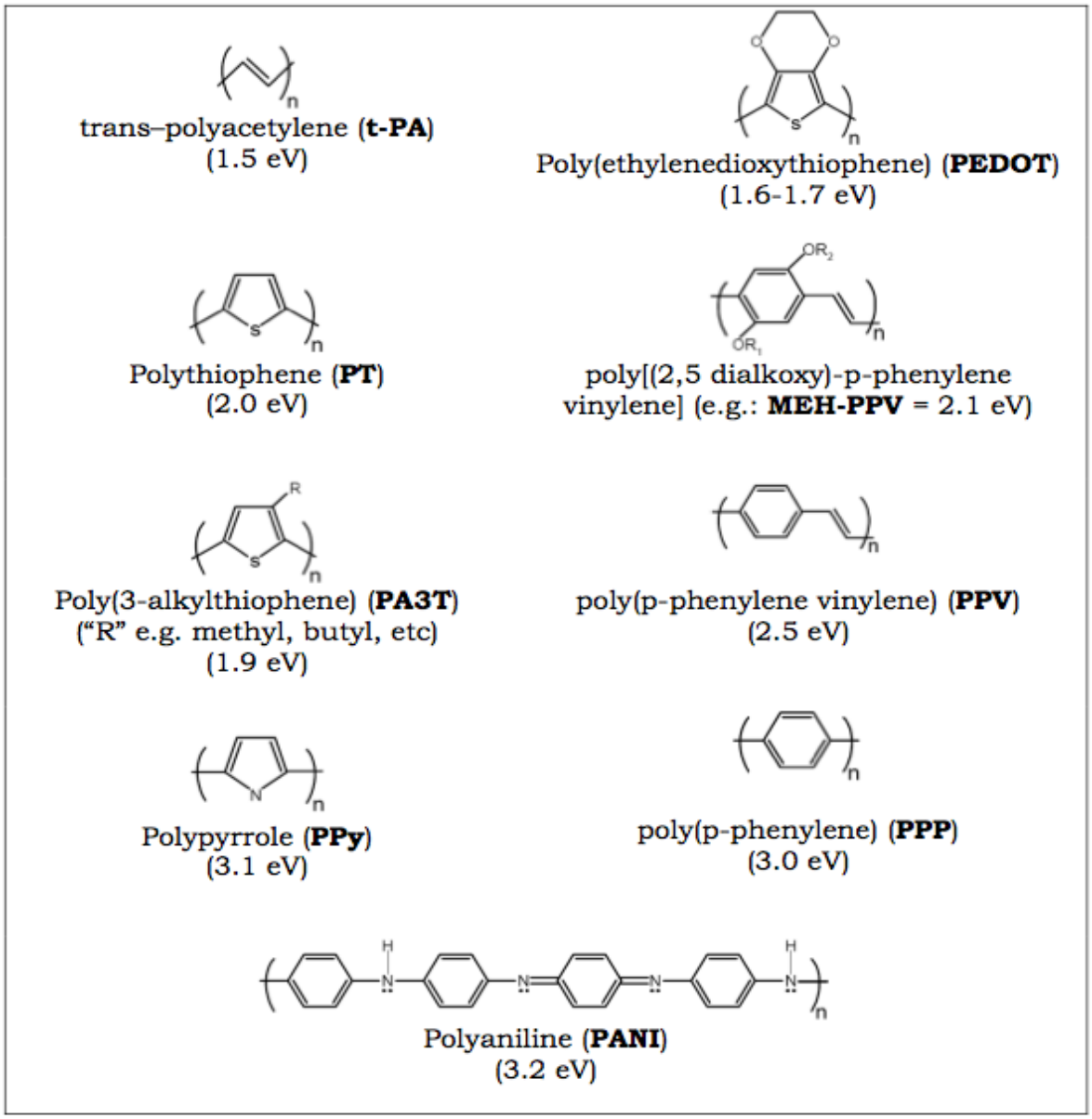

Fig. 1.1 Structure and corresponding energy gap of the main conducting polymers present in the market.

1.3 POLY(3,4-ETHYLENEDIOXYTHIOPHENE) (PEDOT):

PROPERTIES, SYNTHESIS AND APPLICATIONS

1.3.1 PEDOT general properties

Among the numerous electrically conductive polymers that have been studied and developed over the past four decades, PEDOT seems to be one of the most successful material, playing a significant role in industry, mainly in antistatic, electric and optoelectronic applications.
Compared to polypyrrole and polyaniline, it possesses advantageous properties due mainly to the presence of the two electron donating oxygen atoms coupled to the thiophene ring by the ethylenedioxy group. It combines a low oxidation potential and moderate bandgap (1.5-1.6 eV) with good environmental stability in the oxidized state. In fact, the lower band gap relative to PT is thought to originate from the influence of the electron-donor ethylenedioxy groups on the energies of the frontier levels of the π system.[11]
Two structures for neutral PEDOT are possible in principle: aromatic-like and quinoid-like form. Among many studies, a theoretical investigation by Dkhissi et al.[12] suggested that the ground state of neutral PEDOT was aromatic-like. They evaluated the structure from quantum-chemical calculation by both restricted Hartree-Fock (RHF) and density functional theory (DFT). To confirm the conclusion, the vibration spectra of the two forms were calculated and compared to the experimental spectra recorded by Kvarnströmat al..[13,14]

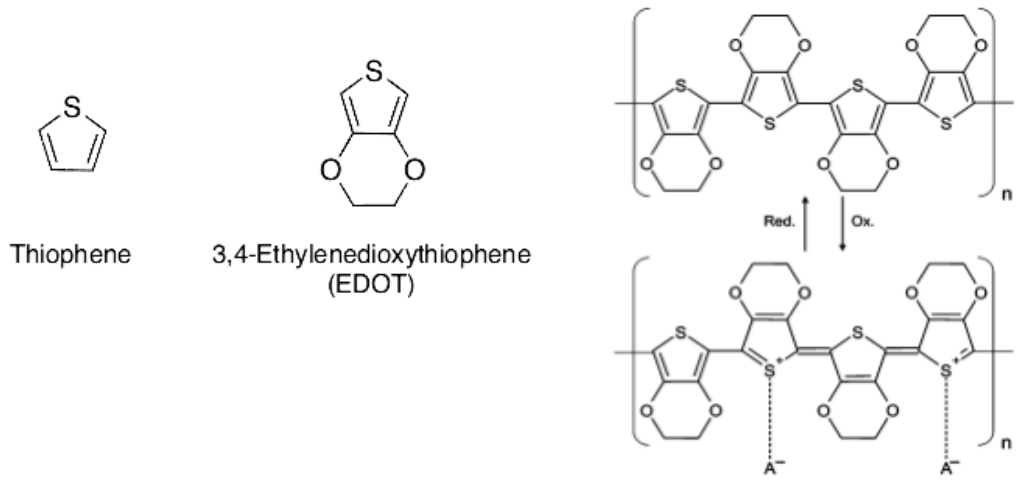

Fig. 1.2 From left: thiophene, its derivative EDOT monomer and PEDOT polymer showed as reduced (neutral) and oxidized (*p*-doped) form.

Commonly PEDOT is obtained by chemical or electrochemical oxidative polymerization of EDOT monomer. Further oxidation of PEDOT chain (*p*-doping) leads to the conductive oxidized form (polaronic and bipolaronic states) (Fig. 1.2). After doping, PEDOT exhibits reduced absorption in the visible: the lowest π-π* transition shifts from 1.5 eV to below 1 eV in the metallic state.[15] Thus it shows high electrical conductivity (up to 1000 S/cm) in the doped state. The high stability of its oxidized doped state is also attributed to the electron-donating effect of the oxygen atoms at the 3,4-positions stabilizing the positive charge of the doped state in the polymer backbone.[16]

Conductivity appears to remain almost unaltered after aging in environmental conditions. By blocking the β-positions of the thiophene ring, also the formation of α-β linkages during polymerization is prevented, thus resulting in a more regio-regular material. In addition to the high conductivity, PEDOT shows reversible doping state. It can be repeatedly doped and undoped. Moreover, it is highly optically transparent and light blue in the form of thin oxidized films and can be easily changed into opaque and dark blue appearance after reduction. Its color changes visibly when its doped state changes and may be suitable for optical applications, such as electrochromic displays.

In order to summarize, the conducting form of PEDOT stands out for high degree of visible light trasmittivity and environmental stability, which are important for industrial applications. In addition, EDOT polymerizes rapidly and efficiently, leading to highly electroactive PEDOT films that well adhere to typical electrode materials and have low oxidation potential, which provides for facile, long-term electrochemical switching.

1.3.2 PEDOT morphology and structural aspects

Many X-ray structures of PEDOT salts have been reported, such as perchlorate[17], *p*-toluene sulfonate [18] and hexa-fluoro phosphate. [19] The high electrical conductivity measured for PEDOT agrees well with metallic state behavior in the surface plane of the film. The optical anisotropy of PEDOT films is of uniaxial character with the optic axis normal to the film surface, as determined by variable-angle spectroscopic ellipsometry together with intensity reflectance and transmission spectrophotometry. The (ordinary) index of refraction in the plane shows a metallic state behavior while the out-of-plane (extraordinary) index or refraction was character similar to that of a dielectric.[20] The optical anisotropy corroborates with a structural model of thin-film tosylate-doped PEDOT, based on diffraction peak positions and intensities.[21,22]

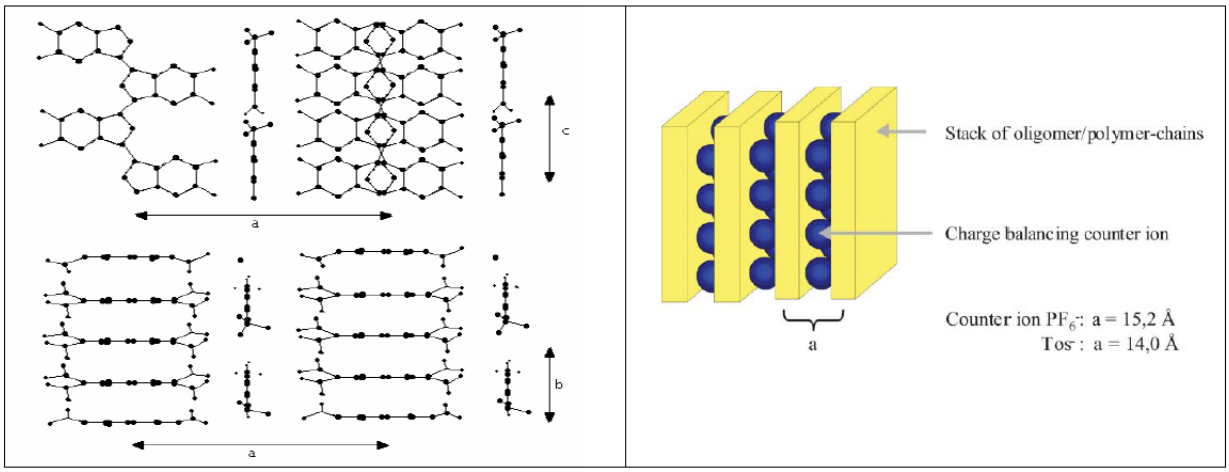

Fig. 1.3 Doped PEDOT structural model.[23]

The structural model has a pseudo-orthorombic unit cell with four monomers and one tosylate ion per cell and lattice parameters a=14.0 Å, b=6.8 Å and c=7.8 Å. The thiophene backbone of the polymer chain along the c-axis is flat and the polymer repeating distance is assumed to be 7.8 Å. The chains stack on top of each other with a stacking distance of b/2=3.4 Å, resembling the tendency of thiophene towards π-stacking. These bc-layers are separated along the a-axis by layers of tosylate ions (Fig. 1.3). Therefore, the orientation of the material is such that the a-axis is oriented along the surface normal so that the thin films are highly anisotropic, in agreement with the observed optical anisotropy of the materials.[24]

1.3.3 PEDOT synthetic routes

The main PEDOT synthesis routes are chemical oxidative and electrochemical [25, 26] polymerization of the monomer EDOT (Fig. 1.4). In addition, another chemical method is based on the transition metal-mediated coupling of dihalo derivatives of EDOT.[27] This methodology was applied mainly to the direct formation of neutral PEDOT[28, 29] and to monomers with solubilizing side groups.

Commonly, PEDOT films are obtained by wet chemical oxidation of the monomer, using iron(III) salts as oxidants, and then applying several types of solution processing. The classical method employs oxidizing agents such as iron(III) chloride ($FeCl_3$) or iron(III) *p*-toluene sulfonate (tosylate) ($Fe(PTS)_3$). Generally the oxidant and the monomer are mixed in alcoholic solutions, that are then used to coat a specific surface. As the polymerization occurs, such a method results in a insoluble and infusible PEDOT layer. The material is purified by

solvent rinsing to remove spent oxidant, unreacted monomer and by-products. This method allows to produce substrate-supported films with useful electrical and optical properties.

The overall reaction for wet chemical oxidative polymerization of EDOT, similar to the oxidative polymerization mechanism for PTs, can be separated into two principal steps: *(I)* oxidative polymerization of the monomer to the neutral PEDOT and *(II)* oxidative doping of the neutral polymer to the conductive polycation. This two steps are not separated in a sequential way, but overlap. A complex mechanism is revealed by detailed studies of the reaction kinetics.[30] Briefly following a mechanism proposed [23] (Fig. 1.4 A), the reaction starts with the slowest, rate determining step, the EDOT oxidation to the radical cation followed by the dimerization of the free radicals. End-group oxidation of oligomers, beginning with dimers, is faster than the monomer oxidation and leads, after recombination of two radical cationic end groups, to higher oligomers with the same rate constant for the recombination as with the monomer cations. At the end, oligomers or polymers, respectively, are doped by further oxidation by excess oxidant. The highly conductive, diamagnetic bipolaron state, stabilized by the charge balancing counter ion (for example, tosylate ion) from the oxidant salt used (such as Iron (III) tosylate salt) is shown in figure 1.4 B.

A chain mechanism for the oxidative synthesis of aqueous PEDOT microdispersions has been suggested.[31]

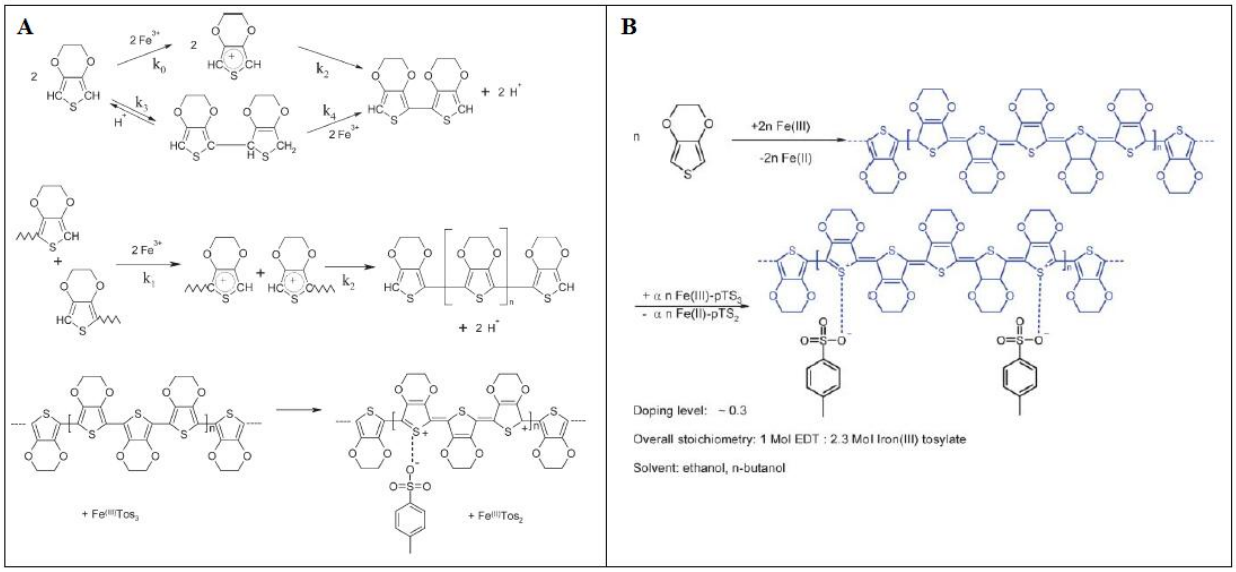

Fig. 1.4 (A) Mechanism proposed for EDOT oxidative polymerization; (B) Molecular structure of tosylate-doped PEDOT.[23]

Acidic environment enhances significantly the reaction rate and the effects of protons concern mechanicistic aspects. Protic acids (sulfuric acid, trifluoroacetic acid, etc.) and a variety of Lewis acids (BF_3, $AlCl_3$, $TiCl_4$, $SnCl_4$, $SbCl_5$, etc.) catalyze an equilibrium reaction of EDOT to the corresponding dimeric and trimeric compounds without further oxidation or reaction. [32] Acidity control by using a weak base, the so-called base-inhibited polymerization method, allows to prevent these undesired side-reactions, reducing the polymerization reaction kinetics and enhancing conductivity and transparency of PEDOT coatings.

Besides the classical methods, other important chemical oxidative polymerization methods have been reported. In the method of de Leeuw et al. [33] $Fe(PTS)_3$ is used at elevated temperature in combination with imidazole as a base, resulting in a black insoluble and infusible PEDOT film that after rinsing with water and *n*-butanol, exhibited high conductivities (up to 550 S/cm).[34]

The third, and most practically employed chemical oxidative method, is the so-called Baytron P synthesis developed at Bayer AG.[35- 38] This method implies the polymerization of EDOT in an aqueous polyelectrolyte (commonly polystyrene sulfonic acid, PSS) using an oxidizing agent. The reaction is generally carried out at room temperature and results in a easy-to-process dark blue aqueous PEDOT/PSS dispersion, that is commercially available with different formulations under the trade name of Baytron® P. PEDOT/PSS complex will be better described in following subsection 1.3.5.

Other methods that use chemical oxidative polymerization based on a heterogeneous phase process are chemical vapor deposition (CVD) methods. In particular, many works have been produced exploiting the method of vapor phase polymerization (VPP) of EDOT. A substrate is exposed to monomer vapors in presence of polymerization initiator at controlled conditions. VPP method related to PEDOT synthesis, is treated in chapter IV (subsection 4.1.1) as object of the research.

In order to alternatively resume the topic of PEDOT synthesis, a general classification of PEDOT synthetic routes can be derived by considering applicative aspects. In fact, PEDOT technological drawbacks, such as low solubility, limited processability and poor mechanical properties, require specific synthetic procedures, according to the application and desired properties. It is possible to distinguish the synthesis of the so-called *(I) in situ* PEDOT, as obtained by electropolymerization, *in situ* solution-based chemical oxidative polymerization and chemical oxidative vapor phase polymerization (VPP) methods, from the synthesis of *(II)* PEDOT aqueous complex with polyanionic dispersants, as in the case of PEDOT/PSS complex. In the case of *in situ* PEDOT methods are used, the ICP is generated in the course of

the manufacturing process by the end user and a close connection to the application is required together with a high control of synthesis parameters. On the contrary, the latter is an example of template polymerization method that leads to preformulated PEDOT complexes, usually in the form of colloidal microdispersions, that can be easily processed by several deposition methods.

1.3.4 PEDOT derivatives and composites

Several EDOT derivatives have been synthesized by various research groups. Starting from the first ones, Heywang and Jonas reported the synthesis of alkyl-substituted EDOT derivatives.[15] Groenendaal et al.prepared alkylated PEDOT derivatives and the influence of such modifications on electrical properties was studied.[39] Hydroxymethylated EDOT derivative was synthesized by Ng et al..[40] This was subsequently converted to the water-soluble sodium salt of the butanesulfonic acid-functionalized EDOT[41] and into alkoxy-substituted EDOT derivatives.[42]

Several derivatives have been produced changing the dimension of 3,4-alkylenedioxy ring (ProDT[43], BuDT[44] series) and, from these, all the range of substituted 3,4-alkylenedioxythiophenes, such as dialkyl derivatives of ProDT[45] available for the preparation of conducting and electro-active polymers (PXDOTs) suitable for electrochemically-driven applications, such as electrochromism, smart windows and chemical sensors.[46] Another family of derivatives is that one introduced by the synthesis 3,4-dibromothiophene[47] from which the synthesis of 3,4-ethylenedithiathiophene (EDTT) where the two oxygen atoms of ethylenedioxy group are substituted by sulfur atoms.[48]

Polymerization of EDOT based monomers, including co-polymerization, can be achieved taking into account the same reactions used for EDOT. Chemical polymerization of alkylated or alkoxylated EDOT derivatives ($R \geq C_{10}H_{21}$) results in regio-random PEDOT derivatives that are soluble in common organic solvents ($CHCl_3$, CH_2Cl_2, THF). Then these derivatives can be characterized using standard structural methods and can be solution processed by casting and spraying methods.

Moreover, PEDOT and its derivatives represent the component for variable-bandgap conjugated polymers, resulting in films colored over the entire spectral range. In fact, the degree of π-overlapping along the backbone controls the electronic bandgap of a conjugated chain, varying the energy levels of molecular orbitals (HOMO-LUMO). This can be adjusted via steric interactions and by controlling the electronic character of the π-system with electrodonating or accepting substituents. A broad family of PEDOT derivatives with higher

energy gaps, in the range of 1.4-2.5 eV, is that one derived from the series of oxidatively polymerizable EDOT-arylenes. In other cases, EDOT has been used to form complex monomers that can provide polymers with bandgaps lower than PEDOT. An example is the cyano vinylene (CNV) acceptor unit as a conjugated spacer between two EDOT units yielding a polymer (PBEDOT-CNV) with energy gaps in the range of 1.1-1.2 eV. Other works use a donor-acceptor methodology to control the electronic properties of PEDOT-based materials, that leads to polymers that can be both p- and n-type doped and provide for multicolor electrochromism.[49]

Also copolymerization is a powerful method to enhance the electrochemical, optical and electrochromic properties of the parent homopolymers. In fact, copolymerization of EDOT with other monomer serves to reduce its band gap, shorten switching time, enhance its capacity stability. Chemically polymerized vinylene copolymers (poly(EDOT-vinylene)s) exhibit slightly reduced electronic band gap relative to PEDOT itself.[50] Moreover, several copolymers were assembled into electrochromic devices and measured in many aspects. For example, electropolymerization of EDOT with 4-(2,5-di(thiophen-2-yl)-1H-pyrrol-1 yl)benzenamine (SNS-NH_2) revealed a multichromic copolymer (P(SNS-NH_2-co-EDOT)) with different colors at different applied potentials.[51] While electropolymerization with other thiophene derivatives monomers, such as 2,5-di(thiophen-2-yl)-1-*p*-tolyl-1H-pyrrole (DTTP) and 1-benzyl-2,5-di(thiophen-2-yl)-1H-pyrrole (SNBS) led to copolymers (P(DTTP-co-EDOT) and P(SNBS-co-EDOT) respectively) characterized by decreased electronic band gap and enhanced electrochromic properties such as optical contrast and switching time.[52,53]

Copolymerization of EDOT with functional EDOT derivatives also serves as powerful method to introduce several functionalities into the conducting polymer backbone, for post-polymerization treatments and targeted applications. This aspect is introduced in chapter 6.

Another way respect to the direct modification with pristine CPs is the formation of composites and nanocomposites, such as the coupling to metal functionalities, in order to further increase the performances of the resulting composite material. Inclusion of noble metal nanoparticles (NPs) leading to CP/NP nanocomposites represents a possibility, also for PEDOT. For example, following chemical and electrochemical routes, Au_{nano}-PEDOT nanocomposites were prepared showing enhanced performances in electrochemical sensing applications.[54]

Another type of PEDOT composites are the layered nanocomposites prepared by in situ oxidative polymerization of EDOT intercalating in a host material in presence of an external

oxidizing agent, such as in the case of VS_2 as host material leading to improved electrochemical performances as a cathode material for rechargeable lithium batteries.[55]

In general, this represents a very extensive area, including PEDOT composites with carbon materials, carbon nanotubes, other conducting polymers and, in general, several synthetic and natural polymers, with important implications and possibilities in many applicative fields.

PEDOT can be modified also changing the nature of doping. In this case, free-standing PEDOT films with a variety of dopant anions can be prepared, especially when electrochemical polymerization methods are used. The conductivities of these films vary in dependence on the nature of the dopant anion (10^0-10^2 S/cm at room temperature)[56,57], as in the case of the dopant counterion PF_6^- providing a material with high room temperature conductivity (300 S/cm) and a temperature dependence of conductivity suggesting the material to be on the metallic side of the metal-to-insulator transition.

Polymeric electrolytes can be also used as doping agents leading to PEDOT films via electropolymerization or chemical polymerization.[58] For example, PEDOT films doped with sulfated poly(β-hydroxyether) (PEDOT/S-PSE) exhibit mechanical properties imparted by the polyelectrolyte dopant with concurrent high conductivity. Higher conductivities are reported when using a bis-trifluoromethyl-functionalized sulfated poly(β-hydroxyether). The use of more flexible polymeric dopants led to materials that could be elongated between 80 and 110% when heated. However, this context is better described in next subsection 1.3.5 focusing on the greatest importance assumed by polystyrene sulfonic acid (PSS) as polyelectrolyte for PEDOT synthesis.

1.3.5 The PSS polyanion for PEDOT synthesis: PEDOT/PSS complex

The problem of low solubility concerning all conjugated polymers may be reduced by the introduction of soluble side-chains or by the use of specific polyelectrolytes, as both solubilizers and doping agents. Relatively to this, in spite of low PEDOT solubility, processability and lack of mechanical properties, its synthesis in presence of polymeric supporting materials, that act as polymerization templates, water solubilizers and stable doping agents at the same time, can reduce or circumvent these unwanted drawbacks. These supporting polymers, specifically anionic polyelectrolytes, are able to coordinate the monomer acting as template during polymerization for the synthesis of many conducting systems.[59] Such a chemical polymerization route, better known as “template polymerization”, may be also useful to provide the resulting conducting systems with mechanical properties

and features tunable for different applications, according to the properties and interactions of the specific supporting polymer used.

As introduced in subsection 1.3.3, traditional water phase template polymerization of EDOT is conducted in presence of water soluble polystyrene sulfonic acid (PSS) by using chemical oxidative methods, in order to give a PEDOT/PSS colloidal water dispersion commercially known under the trade name of Baytron® P.[23]

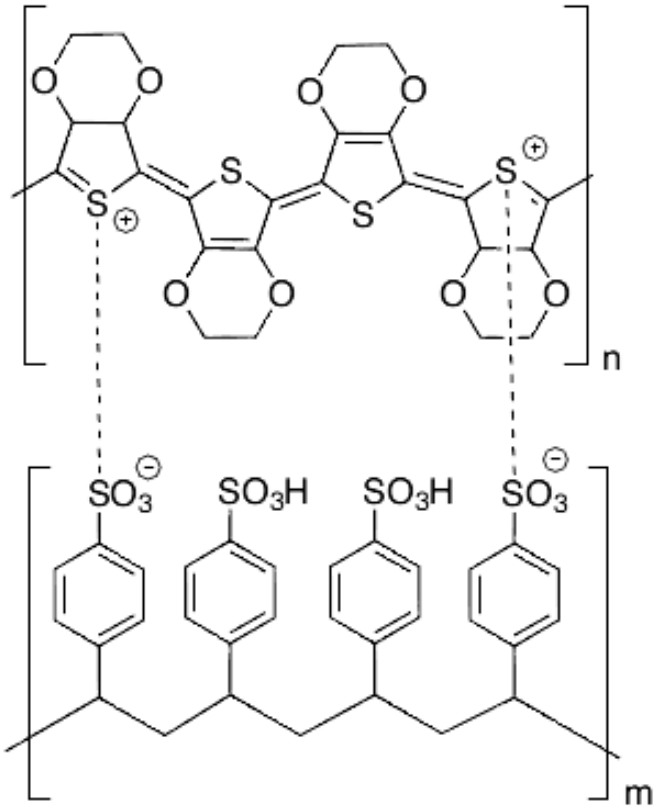

Fig. 1.5 Molecular structure of PEDOT/PSS complex.

A feasible way to obtain the PEDOT/PSS complex in its conductive, cationic form (Fig. 1.5) is the oxidative polymerization of EDOT in aqueous dispersion using sodium peroxodisulfate ($Na_2S_2O_8$) as the oxidant. The PSS phase in the complex has mainly two functions:

I. acting as the source for the charge balancing counter ion.[60]

II. keeping the PEDOT segments dispersed in the aqueous medium, although the resulting complex is not truly water soluble and forms a stable, easy-to-process, deep blue microdipersion.

Experimental evidences about the nature of PEDOT/PSS complex showed that the resulting PEDOT segments, formed during polymerization, in the complex seem to be rather short. From several measurements by MALDI TOF mass spectroscopy on PEDOT/PSS or substituted PEDOT derivatives, including neutral PEDOT segments, a molecular weight of PEDOT molecules not exceeding 1000 to 2500 Da (about 6 to 18 repeating units) resulted, resembling an oligomeric nature of these segments.[61]

Moreover, the PEDOT/PSS complex seems to be very stable. Inganäs et al. demonstrated that the ionic species $PEDOT^+$ and PSS^- cannot be separated by capillary electrophoresis.[62]

An appropriate structural model has been drawn in which oligomeric PEDOT chains are tightly attached to the PSS having a much higher molecular weight (secondary structure of figure 1.6). A stacked arrangement of the polythiophene chains in its tangled particles and films, similarly to the stacks with monomeric counter ions of figure 1.3, is one prerequisite for the high conductivity of PEDOT/PSS. A cross-linked and highly swollen polymer gel is developed, forming gel particles. Baytron P was initially developed for antistatic applications in the photographic industry. Nowadays, it serves as conducting polymer blend for several applications. As result it is available in different formulations, such as the electronic grade used for light-emitting diode (LED) applications.

Some properties depending on the PEDOT/PSS ratio are summarized in figure 1.6. These can be evaluated on the basis of the specific application and requirements.

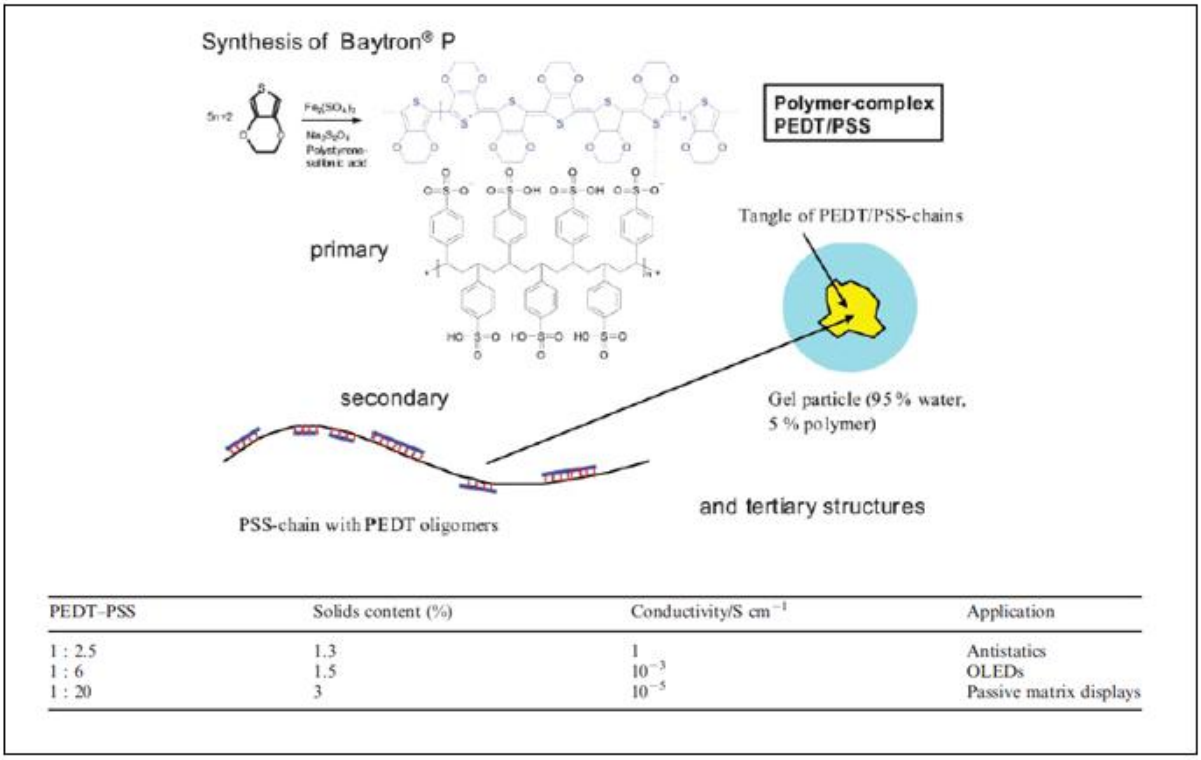

PEDT–PSS	Solids content (%)	Conductivity/S cm^{-1}	Application
1 : 2.5	1.3	1	Antistatics
1 : 6	1.5	10^{-3}	OLEDs
1 : 20	3	10^{-5}	Passive matrix displays

Fig. 1.6 Primary, secondary and terziary structures of PEDOT/PSS complex.[23]

For example, grades of PEDOT/PSS for antistatic applications have low PSS contents, associated with highest conductivity values. Increasing the PSS content logically reduces the electrical conductivity. Moreover, the smaller the particles, the smaller the conductivity. The particle size has been varied by applying different high pressure shear rates to the PEDOT/PSS dispersion. Decreasing the mean particle size decreases also the viscosity. Particle boundaries of dried gel particles seem to contribute significantly to the overall resistivity. A recent work explained in detail the electrical transport properties in PEDOT/PSS syste.[63] Combining scanning probe microscopy with macroscopic conductivity measurements a 3D morphological model explaining the observed anisotropic conductivity of spin coated PEDOT/PSS thin films. In particular, the vertical conductivity ($\sigma_{\perp}$, perpendicular to the substrate) was found up to three order of magnitude lower than the lateral conductivity in the plane of the film ($\sigma_{=}$, parallel to the substrate). In addition, different conductivity mechanisms were found for vertical $\sigma_{\perp}$ and $\sigma_{=}$. A temperature-dependent conductivity study allowed to explain by application of Mott equation, the lateral conductivity mechanism in terms of a

variable range hopping (VRH) model, whereas the vertical conductivity mechanism in terms of a nearest-neighbor (nn-H) hopping type behavior, as a simple Arrhenius thermally activated process. Moreover, observation of pancake-shaped PEDOT rich islands separated by lamellas of PSS in cross-sectional AFM and topographic STM images explained both the large difference in conductivity and conduction mechanism as observed in temperature-dependent conductivity measurements (Fig. 1.7).

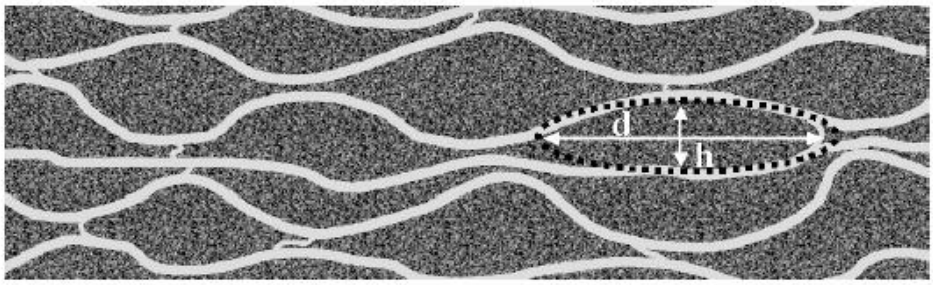

Fig. 1.7 Cross-sectional view of schematic morphological model for PEDOT/PSS thin films. PEDOT rich clusters are separated by lamellas of PSS. Typical diameter (*d*) of PEDOT cluster is about 20-25 nm and the height (*h*) is about 5-6 nm.[63]

While, in general, the conductivity of the best PEDOT/PSS films is reasonably high, there remain some applications for which higher electrical conductivities (> 10 S cm-1) are required, such as stand-alone transparent anodes in flexible electronic devices. In this context, conductivity of PEDOT/PSS can be increased during formulation by one or two orders by use several type of additives, such as:

- Low boiling solvents (alcohol or low boiling ketones):
they are added in order to lower the surface tension and increase wetting of substrates.

- Surface active components:
non-ionic surfactants in very low amount could be added to improve wetting of surfaces by aqueous PEDOT/PSS.

- Polymeric binders:
they are used to improve film properties, especially in case where thermal or mechanical processes are required.

- Silanes and tetraalkylorthosilicates:

they are used to increase adhesion to substrates, hardness and wear resistance.

- High boiling solvents and other polar compounds:

high dielectric solvents, such as amides (*N*-*N* dimethylformamide, *N*-methylpyrrolidone) and sulfoxides (dimethysulfoxide), or polyhydroxy compounds (ethylene glycol and sugar alcohols) are used as "secondary dopants" to increase overall conductivity of the resulting film. Their effect is not due to their presence in the final material, but it was demonstrated that polar solvents dissolve PEDOT stacks in the complex during processing by a screening effect, leading to a favorable morphological rearrangement and clustering and therefore decreasing the resistance between dried gel particles. More mechanisms have been proposed to explain in detail such an effect and it is considered that morphological changes induced by the presence of the dopants are important factors in the increased conductivity for doped films of this type.[64- 66]

Another way for enhancing the properties of electro-active polymers, while preparing useful materials at the same time, is through polymer blending. In this case the high conductivity is attributed to the formation of a continuous network of the conducting polymer, that is phase separated from the insulating host (Interpenetrating Polymer Networks, IPNs). PEDOT/PSS has been blended with polar host polymers, leading to enhanced electrical properties due to different mechanisms. In PEDOT/PSS-poly(vinylpyrrolidone) (PVP) blends a ionic crosslinking with bivalent metals have been exploited.[67] In blends with poly(ethylene oxide) (PEO) a crystallization-induced phase separation has been used.[68] Blends of PEDOT/PSS with poly(vinyl alcohol) (PVA) have been used to give a large effective poling field across a nonlinear optical (NLO) active layer, that is required for dipole orientation.[69]

1.3.6 Applications of PEDOT and PEDOT/PSS

Applications using *in situ* PEDOT need to be distinguished from those ones that use the PEDOT/PSS complex. In case of *in situ* PEDOT, polymerization occurs during the formation process, that, hence, requires a high control of synthesis parameters, such as kinetic parameters. In contrast, the PEDOT/PSS is a prefabricated polymer. All its applicative properties (filming and processing) will be previously adjusted by formulation. In regards to electrical properties, *in situ* PEDOT is generally characterized by the highest values of conductivity.

Applications of PEDOT and PEDOT/PSS complex can be divided into antistatic, electrical, electronic, optoelectronic and electro-chromic applications. Moreover, other applications concern sensors and biomedical fields, such as actuators for artificial muscles, biosensors, tissue engineering and neural probes.

In a general way, applications of PEDOT and related complexes can take advantage of its electrical and electronic properties or its redox properties.

- **PEDOT applications using its electric and electronic properties**

The first industrial application involving PEDOT/PSS complex was the use for antistatic layers in photographic industry (Agfa). The antistatic layer in photographic film is needed to avoid electrostatic discharges within the photographic layers during the processing of the film. Another antistatic application of PEDOT/PSS is the use as outer surface antistatic layer on cathode ray tubes, to avoid dust contamination. The requirements are a surface resistivity of 10^5 up to 10^9 Ω/sq, high optical transparency (low content of large particles), good adhesion and hardness. Further antistatic applications involving PEDOT are antistatic gloves[70], displays and video displays panels, textiles, antistatic release films[71], protective films[72], recording types[73] and polarisers.[74]

Several applications of PEDOT concern production of conducting coatings to conduct current for the operation of a device. Respect to antistatic applications, in this case layers conductivity should be maximized. In most applications PEDOT works as transparent conductor. Hence, thickness, specific optical absorption and specific transparency of conducting layer should be taken into account.

PEDOT/PSS complex is used also as a transparent conductor in electroluminescent (EL) devices. They consist of an emitting layer in contact with two transparent conducting layers. The active layer (a composite, such as the emitter zinc sulfide and dielectric barium titanate) emits light under application of an electric signal. In these devices the transparent conductor indium tin oxide (ITO), commonly used as transparent low work function electrode (anode), can be replaced by PEDOT/PSS layer with some advantages. In fact these devices work at high voltage (~100 V, 400 Hz), hence the specific resistance of the conductor is less critical than for low voltage applications. Moreover PEDOT/PSS is much easier to process (printing techniques) than ITO and can be three-dimensionally shaped.[75] In fact, replacing ITO is an essential target in flexible optoelectronic applications.

Another important application of PEDOT is the use as counter electrode in aluminum and tantalum capacitors. The introduction of a conducting polymer in these capacitors is

advantageous for two main reasons. First, PEDOT increases conductivity of the counter electrode, because it is more conductive than the previously used manganese dioxide and penetrates into the porous structure. Secondly, by substituting manganese dioxide, which forms strong redox couples with metals, it increases the safety of the capacitor during operation, preventing high temperatures and ignition risk in case leakage currents are formed, due to defects of dielectric layer. In order to have a conductor that penetrates deeply into the porous structure, it is necessary to form PEDOT by using an *in situ* solution chemical oxidative polymerization method. The monomer and oxidant are dissolved in lower alcohols (ethanol and *n*-butanol) to give low viscous impregnation solutions. Impregnation is usually performed by dipping procedures which yielded capacitors with PEDOT-layers of few nm thickness and good capacitance recovery.

A wide application field is the production of layers with electronic functions, as hole injection layers (HIL) in organic light emitting diodes (OLEDs), photovoltaic devices and photodetectors, and conducting layers in all-organic thin film transistors (OTFTs). In organic devices applications PEDOT/PSS is used as an electrode/hole-transport layer. Generally, in OLEDs and photovoltaic devices PEDOT/PSS is used as conducting layer interposed between the active material and ITO electrode (anode). In fact, PEDOT/PSS has a higher work function than ITO, even after O_2-plasma treatment[76] and chemical modification of the ITO.

In OLEDs, PEDOT layer has the function of inject holes from anode to emitting active layer; while in photovoltaic devices, it prevents recombination of charges generated inside the active material. Moreover, the usually rough ITO surface is smoothed when a thin PEDOT/PSS is used, resulting in increased efficiency and lifetime of the devices. However, some studies report that in certain conditions PSS could degrade the performance of OLEDs, due to its acidity.[77] In fact, an acidic PEDOT/PSS solution can etch ITO during the spin-coating process, and the hydrolysis of the deposited polymer layer by moisture absorption can also etch ITO, causing indium incorporation into the polymer.

Compare to a photovoltaic cell, a photodetector, as a sensor, just need to detect light. In this case the resistance of the transparent conductor is less crucial. Besides the electronic function it is also possible to PEDOT to replace ITO[78] , such as *in situ* PEDOT or PEDOT/PSS at highly conducting formulations.[79]

All-Organic Thin Film Transistors (OTFTs) are the basis of integrated circuits for applications in low-end electronics and driving electronics for flexible displays. In OTFT configuration, source, drain and gate contacts have been realized using PEDOT/PSS by conventional structuring techniques[80], ink-jet processing and other patterning techniques.

OTFT are widely used also for chemical and biological sensing.[81] In OTFTs-based sensors PEDOT/PSS is frequently employed as semiconductor active material forming the channel.

- **PEDOT applications using its redox behavior**

PEDOT/PSS (and in general PEDOT) exhibits electro-chromic properties, which can be used to build appropriate devices, such as smart windows. On the basis of electro-chromic behavior there is an electron transfer reaction that takes place during the electrochemical oxidation and reduction of PEDOT. In accordance with the cathodic reduction step (+ 2.5 V), PEDOT optical properties vary turning color from slightly blue and transparent to deep blue. The reverse biasing (-2.5 V) leads to the oxidation of the reduced state on the electrode (anode), restoring the original transparency. During reduction process, usually lithium ions as counter ions intercalate into the PEDOT/PSS in order to compensate for the negative charges of the SO_3^- groups on PSS.

- **PEDOT applications in biomedical fields**

Nowadays, several studies have established that PEDOT also represents a biocompatible and biomimetic material, displaying high stability in biological systems. Moreover, it has shown very low cytotoxicity and no inflammatory response upon implantation.[82]

Due to these properties, various applications to the preparation of PEDOT-based biomedical devices, including biosensors[83], neural probes, microelectrode arrays and scaffold for tissue engineering, have spread out.[84- 87]

Moreover, biocompatible doping agents, such as anionically modified polypeptides or glutamate molecules, have been used to increase PEDOT conductivity while improving biocompatibility.[88,89]

Alternatively, in order to promote bioconjugation, PEDOT nanobiointerfaces have been electro-polymerized starting from several functionalized EDOT derivatives.[90] Likewise, methods used to prepare composite materials able to bind specific bioactive species for applications in bioelectronics include EDOT vapor phase polymerization on poly (ethylene glycol) (PEG) or carboxylated PEG.[91]

1.3.7 From PSS to other polyanion systems for PEDOT

EDOT polymerization with the traditional PSS template leads to a product that represents a compromise between performance and processability. In fact a conductivity worsening

respect to pristine PEDOT, ascribed to PSS content, limits PEDOT/PSS use in applications where no high conductivity is required. Moreover, PEDOT/PSS system allows to prepare films with a surface morphology depending on casting process. Moreover, owning to poor thermal and mechanical properties of PSS, some works report the characterization of alternative polyanionic substrates as polymerization templates instead of PSS, such as, for example, a thermally stable sulfonated poly(imide), to provide the resulting conducting systems with higher temperatures resistance [92, 93] or sulfonated poly(2-acrylamido-2-methylpropane) sulfonic acid, to prepare electrically conductive hydrogels.[94,95] Another work reports the use of partially sulfonated poly(styrene-butadiene-styrene) copolymers, considering applicative problems related to PSS acidity.[96] Others propose to replace the nonconductive PSS with conductive poly[2-(3thienyl)-ethoxy-4-butylsulfonate] (PTEB) as surfactant for the emulsion EDOT polymerization, to enhance the conduction properties of the resulting PEDOT systems.[97]

1.4 ETHYLENE VINYL ALCOHOL COPOLYMER (EVAL)

1.4.1 EVAL general properties

Ethylene vinyl alcohol copolymers, known as EVAL or EVAOH, are a family of random polymers constructed of casual sequencing of hydrophobic ethylene and hydrophilic vinyl alcohol monomeric units in variable percentage (Fig. 1.8).

They are obtained from ethylene vinyl acetate copolymers (EVA) by complete hydrolysis of vinyl acetate group.[98] They are known for their excellent barrier properties to gas like O_2, N_2, CO_2, especially at high contents of vinyl alcohol (>= 68%), that make them important materials mostly in food packaging industry, production of gasoline tanks and other materials.[99]

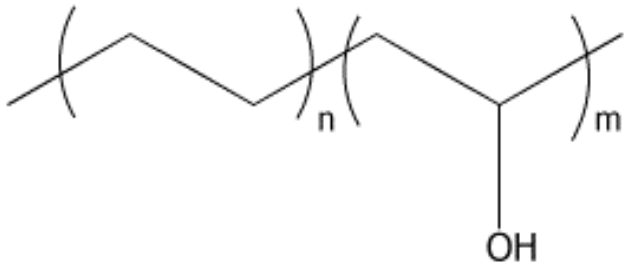

Fig. 1.8 Molecular structure of EVAL with general co-polymer composition.

EVAL is considered as one of the soft materials for ecology because of absence of emission of poisonous gas upon incineration. This is because EVAL is composed of hydrogen, carbon and oxygen and it is chlorine-free. EVAL is characterized by the high content of hydrogen bonding. Moreover, all the members of EVAL family with various vinyl alcohol composition can be crystallized, although the lack of stereo-specificity of the chain. In fact, the reduced volume of hydroxyl groups doesn't impede crystallization. However, its thermal and mechanical properties vary drastically with the copolymer composition. An understanding of the variation of physical properties with the vinyl alcohol content derives from the study of the aggregation structure of chains in both the amorphous and crystalline regions and also in the so-called high-order system. The crystallite modulus and the melting point varies continuously with composition, suggesting a continuous change of crystal structure with composition.[100] Several studies by X-ray diffraction clarified the crystal structure, chain

conformation and chain-packing mode for a series of EVAL crystals with various composition, giving quantitative interpretation of EVAL physical properties.[101]
In spite of their low gas permeation, low solubility to organic solvents and water insolubility, EVAL copolymers generally show poor moisture resistance. In particular, the plasticization effect played by water molecules[102,103], methanol and others alcohols[104,105] have been documented. The reduction of barrier properties by moisture uptake is due to the fact that inter and intra-molecular hydrogen bonding, provided by the hydroxyl groups, is intercepted by water and alcoholic substances. A plasticization effect occurs by increasing of fractional free volume allowing the permeates to travel across the polymer.

1.4.2 EVAL for PEDOT synthesis

In this context EVAL has been evaluated as starting supporting material for EDOT chemical polymerization. The reasons of its choice and the strategies adopted for its employment in combination with PEDOT are clarified in following chapters that illustrate this work. In particular:

- in **Chapter 2** a commercial EVAL is modified by a partial sulfonation reaction of polymer hydroxyl groups in order to obtain a water soluble polyanion, that is partially sulfonated EVAL.

- in **Chapter 3 and 4** alternatively to PSS system, partially sulfonated EVAL (EVALS) is used as optically transparent polyanionic substrate for PEDOT chemical synthesis, by employing two procedures, water and vapor phase polymerization, respectively. Unlike PSS polyanion, EVALS represents a substrate that provides the possibility of functionalizing the system in accordance to applicative purposes, because of the presence of unreacted hydroxyl moieties along the EVALS polymer backbone due to partial sulfonation reaction.

- in **Chapter 5** this latter advantage is exploited by undertaking EVALS to cross-linking reactions in order to obtain EVALS-based electro-active membranes. Results of preliminary tests of optimization of such membranes provide the possibility of realizing ionic polymer transducers (IPTs). In particular, a transducer in the form of a ionic polymer-metal composite (IPMC), in which PEDOT can be potentially coupled and used

in substitution of the metal part, can be designed towards the construction of an all-organic actuator.

- in **Chapter 6** unmodified commercial EVAL is employed as insulating mechanical substrate for integration of a click-functionalizable PEDOT copolymer (PEDOT-PEDOT azide).

It should be specified that the work described in this chapter is a part of a wider research project and derives from a collaboration with the group of the Danish Polymer Centre (DPC) at the Department of Chemical and Biochemical Engineering of the Danish Technical University (DTU), under the supervision of Prof. S. Hvilsted and Dr. A. E. Daugaard.

In particular, the method that has been applied in this context allows to obtain a conducting composite characterized by double surface functionality. In this case, integration of the two phases makes both EVAL hydroxyls and PEDOT azides groups available for surface-limited reactions, following an approach in the field of orthogonal chemistry. This method allows to control surface chemical-physical properties of the conducting system in order to introduce surface targeted applications.

2

PARTIALLY SULFONATED ETHYLENE VINYL ALCOHOL COPOLYMER (EVALS)

2.1 INTRODUCTION

2.1.1 EVALS polyanion for PEDOT synthesis

In the present study, a water soluble polyanion, derived from a statistical ethylene vinyl alcohol copolymer (EVAL) modified by partial sulfonation reaction (Fig. 2.1), was employed and tested for the first time as possible supporting polymer, alternatively to PSS, for PEDOT chemical synthesis. In fact modified EVAL (EVALS), already investigated in order to improve bio- and haemocompatibility of EVAL copolymers in biomedical applications[106], shows water solubility dependent on sulfonation degree, high optical transparency and good mechanical properties. In particular, biological tests have displayed that EVALS possesses a good haemocompatibility and that it increases with its sulfate group content.

For all these characteristics, EVALS has been thought as possible doping and charge balancing polyanionic phase and good transparent mechanical support for PEDOT synthesis. In addition, the presence of residual hydroxyl groups deriving from partial sulfonation of EVAL are potentially available for further functionalization or cross-linking reactions in dependence on the specific application, such as, for example, the preparation of biosensors or membranes for actuators assembling.

The use of EVALS as possible supporting polyelectrolyte was evaluated first for PEDOT synthesis in water phase (Chapter 3), in order to investigate the possibility of obtaining adequate pre-formulated PEDOT complexes. Following this preliminary test, anyway, the research was focused mainly on the use of EVALS as substrate for PEDOT synthesis by vapor phase polymerization (Chapter 4), because of the best results obtained with this method together with favorable possibilities of applicative use. Optimization of the synthetic procedure and characterization of the resulting systems directly followed.

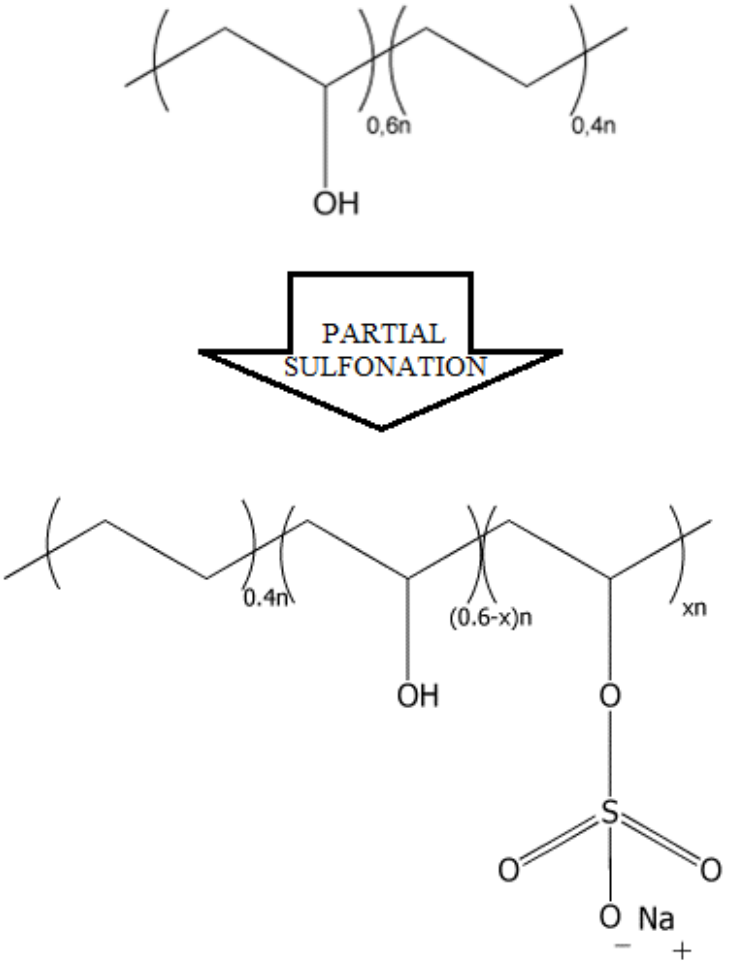

Fig. 2.1 Scheme of partial sulfonation of EVAL 40/60 to give EVALS terpolymer with general sulfonation degree.

2.2 MATERIALS AND METHODS

2.2.1 General methods and instruments

- Transmission Fourier Transform Infrared Spectrophotometry (Trasmission FT-IR) analysis was performed by using a Nicolet 6700 FT-IR Spectrophotometer (Thermo Scientific) operating within the 4000-400 cm^{-1} spectral range and with a resolution of 2 cm^{-1}. Each spectrum was acquired by co-adding 100 intereferograms and baseline corrected.
- Elemental Analysis was performed by using CE Instruments EA 1110 CHNS-O.
- Thermogravimetric analysis (TGA) was carried out employing a TGA-7 Perkin Elmer apparatus.

- Thermal analysis by Differential Scansion Calorimetry (DSC) was performed by using a Mettler Toledo DSC 822[e], operating through the heat flow mode.

2.2.2 Chemicals

All solvents used were acquired from Carlo Erba. All other chemicals, except for ethylene vinyl alcohol copolymer (EVAL) and sodium hydroxide (NaOH), were acquired from Aldrich. EVAL was obtained from Monomer-Polymer&Dajac Laboratories and NaOH from Merck.

2.2.3 Synthesis of EVALS

Commercial ethylene vinyl alcohol copolymer (EVAL) with 27/73 ethylene/vinyl alcohol weight ratio, corresponding to 40/60 repeating unit molar ratio, was used. The hydroxyl groups were partially sulfonated by using sulfur trioxide pyridine complex ($PySO_3$) as sulfonation agent according to the procedure reported by Marconi et al..[106] First EVAL was dissolved under stirring and reflux in dehydrated DMF (3 % wt./V) at T=100 °C. Predetermined amounts of $PySO_3$, previously dissolved in dehydrated DMF at T=0 °C (76 % wt./V), and EVAL solution at T=0 °C were mixed at known $PySO_3$/OH ratios (0.25, 0.50, 1.00, 1.60). For all feed ratios, the relative mixture was kept under nitrogen flux and stirred at T=0 °C for 1 hour followed by 3 hours at room temperature. The partial sulfonation reaction, as described in figure 2.2, introduces sulfate groups into the vinyl alcohol unit of the copolymer. After the addition of NaOH water solution (3N), EVALS sodium salt is collected by precipitation with isopropyl alcohol. The polymer was then repeatedly centrifuged and washed with pure isopropyl alcohol. Then, the dried copolymer was dissolved in distilled water and purified from reaction by-products (Na_2SO_3, NaOH and pyridine) by dialysis (cellulose tube, cutoff 12000-14000 g/mol, Sigma-Aldrich). The purified EVALS in water was then dried on a hot plate (T=50 °C) to form discs. Finally, EVALS discs were vacuum dried until constant weight and stored in dissecator.

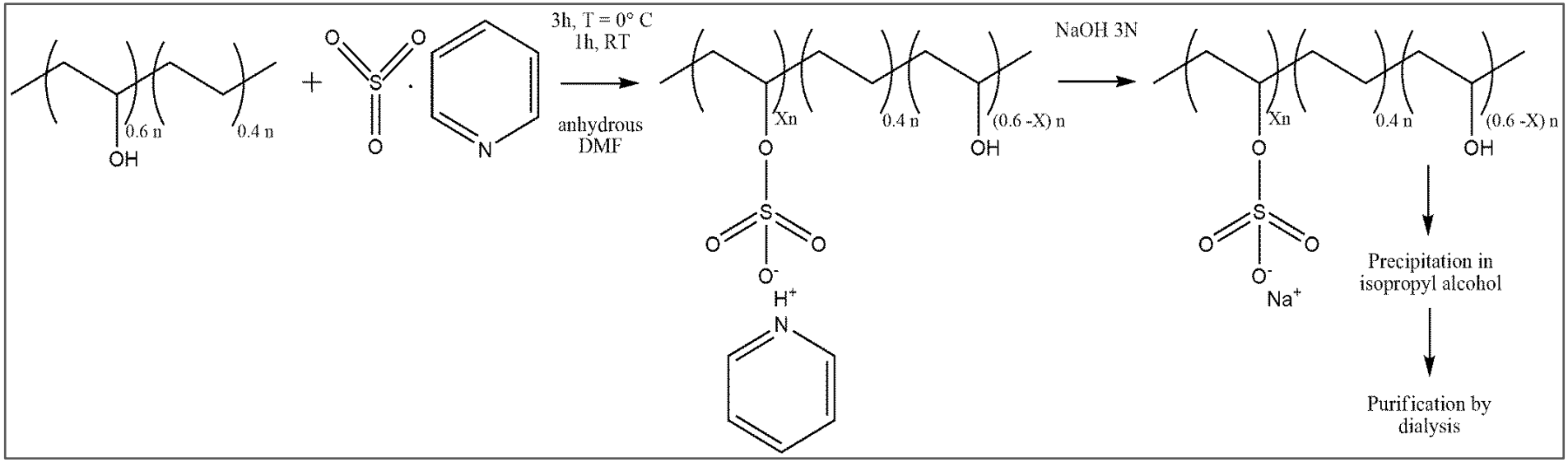

Fig. 2.2 Reaction scheme of EVAL sulfonation by using $PySO_3$ abduct.

2.2.4 Methods for EVALS characterization

EVALS sulfonation degree (SD), expressed as the molar percentage of reacted hydroxyl groups, was varied changing the $PySO_3$/hydroxyl groups molar ratio during synthesis and was determined by elemental analysis through evaluation of C/S atomic ratio. EVALS sodium salt samples were named EVALSXX, where -XX is the generic suffix indicating the percentage of SD.

EVALS was characterized by transmission FT-IR spectrophotometry analysis. For FT-IR characterization, EVALS thin films were cast on a ZnSe plate from a water solution (0.1 wt/V %) and dried at 50° C under vacuum before analysis.

Thermal stability of EVALS was evaluated respect to unmodified EVAL by thermogravimetric analysis (TGA). About 10 mg of previously dried polymer were used employing a scanning speed of 10 °C/min in the temperature range from 25 to 600 °C.

Characterization of EVALS by DSC thermal analysis was conducted on previously dried samples (about 4 mg). A single heating scansion from -50 °C to 110 °C was conducted by using a heating rate of 10 °C/min and under nitrogen flow (30 ml/min).

Among all the synthesized polyanions, EVALS at intermediate sulfonation degree of 32 % (EVALS32) showed the best balance in terms of moisture absorbing, thus processability, and mechanical and filming properties. Hence EVALS32 was selected as substrate for following experiments, unless otherwise specified.

2.3 RESULTS AND DISCUSSION

2.3.1 Characterization of EVALS

The number of hydroxyl groups involved in the sulfonation reaction of EVAL was estimated by elemental analysis. The series of the sulfonated samples was designated as EVALSXX, where -XX specifies the sulfonation degree (SD). In table 2.1 the reactants molar ratio ($PySO_3$/OH), the C/S atom ratio found in elemental analysis used to calculate SD, the SD values and the reaction yields are reported.

Sample code	PySO3/ OH molar ratio	C/S atomic ratio (elemental analysis)	SD (%)	Reaction Yield (%)	Water solubility	Notes
EVALS10	0.25	76.1	10	0.40	+ (hot)	
EVALS19	0.50	35.4	19	0.38	+ (hot)	hygroscopic
EVALS32	1.00	18.4	32	0.32	+	hygroscopic
EVALS55	1.60	8.7	55	0.34	++	highly hygroscopic, sticky in air

Tab. 2.1 Reactants molar ratio used to obtain the series of EVALS together with C/S atomic ratio from elemental analysis, calculated SD and reaction yields, respectively. Qualitative information about water solubility is also reported.

In particular, by varying the molar ratio between the sulfonation agent (sulfur pyridine complex, $PySO_3$) and EVAL hydroxyl groups, it was possible to vary the EVALS SD, as showed in figure 2.3.

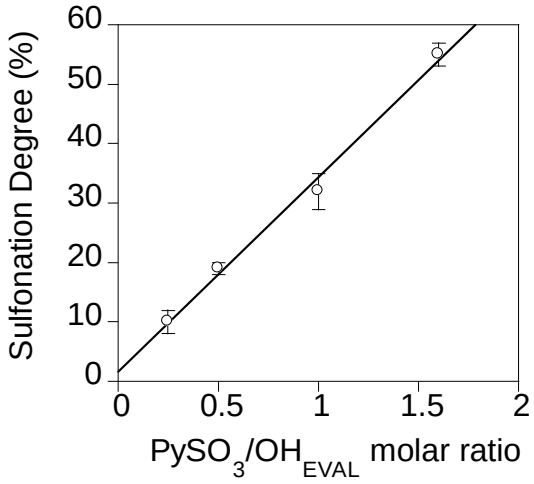

Fig. 2.3 EVAL sulfonation degree (SD) vs $PySO_3/OH_{EVAL}$ molar ratio.

In figure 2.4 transmission FT-IR spectra of EVAL and EVALS55 samples are reported.

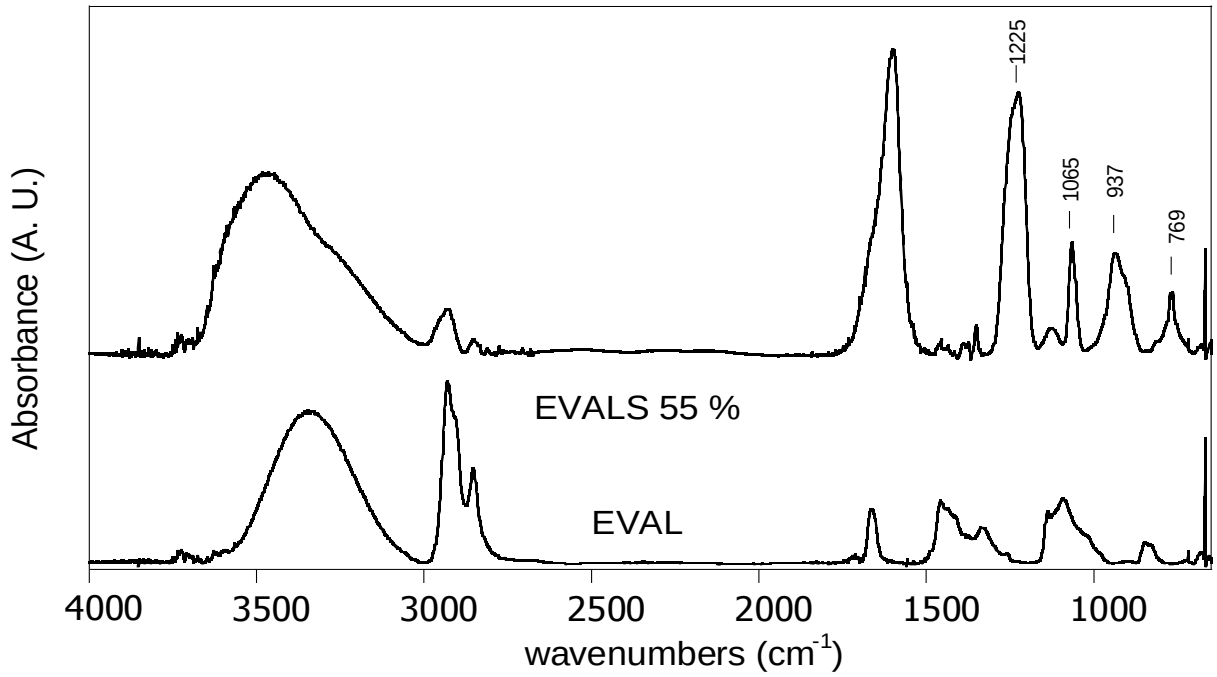

Fig. 2.4 Transmission FT-IR spectra of EVAL and EVALS (SD=55 %). (Inset) Intensity ratio I_R as a function of SD.

Besides of the characteristic absorption peaks of the pristine polymer, it may be observed the specific band of the sulfate group at 1225 cm^{-1} (SO_3 asymmetric stretching), 1065 cm^{-1} (SO_3 symmetric stretching), 937 cm^{-1} (S-O-(C) asymmetric stretching) and at 769 cm^{-1} (S-O-(C)

symmetric stretching). The peaks at about 1700 and 1640 cm^{-1} are probably due to DMF traces and absorbed water.

In figure 2.5 the intensity ratio I_R between the bands at 2930 cm^{-1}, due to the asymmetric stretching of $-CH_2$ not involved in the reaction, and at 1225 cm^{-1} is reported as a function of SD determined by elemental analysis. As expected, a linear correlation was obtained.

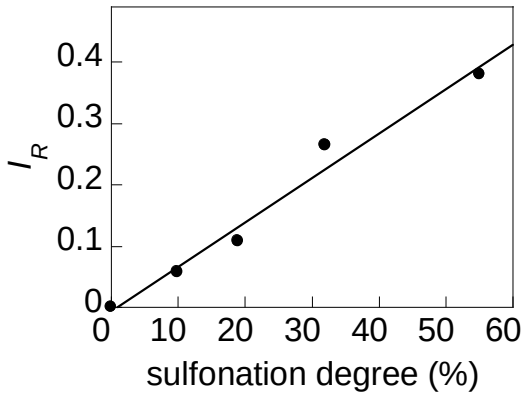

Fig. 2.5 Intensity ratio I_R as a function of SD.

EVALS shows water solubility dependent on SD. Water solubility and hygroscopicity of EVALS varies so that at *SD* <10% the polymer results insoluble in cold water whereas at *SD*>55% it is highly hydrophilic and hygroscopic and becomes rapidly sticky in air by absorbing environmental moisture (Tab. 2.1).

Thermal stability of synthesized EVALS was evaluated respect to pristine unmodified EVAL. Figure 2.6 shows a comparison between TGA thermograms of EVALS32 and EVAL, respectively.

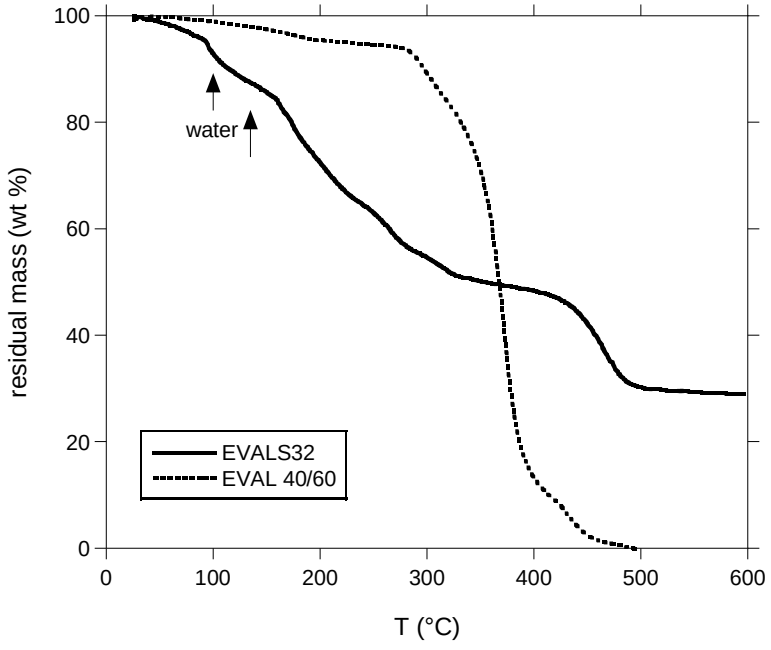

Fig. 2.6 Thermogravimetric curves of EVAL and sulfonated EVAL at 32 % SD (EVALS32 sodium salt).

While EVAL starts to sharply decompose at 280 °C, EVALS32 sample shows a progressive and broad decomposition process in the temperature range of 140 up to 350 °C associated to a weight loss of about 40 %. Presence of atmospheric water traces are evidenced by the slight weight loss above 100 °C, owning to EVALS hygroscopicity. Hence, pyrolysis products are supposed to be mainly SO_2, SO_3 and water.[106] Moreover, it is supposed that thermally activated cross-linking processes between sulfate groups occur in EVALS as the temperature increases. In fact, the occurring of cross-linking reactions could explain the observed incomplete decomposition of EVALS respect to EVAL, as it is evidenced in EVALS thermogram by the presence of a residual amount of mass at high temperatures. As expected, these phenomena are more pronounced the higher is the EVALS sulfonation degree.

Differential scanning calorimetry (DSC) measurements showed also that sulfate groups introduction causes modification of physical-chemical properties, as the comparison between EVALS32 and unmodified EVAL shows in figure 2.7.

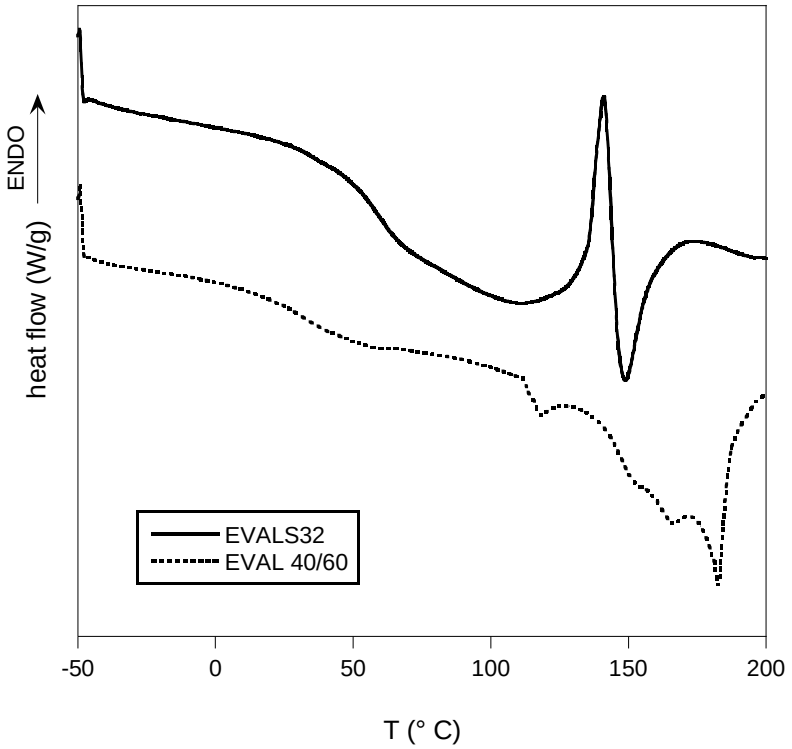

Fig. 2.7 DSC of EVAL 40/60 and sulfonated EVAL at 32 % SD (EVALS32 sodium salt).

In particular, unmodified EVAL shows intense and complex melting processes in the range of 140 to 200 °C, due to the presence of semi-crystalline regions. In addition a broad glass

transition process centered around 50-60° C is found. The smaller peak above 100 °C is attributed to water strongly bonded to polymer hydroxyl groups. In fact, this peak tends to disappear when the sample is subjected to second scanning.

On the other hand, the thermogram of EVALS32 sodium salt shows a more pronounced glass transition process, in which manly two processes can be observed, centered at about 35 and 70 ° C respectively. Here the peak related to bonded water above 100 °C, that is supposed to be more intense due to increase of polymer hydrophilicity after sulfonation reaction, can't be observed, probably because it is covered by the nearest sharp exothermic peak at 150 °C. This exothermic peak was attributed to the possible cross-linking reactions involving the sulfate groups of the chains. This is in agreement with the results observed in TGA analysis, showing that, in the complex, above 150 °C heated EVALS32 sample undergoes intense loss of functional groups and possible cross-linking reactions. These effects were confirmed also by qualitative observation that EVALS32 samples started to change appearance, becoming, moreover, water insoluble when heated just above 130 °C.

Hence, in particular, EVALS32 was chosen as supporting polyelectrolyte for EDOT polymerization experiments described in following chapters, because of best compromise between a tolerable risk of decomposition and thermally activated cross-linking reactions, high water solubility and moderate moisture absorption. In fact, in this case, sulfonation at 32 % degree doesn't adversely affect mechanical properties neither processability of the terpolymer. Moreover, EVALS32 showed high optical transparency, good mechanical and filming properties on several types of substrates.

3

EVALS FOR EDOT WATER PHASE POLYMERIZATION

3.1 INTRODUCTION

The use of EVALS in combination with PEDOT was tested at first by carrying out EDOT water phase polymerization in presence of EVALS. Following preliminary tests performed using EVALS at different sulfonation degrees, finally oxidative chemical PEDOT synthesis was carried out employing EVALS32 water solutions at different formulations with $FeCl_3$ as oxidant salt. The influence of EVALS sulfate groups/EDOT molar ratios on the PEDOT/EVALS systems resulting from water phase polymerization was investigated, mainly in terms of electrical properties and suspension stability. While the results of these tests are reported in this chapter, other tests are ongoing that imply the use of other oxidant systems such as the $K_2S_2O_8$ + $Fe_2(SO_4)_3$ system[107], similarly used in many procedures for PEDOT/PSS synthesis.

3.2 MATERIALS AND METHODS

3.2.1 General methods and instruments

- Optical microscopy (OM) images were acquired on a Nikon Opti Hut2-pol Polarized Optical Microscope (POM) at 40x-200x magnification and recorded with a Moticam 2500 5.0 Mpixel camera.
- Scanning Electron Microscopy (SEM) images were acquired by a SEM, LEO 1450 VP, characterized by a resolution of 3.5 nm and maximum magnification of 300000x.
- Electrical surface conductivity measurements were performed by using a four points probe (Jandel Engineering) equipped with 1 mm spaced four tungsten carbide spring-loaded needles. The ratio between the measured inner probe voltage (*V*) and the source DC current passing through the outer probes (*I*) was directly given by a digital multi-meter Keithley 2700 (4-wire resistance mode). The applied current was in the range

10^{-2} - 1 mA. At least three different measurements of *V*/*I* for each test were carried out and then the mean value was used to calculate the surface electrical properties.

3.2.2 Chemicals

All solvents used were acquired from Carlo Erba. All other chemicals were acquired from Aldrich, except for EVALS32 synthesized according to the procedure described in chapter 2.

3.2.3 Water phase polymerization of EDOT in presence of EVALS

Oxidative polymerization of EDOT in presence of EVALS with different $SO_3^-Na^+$/EDOT molar ratio (from 0.4 to 20 with SD=32 % EVALS) was carried under stirring for 24 h at RT in aqueous medium by using the iron(III) salt, $FeCl_3$, as oxidant (molar ratio $FeCl_3$/EDOT=10). The resulting suspensions were purified from iron salts and by-products through dialysis tube (12000-14000 g/mol) in HCl 0.01N and distilled water and stored in sealed bottles.

3.2.4 Methods for water phase EVALS/PEDOT system characterization

EDOT water phase polymerization in presence of EVALS at different formulations led to suspensions with different grade of stability. Optical and scanning electron microscopy were used to observe morphology of EVALS/PEDOT suspended particles, as obtained by water phase synthesis. The suspensions were deposited by dropping on glass microscope slides and left to dry. The obtained optical images were elaborated by Sigma Scan Pro software, in order to calculate the mean diameter of suspended particles. At least three images of the same sample and 20 objects for each image were analyzed. Anyway, such suspensions didn't form homogeneous films when dried on a support, especially at the lowest $SO_3^-Na^+$/EDOT molar ratios. For this reason, conductivity measurements were carried out by four points probe method on dried EVALS/PEDOT samples previously reduced to powder and pressed at the same conditions in order to form thin pellets with diameter of 12 mm and thickness of about 0.1 up to 0.3 mm. Bulk conductivity (σ) was calculated by $\sigma = \sigma_s/d$, where σ_s is the surface conductivity obtained by applying equation 1 reported in following subsection and d is the thickness of pellet.

3.3 RESULTS AND DISCUSSION

3.3.1 EVALS/PEDOT system from water phase

Generally, by using PSS as polyanion, the EDOT polymerization brings about a stable suspension of PEDOT particles (D=10-50 nm).[108] Other morphologies were observed according to the templating agent used. The EDOT polymerization in presence of EVALS32 brought about star-like PEDOT microparticles, whose dimension and stability in suspension depended on polymerization condition. In figure 3.1, the images obtained by optical and scanning electron microscopy are reported. In figure 3.2 it may be observed that the lower is the $SO_3^-Na^+$/EDOT molar ratio, the higher is the particle dimension and, hence, the lower the stability of the water suspension. For this reason, with slight exception for the suspensions obtained at higher $SO_3^-Na^+$/EDOT molar ratio, most of the samples resulted non adequate for conductivity measurements after direct deposition on substrate and drying in form of films, due to inhomogeneous structure of the resulting films, created by PEDOT aggregates. In fact, a qualitative measurement of conductivity of these EVALS32/PEDOT systems was possible only after drying of the suspensions and preparation of pellets.

Conductivity measurements on EVALS32/PEDOT systems in form of pellets show that the conduction decreases with increasing of the $SO_3^-Na^+$/EDOT molar ratio, hence, with increasing of the amount of EVALS32 respect to PEDOT in the synthesis formulation (Fig. 3.3).

EVALS32/PEDOT samples obtained at lower $SO_3^-Na^+$/EDOT molar ratio show high conductivity (up to 2×10^1 S cm^{-1}). Although the conductivity of the systems is high, on the contrary of the usual PEDOT/PSS complex, the EVALS32/PEDOT suspensions were not very stable, involving the rapid settlement of the conducting polymer aggregates. However, EVALS32/PEDOT obtained at $SO_3^-Na^+$/EDOT molar ratio= 20, even though it shows modest electrical properties, forms a quite stable suspension, characterized by fine particulate. Figure 3.1 C shows that after casting this suspension forms the finest network of aggregated particles. In this case, the low dimension of particles didn't allow elaboration of optical images.

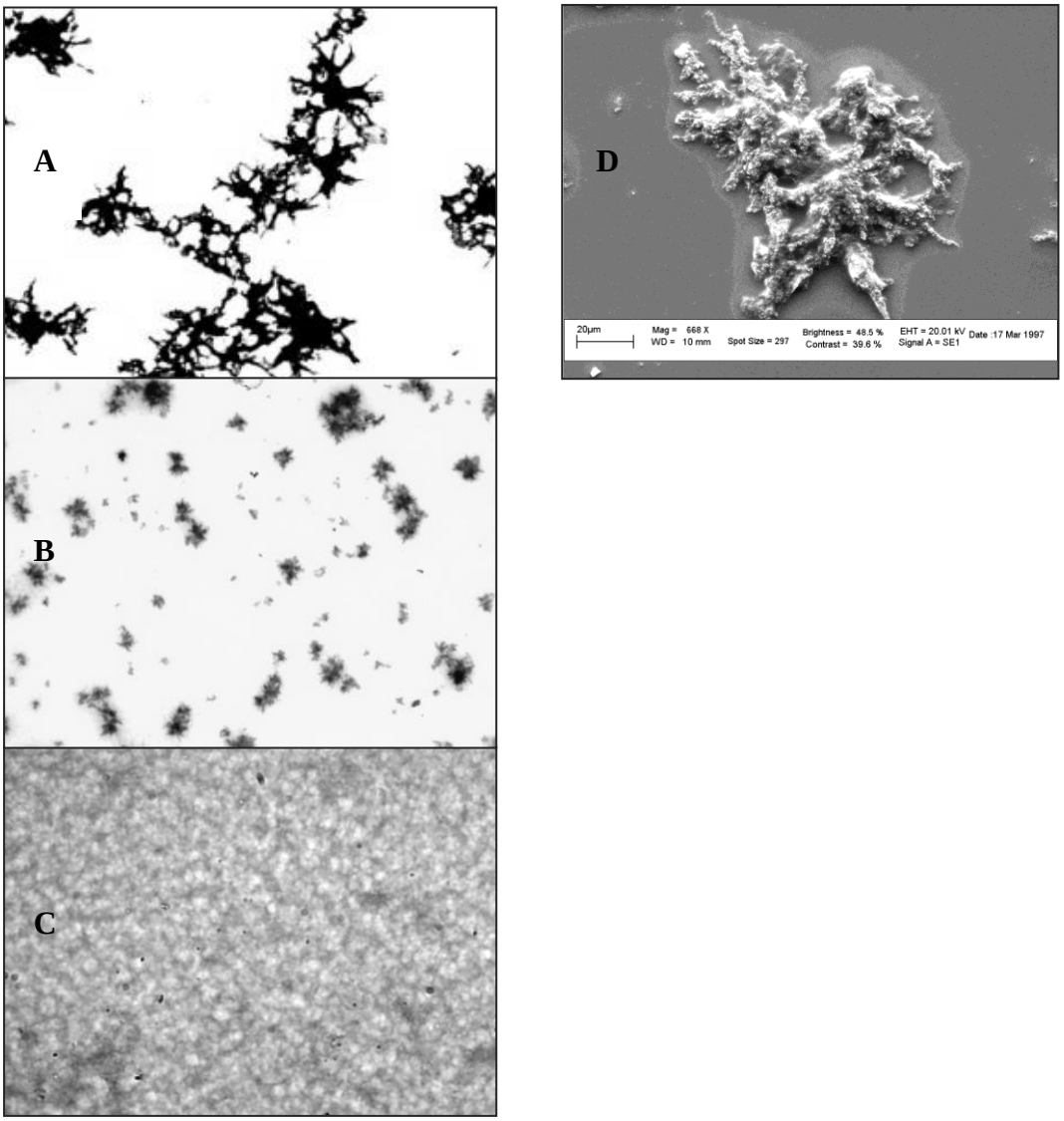

Fig. 3.1 Optical (left) and SEM (right) images of EVALS32/PEDOT suspended particles obtained from water phase. (A) $SO_3^-Na^+$ = 0.4, 100X magnification; (B) $SO_3^-Na^+$ = 0.8, 100X; (C) $SO_3^-Na^+$ = 20, 200X; (D) $SO_3^-Na^+$ = 0.4, 670X.

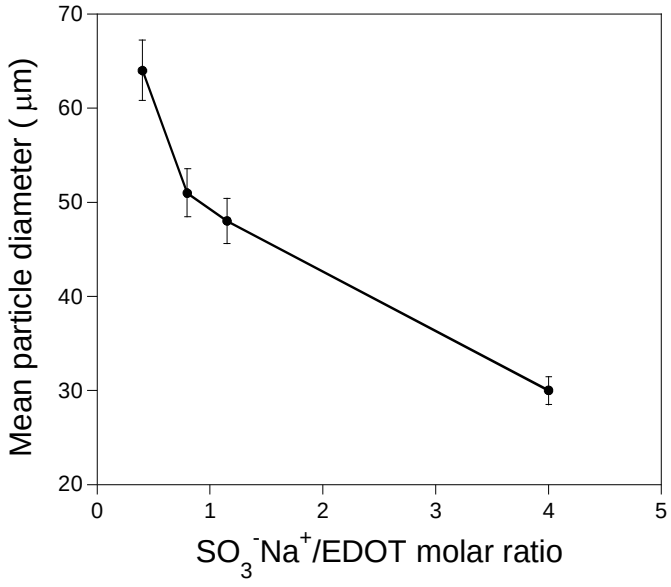

Fig. 3.2 Mean diameter of suspended EVALS32/PEDOT particles obtained in water phase as a function of $SO_3^-Na^+$/EDOT molar ratio. The values were obtained from elaboration of optical microscopy images and error bars represent the particles diameter distribution. The line is guide for eyes. The graph doesn't show the data of EVALS32/PEDOT sample at $SO_3^-Na^+$/EDOT molar ratio = 20.

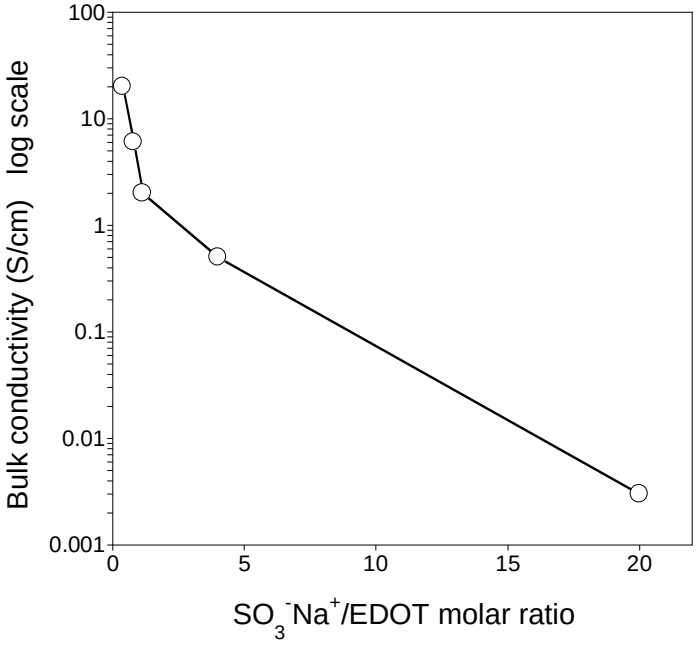

Fig. 3.3 Bulk conductivity (four points probe method) of EVALS32/PEDOT samples obtained in water phase as a function of $SO_3^-Na^+$/EDOT molar ratio. The line is guide for eyes.

4

EVALS AS SUBSTRATE FOR EDOT VAPOR PHASE POLYMERIZATION

4.1 INTRODUCTION

4.1.2 PEDOT synthesis by Vapor Phase Polymerization (VPP): advantages, related problems and strategies

Another advantageous chemical synthetic route that overcomes drawbacks associated with performance and processability of ICP, is that one known as vapor phase polymerization (VPP). This *in situ* polymerization method retains some advantages respect to other synthetic procedures, first of all the high conductivity values that can be reached. In fact, PEDOT/ PSS films exhibits a relatively low electrical conductivity (~10 S/cm)[109], which is not suitable for the high conductivity requirements in most applications, such as the low voltage ones. Moreover a PSS rich layer has been found at the top of the spin-coated PEDOT/PSS films. So the excessive amount of PSS is needed to stabilize the dispersion, but the resulting films may contain amounts of PSS that segregates from the complex and, since PSS is an electrical insulator, the excessive PSS could limit the final conductivity. In order to obtain highly conductive PEDOT films, *in situ* methods should be used. *In situ* electrochemical polymerization generally results in a poor transparency and needs to be carried out on conducting substrates. These factors limit the practical applications of this method. From this point of view, *in situ* solution oxidative chemical polymerization is more versatile in process design and applications, because it is less restricted by the substrate. Nevertheless, the mixtures used, containing both monomer and oxidant, have a limited pot-lifetime. In order to avoid and overcome this inconvenient, separate pots containing monomer and oxidant can be prepared and mixed just before use. In some cases, the use of retardants for prolonging the pot-lifetimes has been proposed.

Another way to achieve this is to apply the oxidant using a solvent coating process and, then, exposing the coated surface to a monomer vapor, that represents the VPP method itself.

VPP is better described as a chemical vapor deposition process that was first applied for ICP by Mohammadi et al.[110] using $FeCl_3$ and H_2O_2 as oxidants for polypyrrole (PPy) synthesis.

Conductive films characterized by nanometric thickness, morphological homogeneity (few nanometers roughness) and complex geometry may be obtained in controlled conditions. It was adapted for the formation surface patterns of PPy using patterned copper converted to $CuCl_2$ as oxidizing agent.[111] VPP method has also been used for *in situ* polymerization of PPy inside a number of different non-conducting polymeric matrixes and rubbers, such as PVC [112] and polyurethane foams.[113]

This method then was applied to the synthesis of PEDOT using $FeCl_3$ as oxidant, to give films at nano-level thickness and with conductivities around 70 S/cm.[114] Nevertheless the main problem connected to the use of $FeCl_3$ as the oxidizing agent is that it easily forms crystal-like structures as the solvent evaporates, retaining a grainy morphology that may act as seeding template to cause discontinuous and poor quality film formation. De Leeuw et al.[115] found that ferric *p*-toluenesulfonate (Fe(III) tosylate or $Fe(PTS)_3$) represents a well-suited oxidant for chemical polymerization of EDOT. Further work by Winther-Jensen e al.[116,117] has shown that Fe(III) tosylate produces smooth homogeneous films, but an undesirable polymerization mechanism may also occur, resulting in partially conjugated polymer chains. This undesirable evidence has been attributed as consequence of an acid-driven polymerization route to produce greenish films (low conjugation length) with poor conductivity. In order to solve such a problem, a method for controlling acidity of the system was widely described. It is better known as base-inhibited vapor-phase polymerization method[118,119], where a surface covered with Fe(III) tosylate mixed with a volatile base is exposed to EDOT vapors. The weak base (pyridine or imidazole[120]) is added to raise the pH of the Fe(III) tosylate solution and suppress the unwanted acid-initiated polymerization. During base evaporation the pH of the oxidant is lowered entering a window where conditions are favorable for high-conductive PEDOT formation (10^3 S/cm). Other additives, such us humidity, poly(ethylene glycol)-*ran*-(poly(propylene glycol) or diethylene glycol, glycerol and sorbitol, have been used to reduce acidic side reactions during the vapor phase polymerization process, suppress the oxidant crystal growth or as secondary dopants, respectively.[121- 123] In these works generally a solution containing oxidant and the specific additives in high viscosity solvents (butanol) is spin-coated on ITO or glass and plastic supports, and exposed to EDOT vapors. In other cases the oxidant is sublimated in a heated crucible and sent to the support together with the monomer vapors.[124]

However, in the VPP process oxidant crystallization remains the main problem to be limited in order to improve PEDOT films quality and homogeneity.

As an advantageous *in situ* chemical synthetic method, vapor phase polymerization has been used for PEDOT synthesis onto several substrates and into several polymeric matrices. Highly conductive PEDOT coatings with nanometric thickness have been recently obtained by VPP on polymeric substrates for flexible optoelectronic applications (enhanced transparent electrodes for ITO "free" devices), such as PET[125], surface modified PET with ethylene diamine to improve interactions with the conductive layer[126] or polyethylene naphthalate (PEN).[127]

Traditionally, VPP has been used for growing smooth textured films with high light transmittance (up to 95 %). More recently, VPP has been used in biomedical field to incorporate tosylate doped PEDOT into gelatin polymer matrix in order to prepare composites as biocompatible substrates for use in tissue engineering, mediating brain endothelial cell adhesion.[128] In general, it has been also used to produce nano-structured PEDOT films comprised of nanofibers, nano-bowls and nano-snowflakes.

4.2 MATERIALS AND METHODS

4.2.1 General methods and instruments

- Spin-coating depositions were performed with a spin-coater PWM32, operating by proper parameters selection.
- Optical microscopy (OM) images were acquired on a Nikon Opti Hut2-pol Polarized Optical Microscope (POM) at 40x-200x magnification and recorded with a Moticam 2500 5.0 Mpixel camera.
- Trasmission Fourier Transform Infrared Spectrophotometry (Trasmission FT-IR) analysis was performed by using a Nicolet 6700 FT-IR Spectrophotometer (Thermo Scientific) operating within the 4000-400 cm^{-1} spectral range and with a resolution of 2 cm^{-1}. Each spectrum was acquired by co-adding 100 intereferograms and baseline corrected.
- Visible-Near Infrared Spectroscopy (Vis-NIR) analysis was performed by using a Hitachi U-2000 double-ray spectrophotometer operating in the 350-1100 nm range and with a resolution of 2 nm.
- Scanning Electron Microscopy (SEM) images were acquired by a SEM, LEO 1450 VP, characterized by a resolution of 3.5 nm and maximum magnification of 300000x.

- High Resolution Field Emission Scanning Electron Microscopy (HR FE-SEM) images were acquired through an Auriga Zeiss apparatus at CNIS Laboratories, Sapienza.
- Electrical surface conductivity measurements were performed by using a four points probe (Jandel Engineering) equipped with 1 mm spaced four tungsten carbide spring-loaded needles. The ratio between the measured inner probe voltage (*V*) and the source DC current passing through the outer probes (*I*) was directly given by a digital multi-meter Keithley 2700 (4-wire resistance mode). The applied current was in the range 10^{-2} - 1 mA. At least three different measurements of *V*/*I* for each test were carried out and then the mean value was used to calculate the surface electrical properties.

4.2.2 Chemicals

All solvents used were acquired from Carlo Erba. All other chemicals were acquired from Aldrich, except for EVALS32 synthesized according to the procedure described in chapter 2.

4.2.3 Vapor Phase Polymerization of EDOT on EVALS

Preparation of EVALS/PTS supports

EVALS32 was used as supporting matrix for EDOT vapor phase polymerization by using iron(III) *p*-toluenesulfonate hexahydrate ($Fe(PTS)_3 \cdot 6\ H_2O$ or simply PTS) as oxidizing agent. In order to prepare EVALS32/PTS supports, PTS was added to the EVALS32 matrix by following two procedures of deposition by spin-coating:

I. Double step method.
II. Single step method.

For both methods, solutions of EVALS32 and PTS were prepared and each solution was filtered with a 0.45 µm syringe filter before the use. Spin-coating deposition of EVALS32 and PTS solutions to give EVALS32/PEDOT supports, was carried out on carefully cleaned glass slides.

As far as the *I*) method is concerned, about 1 µm thick EVALS32 film was spin-coated at 3000 rpm on 150 µm thick glass slides by dropping for 30 s 500 µl of EVALS32 water solution (6 % wt/V). The film was left to dry for further 210 s. Then, 200 µl of PTS methanol

solution (40 % wt/V) containing pyridine as acidity inhibitor (PTS/pyridine molar ratio =2) was spin-coated on the previously deposited EVALS32 films by using the same conditions. Then the sample was vacuum dried at room temperature for 1h and stored in desiccator.

As far as *II*) procedure, reported in figure 4.1, the two previous EVALS32 and PTS solutions were mixed in 2.5:1 volume ratio, respectively. In this way a MeOH/water solution with a final PTS content of 11.4 % wt/V was obtained. Similarly, solutions with higher PTS final concentration, up to 31.4 % wt/V, were obtained by mixing in the same volume ratio the previous EVALS32 water solution with MeOH solutions of PTS at increasing concentration and containing pyridine at the same PTS/pyridine molar ratio (PTS/pyridine molar ratio =2). EVALS32/PTS supports were obtained by depositing all the solutions on glass slides through direct spin-coating (V=500 µl) at 3000 rpm for 4 min (t=120 s for dropping and t=120 s for drying). At the end, the EVALS32/PTS-coated glass slides were kept in desiccator.

EDOT Vapor Phase Polymerization

Vapor phase polymerization was carried out in a chamber at controlled conditions (T=60 °C, N_2 flux=30 ml/min, t=0-20 h) on EVALS32/PTS supports by bubbling nitrogen inside a vial with liquid EDOT, as represented in figure 4.2. In order to limit water absorption onto the hygroscopic EVALS32 and PTS, the supports were then quickly transferred from desiccator to the reaction chamber.

Glass slides were substituted with a 1 mm thick silicon wafers for FT-IR analysis using the same deposition conditions.

At the end of the VPP, each sample was rinsed by methanol up to 2 h to remove spent oxidant, unreacted monomer and polymerization by-products (EDOT, Fe(III) and Fe(II) salts and pyridine) and vacuum dried. After the deposition, the samples were transferred and stored in a desiccator.

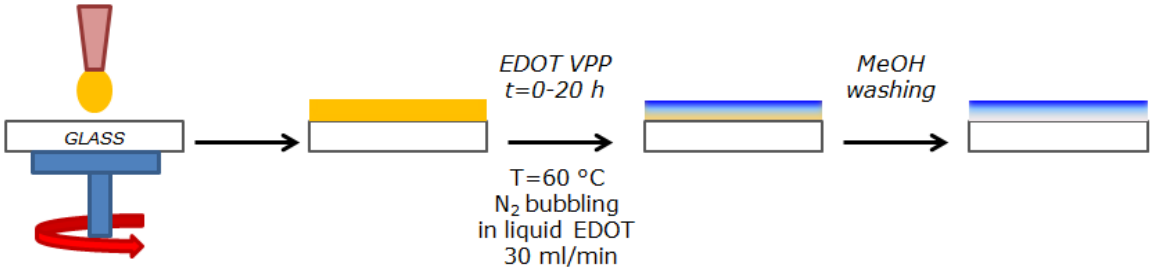

Fig 4.1 Single step deposition of the substrate (EVALS32+ $Fe(PTS)_3$/pyridine water/MeOH solution) and VPP process scheme.

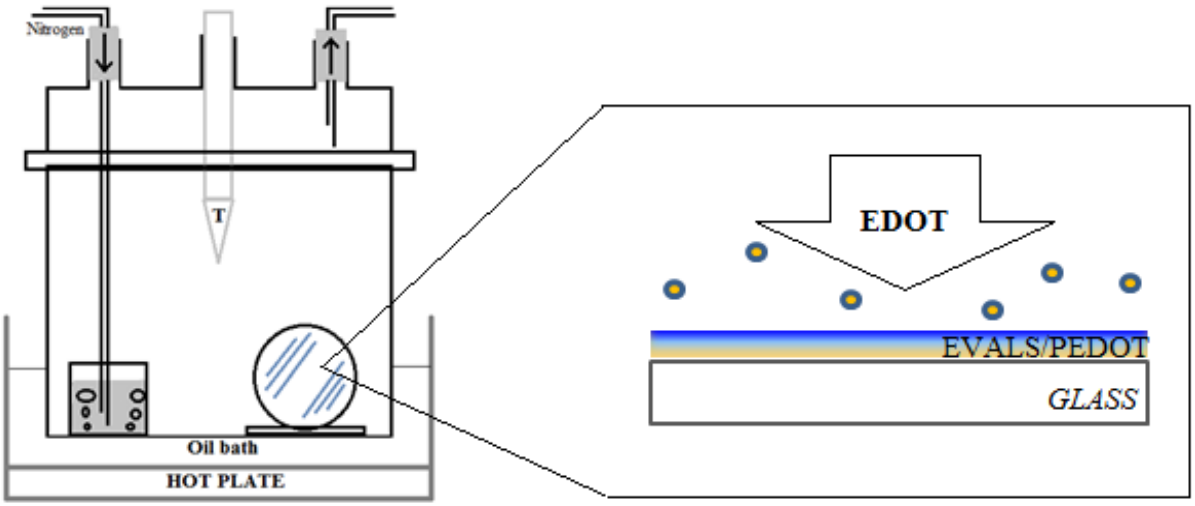

Fig. 4.2 Scheme of the chamber used for EDOT vapor phase polymerization on EVALS32.

4.2.4 Methods for vapor phase EVALS/PEDOT system characterization

EDOT vapor phase polymerization on EVALS32 was employed in order to obtain homogeneous EVALS32/PEDOT thin films, after comparing the two deposition procedures as described previously, by double and single step respectively.

The possible PTS crystallization onto the support and the film microstructure were analyzed by polarized optical microscopy (POM).

The single step deposition method for EVALS32/PTS supports preparation resulted as the best way to conveniently prepare homogeneous EVALS32/PEDOT conducting films by VPP. Thus, all following characterization was achieved on samples prepared by this method.

VPP kinetics measurements of EVALS32/PEDOT samples were obtained by transmission Vis-NIR and FT-IR spectrophotometry by carrying out *ex situ* measurements, that are after extraction of the samples from the reaction VPP chamber at predetermined intervals of time.

In particular, Vis-NIR spectra were collected after different polymerization time on samples spin-coated on glass slides. Almost three samples per VPP time period were analyzed. Before the analysis, all the samples were rinsed with methanol for few minutes and then vacuum dried. A clean glass slide was used as reference.

In case of FT-IR analysis, spectra were acquired after different polymerization times on samples spin-coated on silicon wafers instead of glass slides.

For both Vis-NIR and FT-IR analyses, EVALS/PEDOT supports were placed in the spectrophotometer sample holder perpendicularly to the light beam.

The surface morphology and the thickness (*d*) of EVALS32/PEDOT films were observed by field emission scanning electron microscopy (FE-SEM). For FE-SEM analysis, EVALS32/PEDOT-coated glass slides were fractured in liquid nitrogen and fracture surface of samples was observed.

The variation of the electrical resistance (*V*/*I*) during the EDOT VPP process was measured *ex situ* by the four-point probe method. The measurements were performed putting the probe needles in contact with the outermost film surface previously exposed to the EDOT vapor and methanol rinsed. The conductivity, σ, of each sample (almost three per VPP time period) was obtained according to the equation (Valdes)[129,130] for thin and finite films by:

$$\sigma = \frac{\ln(2) I}{\pi V d} \qquad (1)$$

where where *d* is the thickness of the sample.

Three different measurements of *V*/*I* for each sample were obtained and then the mean value was used to calculate the conductivity by equation 1.

Additional analysis about the kinetics of the VPP process was carried out by *ex situ* measurements of electrical properties on samples prepared with increasing amount of oxidant in the EVALS32 matrix. Different MeOH/water solutions containing invariant amount of EVALS but at increasing concentrations of oxidant ([PTS]=11.4-31.4 % wt/V) were spin-coated on glass slides by the single step deposition method at the same conditions. The variation of the electrical properties of the samples was followed during VPP time, as previously done.

4.3 RESULTS AND DISCUSSION

4.3.1 EVALS/PEDOT system from VPP

In order to find the best procedure for the support preparation, two different conditions for the addition of oxidizing initiator were investigated: double and single step respectively.
If the PTS solution is directly spin-coated on already deposited EVALS32 (double step deposition method), initiator crystallization occurred, as evidenced by birefringent large crystals formation (light regions) in polarized optical microscopy image of figure 4.3 A. The EDOT VPP carried out on such support brings about to a highly inhomogeneous PEDOT film formation. In fact, once the PTS salt was removed by rinsing the sample, polymer appeared localized predominantly on the underlying PTS crystals regions, as displayed by the dark regions correspondent to PEDOT aggregates in optical microscopy image of figure 4.3 B. Moreover, at the end of the VPP, the EVALS32/PTS support obtained by a double step deposition method, resulted mostly soluble and PEDOT aggregates crumbled in water.

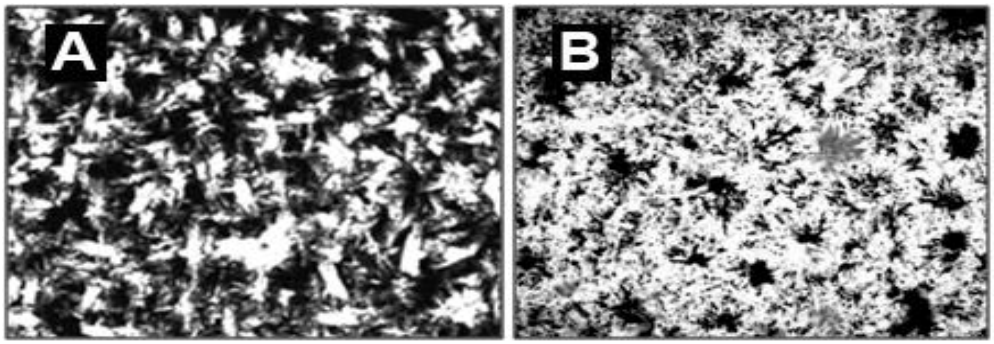

Fig. 4.3 (A) Optical image (crisscross nicols, 400X magnification) of an EVALS32 support as obtained by double step deposition; (B) optical image of the same sample after 2 hours VPP and methanol rinse.

On the other hand, an alternative coating procedure was adopted, that is the method designated as single step deposition. In this case, when EVALS32 and PTS were contemporaneously spin-coated on glass slide, no macroscopic PTS salt crystals were observed by optical microscopy (magnification 400X) both before and after EDOT polymerization. This indicates a homogeneous dispersion of PTS initiator into EVALS32 polymer matrix, which hindered the initiator crystallization without the use of specific additives. At higher PTS concentrations, initiator crystallization occurred. Small and

dispersed micrometric crystallites segregated on the film surface, making the sample opaque (Fig. 4.4).

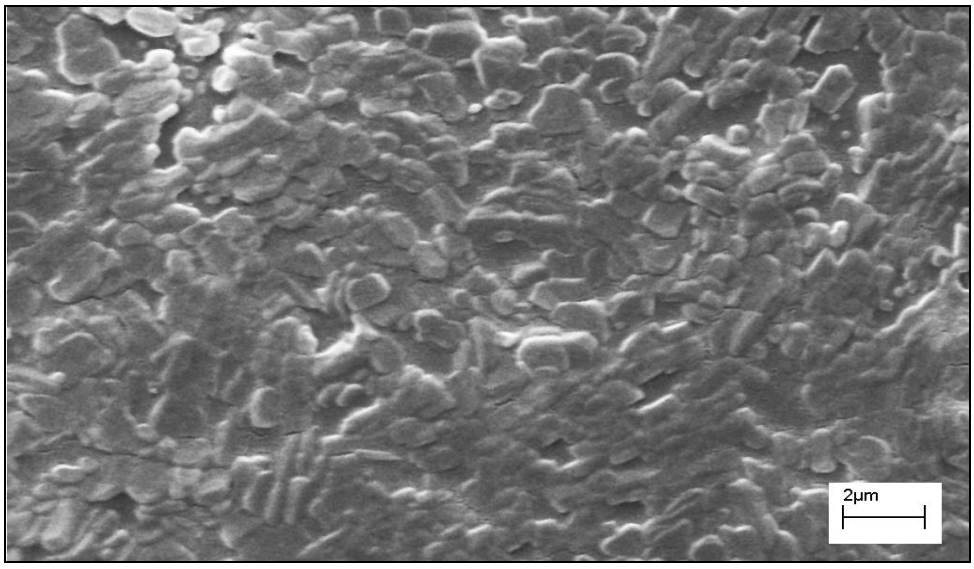

Fig. 4.4 SEM image of EVALS32 surface film, spin-coated with PTS (31.4 % wt/V).

Therefore, an EVALS32/oxidant solution with concentration of oxidant [PTS]=11.4 % wt/V was selected and employed for the further deeper characterization.

The qualitative evidence of EDOT polymerization on EVALS32/PTS-coated glass slides was given by UV-Vis-NIR spectroscopy. This technique also permitted to evaluate the nearly complete PTS elimination by sample rinsing in methanol as well as to study the kinetics of EDOT polymerization.

In figure 4.5 A, the UV-Vis spectra in the 320-800 nm wavelength range of EVALS32/PTS-coated glass slides before polymerization and EVALS32/PEDOT after 4 h polymerization (t_{VPP} = 4 h) rinsed with methanol for either 10 min or 2 h are reported. In particular, a significant intensity reduction of the bands at about 360 nm and 320 nm, related to the PTS tosylate group, was observed already after 10 min sample rinsing in methanol. A nearly complete removal of the initiator was obtained at 2 h rinsing.

The kinetics of EDOT VPP onto the EVALS32 support was followed by *ex situ* Vis-NIR and Trasmission FT-IR spectrophotometry. At predetermined time intervals the samples were removed from the reaction chamber and analyzed.

In figure 4.5 B the Vis-NIR spectrum evolution of methanol rinsed EVALS32/PEDOT films layered on glass slides recorded at increasing VPP times is reported.

The broad absorption from about 500 nm to 1100nm, called "free carrier tail" and related to high conjugation length of doped PEDOT, increased with the VPP time without large shape changes, indicating the formation of the doped conducting polymer just in the early polymerization stage and its progressive concentration increase[131]. The small absorption rise at the higher wavelength (800 - 1100 nm) observed in the spectra recorded at t_{VPP} =0.5 h and t_{VPP}=1 h could be due to a higher conjugation of PEDOT formed in the early polymerization stage.

A qualitative indication of the increase in PEDOT concentration with t_{VPP} was obtained by plotting the absorption intensity at 705 nm versus the polymerization time (Fig. 4.5 C). In fact, according to the Lanbert-Beer law and approximating that the PEDOT absorption coefficient did not change at the different polymerization times, the recorded absorbance can be considered proportional to the conducting polymer amount formed during VPP. The absorbance at 705 nm, corresponding to the isosbestic point of the doped and undoped PEDOT, was chosen because it should be linearly related to the concentration of the conducting polymer, being less affected by the doping level.[132]

PEDOT conversion degree, $X_{705\,nm}$, proportional to the polymer concentration, was evaluated from Vis-NIR analysis and defined as

$$X_{705\,nm} = \frac{Abs(t) - Abs(0)}{Abs(20\,h) - Abs(0)} \quad (2)$$

where *Abs(t)*, *Abs(0)* and *Abs(20 h)* are the absorbance values measured at 705 nm at the generic VPP time *t*, at the beginning and at the end of the polymerization, respectively.

In literature, PEDOT VPP is described as a fast process that takes place in few minutes. In our system, where the PTS oxidant initiator is dispersed into an insulating polyanion matrix, the kinetics of polymerization resulted to be slower, presumably because of the monomer diffusion into the supporting insulating polyanion and of the polymerization taking place in EVALS32.[131,110] This hypothesis could explain the linear trend of the initial 705-nm absorbance variation as a function of the square root of the t_{VPP} (inset of Figure 4.5 C) expected for a diffusion controlled reaction according to Fick second law for medium conversions. Moreover, the EVALS32/PEDOT films obtained for t_{VPP} ≥0.5 h resulted insoluble in water because of the formation into the sample bulk of multiple electrostatic associations between the polyanion and the PEDOT chains, as described also by DeLongchamp and colleagues.[133] This indicates that the EVALS32 sulfonic groups acted as PEDOT doping agents.

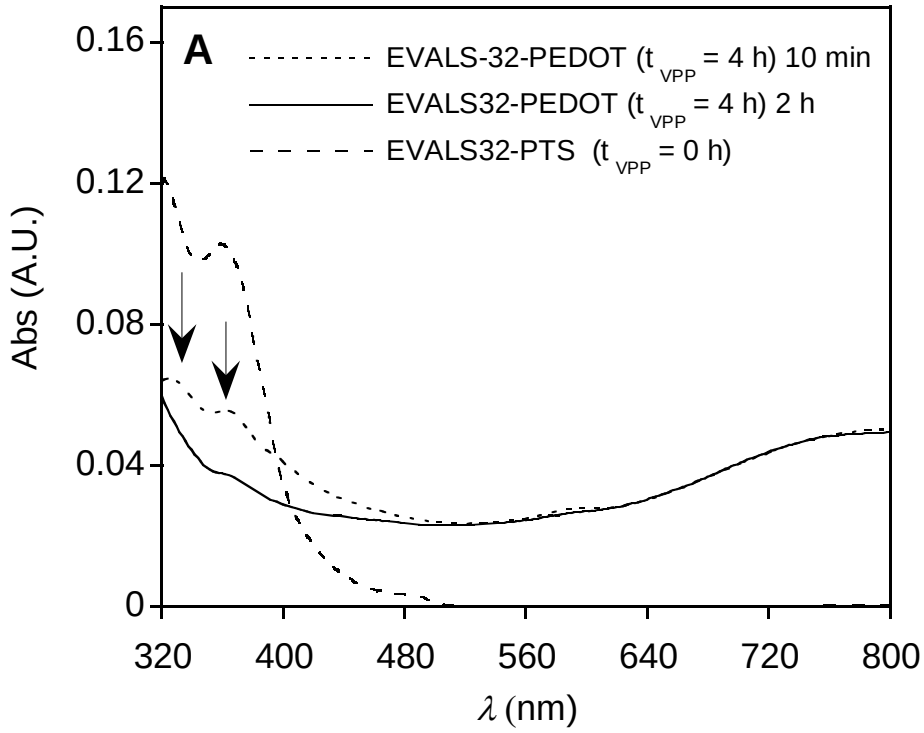
A
EVALS-32-PEDOT (t VPP = 4 h) 10 min
EVALS32-PEDOT (t VPP = 4 h) 2 h
EVALS32-PTS (t VPP = 0 h)
Abs (A.U.)
0.16
0.12
0.08
0.04
0
320
400
480
560
640
720
800
λ (nm)

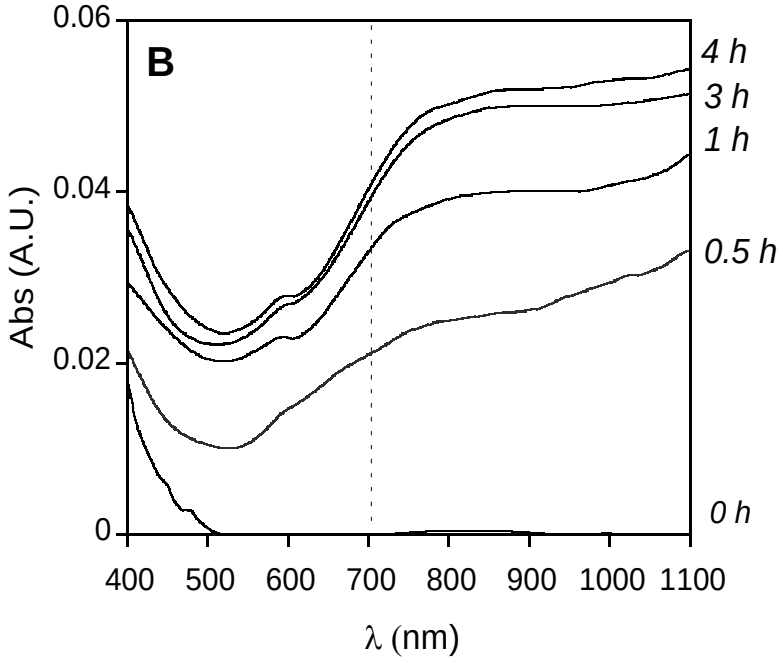
B
4 h
3 h
1 h
0.5 h
0 h
Abs (A.U.)
0.06
0.04
0.02
0
400
500
600
700
800
900
1000
1100
λ (nm)

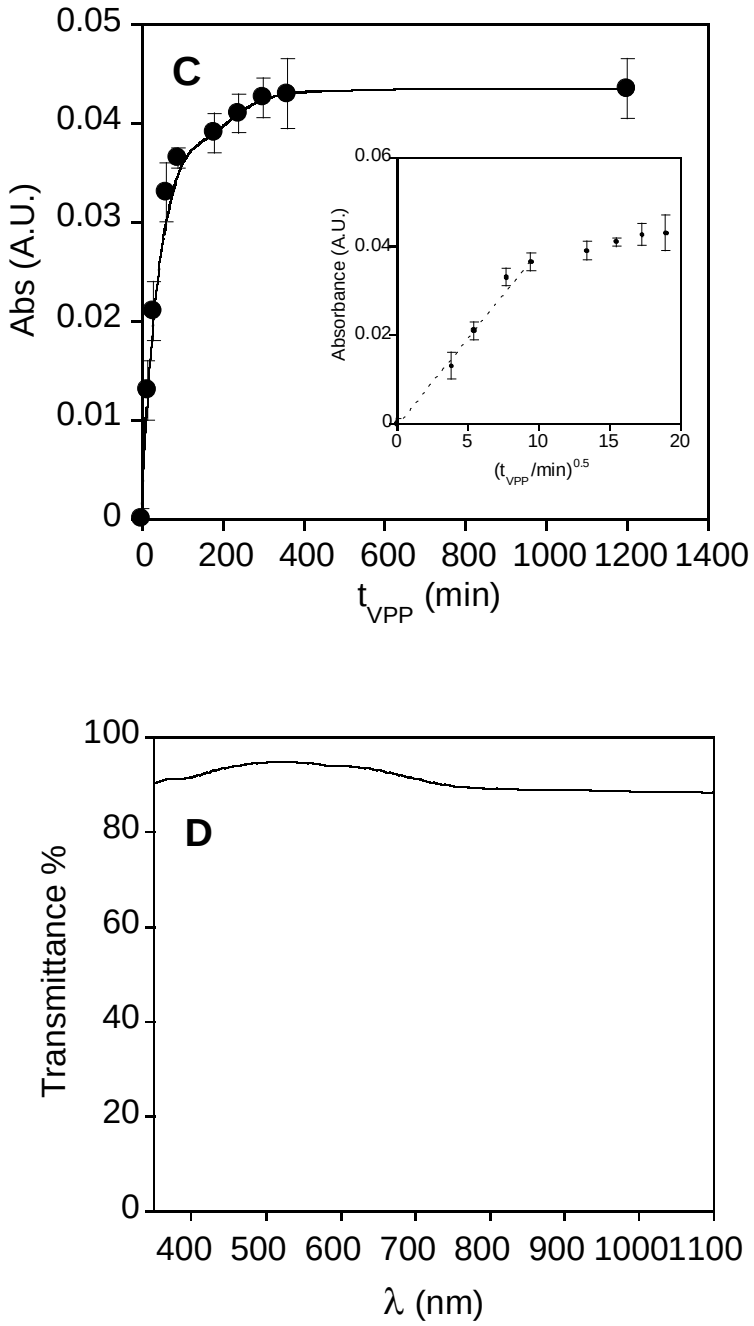

Fig. 4.5 (A) *Ex situ* UV-Vis spectra (320< λ<800 nm) of EVALS32/PTS-coated glass slides before polymerization (t_{VPP} = 4 h) and EVALS32/PEDOT samples (t_{VPP} = 4 h) dwelled in methanol for 10 min and 2 h. The arrows indicate the PTS absorption bands; (B) *Ex situ* Vis-NIR absorption spectra of methanol rinsed EVALS32/PEDOT films on glass slide recorded at increasing VPP times; (C) Absorbance at 705 nm as a function of VPP times. In the inset, the absorbance variation is reported as a function of the square root of VPP time; (D) Sample optical transmittance measured in the 300-1100 nm range (t_{VPP} =20 h).

As can be observed in figure 4.5 C, the 705-nm absorbance increased up to t_{VPP}=6 h and remained constant for higher polymerization time up to t_{VPP} =20 h.

The film obtained after a VPP of 20 h was transparent and the optical transmittance resulted to be above 90 % in 300-1100 nm range (Fig. 4.5 D).

In order to have further confirmation of UV-Vis kinetic results, *ex situ* kinetic analysis of EDOT VPP on EVALS32/PTS matrix was carried out on identical samples at the same conditions by transmission FT-IR spectrophotometry using silicon support instead of glass slide for the matrix deposition.

Because of the high reproducibility of the spin-coating process, the intensity ratio of the EVALS32 support and silicon substrate spectra was constant. In figure 4.6 the spectra evolution as a function of VPP time is reported up to 4 h. Further polymerization time does not leads to any substantial spectrum change. All the spectra are quite complex, being the superimposition of the absorption bands of the silicon substrate, EVALS32/PTS support and PEDOT. Although most of the EVALS32 and PEDOT peaks overlap, the absorption at 1306 and 974 cm^{-1} may be assigned exclusively to PEDOT. In particular, they were attributed to PEDOT *p*-doping induced bands.[134,135] A linear agreement between transmission FT-IR and Vis-NIR spectroscopy kinetic data was expected, as showed in figure 4.6 B.

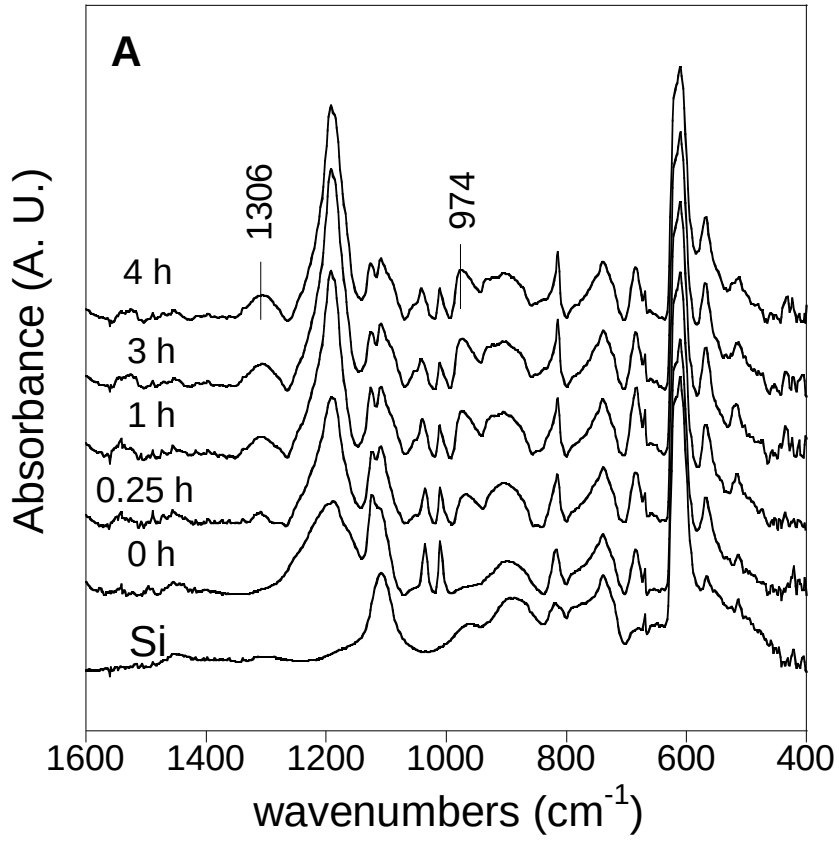

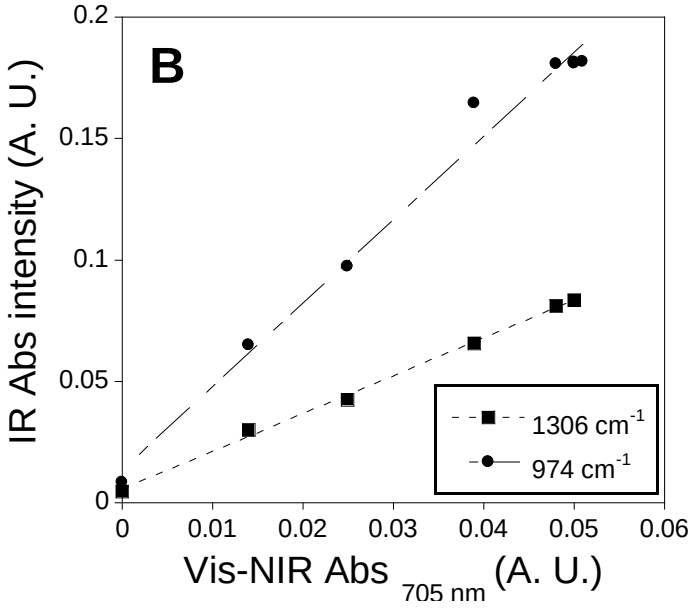

Fig. 4.6 (A) *Ex situ* FT-IR absorption spectra (1600< wavenumebers<400 cm^{-1}) of EVALS32/PEDOT films on silicon slide recorded at increasing VPP times. The arrows indicate absorption bands assigned to PEDOT; (B) Linear agreement between infrared and Vis-NIR kinetic data.

The thickness (*d*) of methanol rinsed EVALS32/PEDOT films was measured by FE-SEM, after fracturing the coated glass slides and observing the fracture surface of the sample. In figure 4.7, SEM images of the fracture surface of the EVALS32/PEDOT film obtained after 6 h of polymerization are reported.

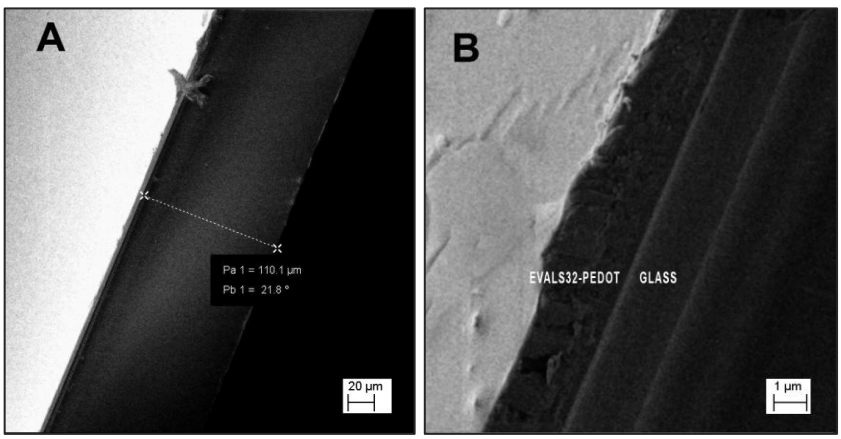

Fig. 4.7 FE-SEM images of fracture surface of a EVALS32/PEDOT film supported on glass slide (t_{VPP}=6 h) at 600X (A) and 25000X (B) magnifications.

The real glass slide thickness (150 µm) was used for the tilt angle correction. The variation of the sample thickness as a function of t_{VPP} was very small and within the variability of the measurement carried on the different samples. Then, the average thickness 3.5 ± 0.2 µm found was used in following conductivity measurements.

The electrical resistance (*V*/*I*) of the EVALS32/PEDOT films was measured *ex situ* at increasing VPP times by using a four points probe. The film conductivity (σ), calculated by equation 1 , is reported as a function of t_{VPP} in figure 4.8 .

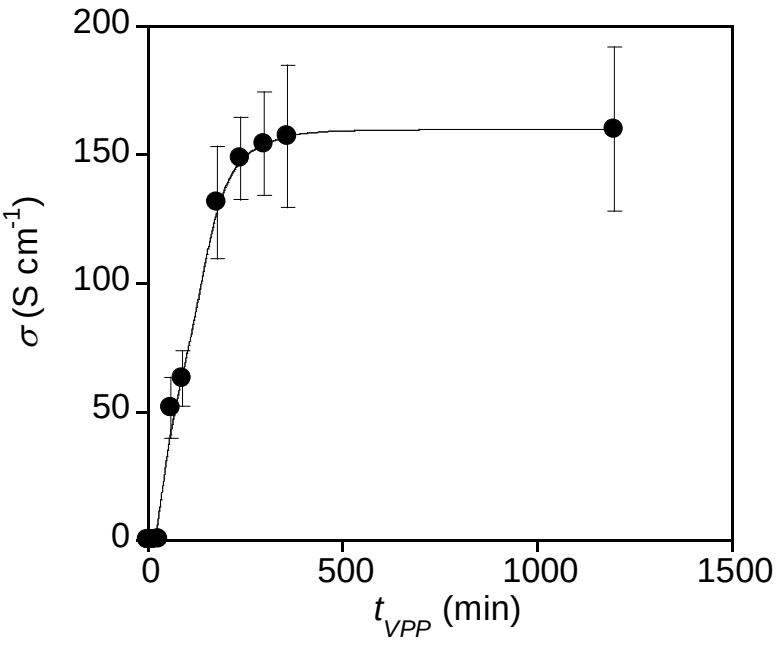

Fig. 4.8 Conductivity (σ) variation of EVALS32/PEDOT films during the VPP time; the line is guide for the eyes.

The graph shows that during an initial period of time the conductivity was very low and close to the value of that of the matrix (σ=3x10^{-3} S cm^{-1}). After this induction time, it dramatically increased becoming stable after 6 h of the VPP process. After a 20 h VPP time a conductivity σ = (1.6±0.3)x10^{2} S cm^{-1} was reached. The obtained σ =1.6x10^{2} S cm^{-1} value is quite high if

compared with other PEDOT films grown from VPP having similar transmittance to visible light.[136]

In order to correlate the sample electrical behavior with the PEDOT amount grown into the EVALS32 insulating matrix during the VPP process, the sample surface conductivity (σ_s), expressed as $\sigma \cdot d$ [137], was related to PEDOT conversion degree ($X_{705\ nm}$) derived by UV-Vis kinetic analysis and previously defined in equation 2, that is proportional to the polymer concentration.

σ_s values measured at increasing VPP times were reported as a function of the conversion degree $X_{705\ nm}$ as displayed in figure 4.9. Figure 4.9 shows that the surface conductivity of EVALS32/PEDOT films was not linearly related to the PEDOT concentration.

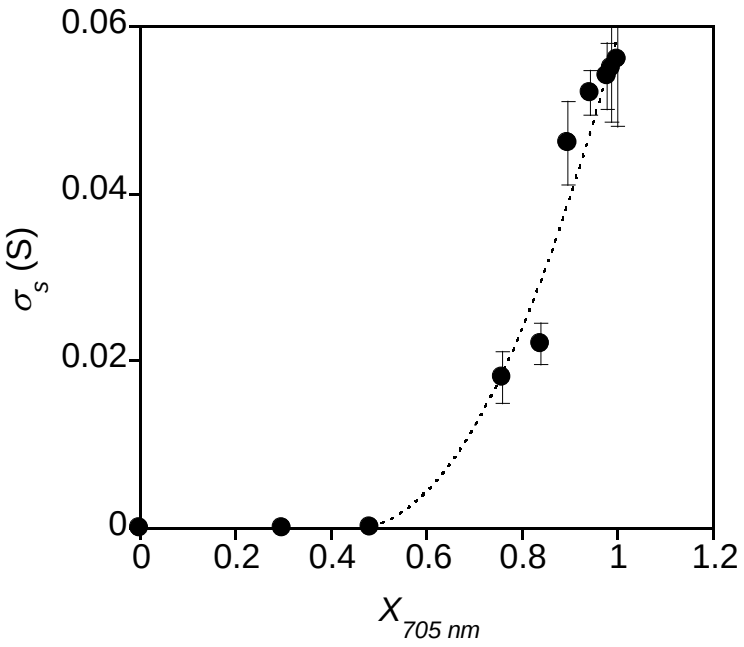

Fig. 4.9 Surface conductivity (σ_s) of EVALS32/PEDOT films as a function of VPP conversion degree, $X_{705\ nm}$, as evaluated by Vis-NIR analysis. The line is the best fit curve according to the general percolation model of Equation 4 at a percolation threshold X_c=0.45.

Particularly, at low polymerization times (0< t_{VPP} <30 min, $X_{705\ nm}$ values up to 0.45), for which the PEDOT formation is fast (Fig. 4.5 C), the σ_s increase was very low. Probably, the PEDOT grown in the early polymerization stage, although characterized by a high conjugation, did not form a continuous conductive path, being dispersed into the insulting EVALS32 matrix. The sample surface conductivity, then, increased rapidly from t_{VPP} > 30

min. This type of dependence could be explained in term of a percolation mechanism of conduction.[138]

For this mechanism, the general equation that correlates the conductivity $\sigma(p)$ to the volume fraction p of a conducting filler in an insulating matrix is:

$$\sigma(p) \propto (p - p_c)^n \quad (3)$$

where p_c is the volume fraction of the conducting filler at the percolation threshold, that is when a continuous conductive path is formed, and n the critical exponent.[139]

If the variation of the sample volume during the polymerization is neglected, the conversion degree X_{705} can reasonably replaces the parameter p in equation 3 to give the following equation:

$$\sigma(X) \propto (X_{705nm} - X_c)^n \quad (4)$$

where X_c is the critical conversion degree, proportional to the PEDOT concentration, at the percolation threshold.

In order to find the best values of the parameter X_c and n, the conductivity results as a function of X_{705} were interpolated by a least square fitting procedure. In equation 5 different trial values of X_c in the range 0.2-0.7 were inserted and for each $\sigma(X_{705\ nm})>\sigma(X_c)$ set of data and the relative errors on n ($\Delta n/n$) were calculated.

The minimum value of $\Delta n/n$ was reached at X_c=0.45±0.05 (VPP time ~ 30 min) for which a n =2.0 ± 0.3 was obtained. The best fit curve was plotted in figure 4.9 as dashed line starting beyond the percolation threshold. The obtained critical exponent n is equal to the theoretical figure expected from three-dimensional percolation conduction model.[139,140] This suggests a homogeneous PEDOT dispersion into the EVALS matrix and the absence of aggregated structures, which, otherwise, would have caused a weaker conductivity dependence on PEDOT concentration than that expected for the ideal (three-dimensional) case. [140]

At the end of the VPP, the conducting EVALS32/PEDOT films obtained by the presented method resulted to be insoluble in ethanol, methanol and water, firmly adherent to the glass support and their conductivity stable up to almost six months after the preparation as well as its transparency (Fig. 4.10 A). The EVALS32/PEDOT conductivity did not significantly changes even when samples were kept in water for 24 h.

The SEM image of the surface of a methanol rinsed EVALS32/PEDOT film obtained after 20 h of VPP showed a smooth or nano-rough morphology and the presence of few nanometric

drops, probably due to isolated PEDOT clusters segregated upon the surface matrix (Fig. 4.10 B).

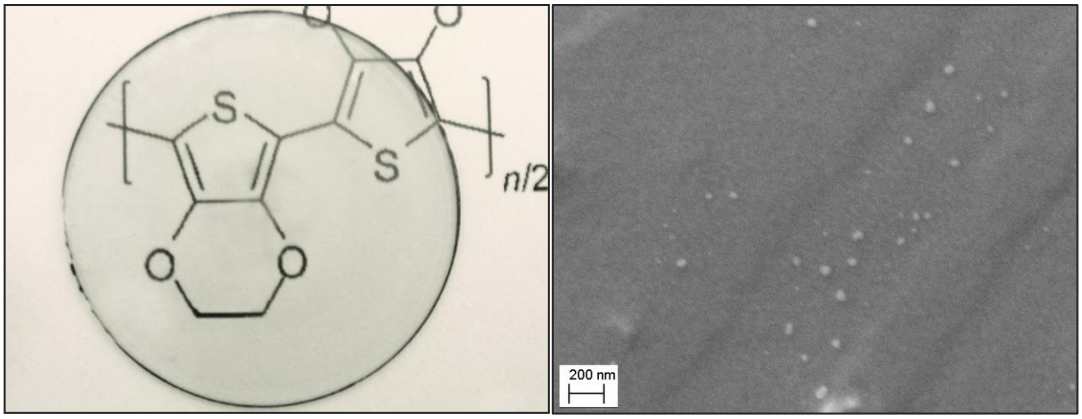

Fig. 4.10 (A) Digital photograph of the EVALS32/PEDOT film supported on glass; **(**B) SEM image of the EVALS32/PEDOT film surface at the end of the VPP (t = 20 h).

In respect of the final electrical properties reached by the material at the end of EDOT VPP, further tests were performed in order to obtain samples with enhanced electrical conductivity. Analogue EVALS32/PTS supports characterized by an increased initial amount of oxidant in the EVALS32 matrix were prepared and analyzed for EDOT VPP. For all EVALS32/PTS solutions ([PTS] = 11.4 - 31.4 % wt/V), both spin-coating procedure and EDOT VPP process on the resulting EVALS32/PTS supports were performed in the previously adopted conditions. The electrical resistance of each EVALS32/PTS support was measured as a function of t_{VPP}. Figure 4.11 shows the comparison of surface conductivity variation σ_s as a function of EDOT VPP time for the EVALS32/PTS supports obtained from EVALS32/PTS solution at 11.4 and 20 % wt/V PTS concentration, respectively. The obtained graphs are labeled by the initial oxidant concentration of the solution used for support deposition by the single step method.

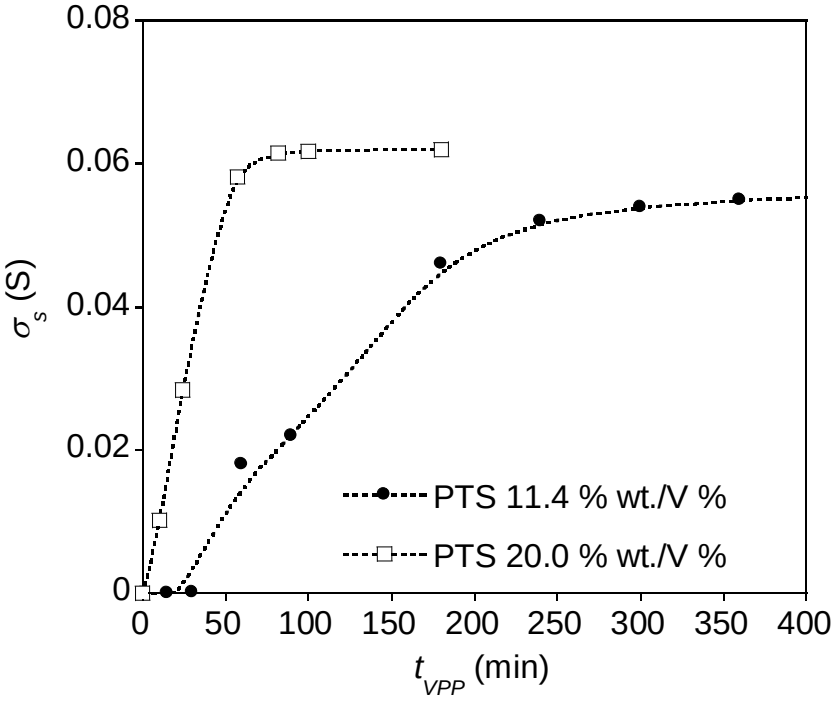

Fig. 4.11 EVALS32/PEDOT surface conductivity (σ_s) as a function of VPP time for two different EVALS32/PTS supports obtained from EVALS32/PTS solutions at PTS concentration of 11.4 and 20.0 % wt/V, respectively.

In particular, the graphs show that the higher the oxidant amount in the EVALS32 matrix, the faster is the kinetic and the higher the conductivity reached at the end of VPP process ($\sigma_{s\ max}$ varying from 5.5×10^{-2} to 6.2×10^{-2} S). However, it must be specified that such an increase of oxidant amount appeared limited within a certain value laying in the range of [PTS] = 20 - 25 % wt/V, beyond which no further variation of final conduction properties was observed in the resulting system .

In addition, the supports obtained at higher oxidant contents ([PTS] $\geq$ 20 % wt/V) resulted affected by visible oxidant crystals formation after deposition with reduction of optical transmission properties after EDOT VPP, due to visible PEDOT aggregates formation on oxidant-rich regions (Fig. 4.12).

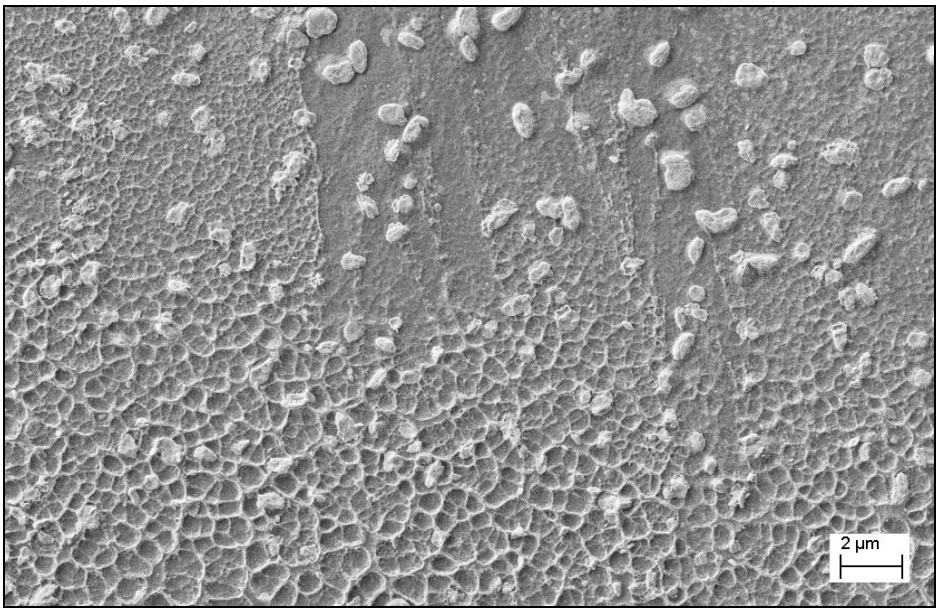

Fig. 4.12 SEM image of the EVALS32/PEDOT (PTS 20.0 % wt/V) sample surface.

This could be due to the fact that a homogeneous dispersion of the oxidant in the EVALS32 matrix is possible until reaching a certain value of oxidant amount, beyond which oxidant segregation phenomena can occur. At PTS ≥ 25.7 % wt/V, the high surface segregation of the polymerization initiator favored the formation of a continuous PEDOT layer of about 300 nm thickness (Fig.4.13).

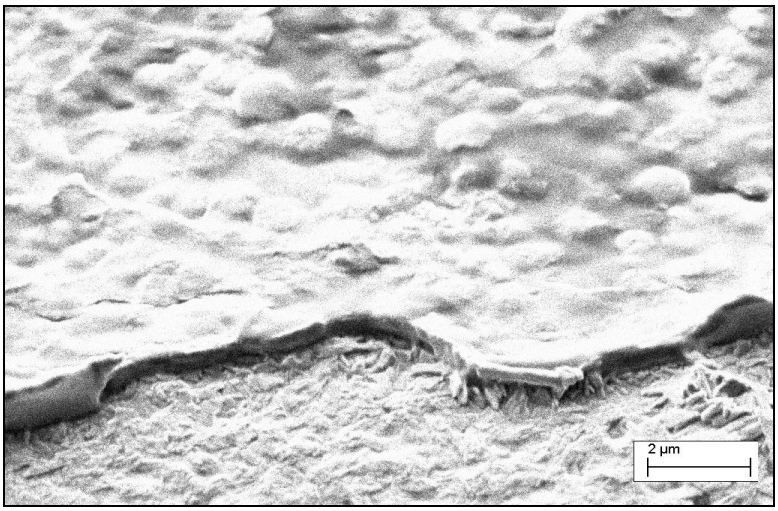

Fig. 4.13 SEM image of the EVALS32/PEDOT (PTS 25.7 % wt/V) sample surface.

The SEM image shows that the conducting polymer film obstacles the removal of the underlying PTS crystals by methanol rinsing. Moreover, it can be presumed that the leveling of the conductivity at the highest PTS concentrations was due to PEDOT film formed over the initiator that, hampering the diffusion of EDOT, suppressed further polymer deposition. Definitively, although they showed increased conductivity, the film obtained with PTS concentration higher than 11.4 % wt/V resulted opaque, characterized by a mean transmittance below 70 % in the range 400-1100 nm, mainly due to the light scattering. Moreover, at the highest concentrations of PTS, the initiator segregated on the sample surface behaved as other reported conducting systems in which the substrate acts just as initiator support, not interacting with PEDOT.

5

EVALS-BASED ELECTRO-ACTIVE MEMBRANES

5.1 INTRODUCTION

5.1.1 Cross-linked EVALS: a ionic Electro-Active Polymer (ionic-EAP)

In recent year, great research efforts have focused on the development of synthetic materials that display biomimetic properties. Among these, one class is represented by stimuli-responsive materials. For example materials responsive to pH, temperature, magnetic and electrical stimuli have been developed. Materials that respond to electrical stimuli are crucial for devices that can function as actuators, specifically as artificial muscles. In this context, mainly two general classes of materials showing electro-active properties are known: Electro-Active Ceramics (EACs) and Electro-Active Polymers (EAPs).

EACs consist of ceramic materials widely used for several mechatronic applications and mechanical devices, for example for production and detection of sound, high voltages generation, electronic frequency generation, microbalances and optical devices. They are characterized by piezoelectric properties, as in the case of $BaTiO_3$ and the class of Lead Zirconate Titanate based materials, also known as PZTs, that are used as ultrasound transducers, ceramic capacitors, ceramic resonators, sensors and STM/AFM actuators and other actuators. Piezoelectric effect can be resumed as the linear electromechanical interaction between the mechanical and the electrical state in crystalline materials that don't possess inversion symmetry (non-centrosymmetric crystals). This effect is a reversible process. In the direct piezoelectric process the internal generation of electrical charge results from an applied mechanical force, while in the reverse process the internal generation of a mechanical strain results from an applied electrical field. When a mechanical stress induces a re-configuration of dipole moments, hence the variation of polarization vector (about its strength, its direction or both), that is the dipole density in the bulk of materials without centrosymmetry, a variation of surface charge density upon the crystal faces appears, that is a variation of the electric field extending between the faces caused by the change in dipole density in the bulk.

Conversely, the reverse effect consists of creation of mechanical deformation in the crystal when an electrical field is applied.

Anyway EACs are not lightweight materials as polymers; moreover their high brittleness, their lack of flexibility and low deformations upon piezoelectric effect are important drawbacks that make these materials inadequate for the realization of artificial muscles for robotic and biomedical technology. On the other hand, polymers are resistant, flexible, biocompatible and withstand large deformations at the same time. In particular their elasticity and easy shaping, the ability to induce large implementation of actuation and the possibility of non-linear electromechanical responses are properties that match the operational features of natural muscles, while also making low-dimensional applications possible.

Polymer actuators devices can be classified on the base of actuation process, that is in general the mechanism through which they can convert electrical energy into mechanical strain. A general classification focuses on transport properties of the active material. Polymers that change shape under electrical stimuli can be divided into electronic (electronic-EAPs) and ionic (ionic-EAPs) types. In the first case, actuation mechanism arises from the direct application of the external electric field, such as in the case of dielectric elastomer actuators (DEAs).[141] DEAs consist of a thin elastomeric film (cross-linked polysiloxanes, polyurethanes or polyacrylates) characterized by high relative permittivity, coated on both sides by compliant electrodes. When a differential voltage is applied across the two compliant electrodes, Maxwell stresses are generated in the film and the resulting film thickness reduction causes the film to expand in area. This expansion of area can be captured by a frame to produce a linear extension (Fig. 5.1). Some of these actuators have shown extension up to three times their initial lengths, bulk material force-to-weight ratio of 1000:1 and bulk material specific energy densities of 3-4 J/g, so that they have been proposed as large displacement actuators for use in mechatronic devices. Anyway, although DEAs are simple, potentially low cost and lightweight, their physics of performance mechanisms and their complex viscoelastic behaviors are not yet fully understood. From an applicative point of view, electronic-EAPs, including also classes of conducting polymers, used for such actuators, are in general stiffer than ionic type EAPs, produce higher mechanical stresses and higher lifting capacity with a faster actuation response. Anyway they show low flexibility and moderate displacement and require high voltage compared to ionic-EAPs.

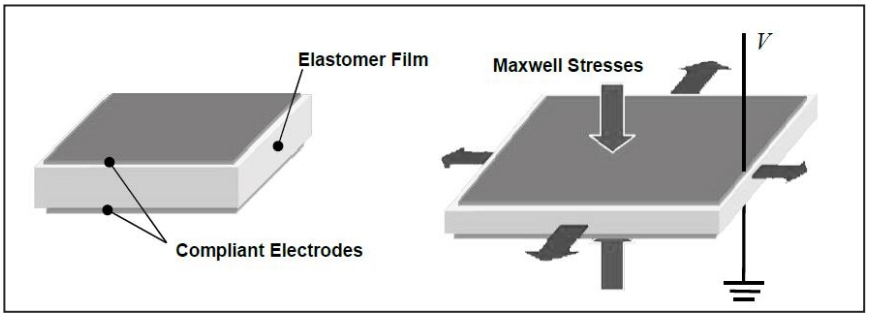

Fig. 5.1 Scheme of DEA operating principle.

Thus, the second type of polymeric actuators, based on the use of the so-called ionic-EAPs, concerns the ionic polymer transducers (IPTs). In this case, actuation mechanism at the active polymer is coordinated by motion of ionic moieties within the polymer matrix across an electrolytic phase. Drawbacks associated to ionic-EAPs include the need to seal the device in its wet state in order to preserve the electrolytic phase and the need to set the applied voltage below a certain value in order to avoid electrolytic effects that can cause irreversible damage in the device. At first, naturally occurring materials and biopolymers were explored as ionic-EAPs that showed some mechano-electric properties, such as contraction or expansion of a gel, for example collagen membranes.[142] This research was expanded into synthetic polyelectrolyte gels[143], demonstrating the response of swollen gels to electrical stimuli following a mechanism based on field-induced migration of ionic species through the gel causing solvent transport, hence contraction or bending of the sample. Polyelectrolyte gels have been shown to undergo reversible deformation under dynamic applied electrical stimulus yet require immersion in solution and in many cases show slow response or lack mechanical stability. For these reasons, solid polymer electrolytes in the form of systems based on ionomer[144] membranes with similar electromechanical properties have been introduced. These systems have been developed mainly as ionic polymers or ionomers in composite form with conductive metallic electrodes. Three groups of researches in the early 1990s studied this ionic polymer-metal composite, known as IPMC: Oguro et al. [145] and Shahinpoor [146] demonstrated their application as actuators, while Sadeghipour [147] demonstrated their application as sensors. Looking at an IPMC membrane cross-section, one can see an inner part composed of a ionomeric polymer membrane and metallic external layers at each surface penetrating microns deep into the surface of the membrane (Figure 5.2). Electrokinetic ion migration and solvent transport represents the mechanism of function of an IPMC. In the water-swollen state, for an ionomer containing fixed anionic groups, application of an electrical stimulus (ddp=1-4 V) causes the mobile counterions (for example, H^+, Li^+, Na^+),

and associated water of hydration to migrate to the anode. Enrichment of water near one membrane face generates an osmotic pressure and a strain that results in bending of the composite toward the opposite electrode.[148]

Generally IPMCs are produced through deposition of a conductive metal onto the surface of such an ionomer membrane. The basic technique involves the neutralization of the ionomer with a platinum salt, which is chemically reduced to its metallic state using a strong reducing agent such as sodium borohydride. The diffusion of both the reducing agent and the metal salt creates surface electrodes by selective deposition at the membrane faces, thus allowing the application of the electric potential across the membrane. Formation of the composite includes multiple reductions, electrochemical deposition, the use of alternative reducing agents and metals.

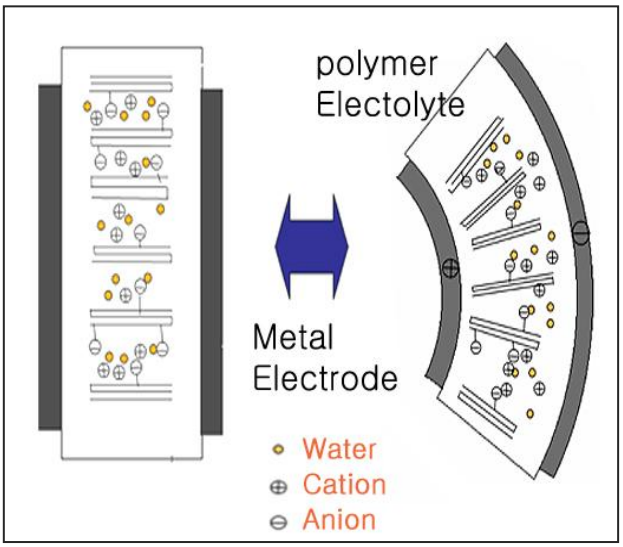

Fig. 5.2 Scheme of IPMC operating principle.

Functional IPMC application have focused almost on the class of perfluorosulfonated ionomers, first of all Nafion® (DuPont), Flemion® (Asahi Glass) and Aciplex® (Asahi Chemical). Nafion is a perfluorinated copolymer composed of tetrafluoroethylene and a perfluorovinyl ether comonomer with a sulfonic acid terminus on the side chain. Nafion morphology consists of ionic aggregates distributed through a PTFE matrix, as a result of phase separation between the hydrophobic matrix and the hydrophilic side chains. Thus, hydration occurs through swelling of ionic aggregates that can be thought as reverse micellar structures distributed in the fluorocarbon matrix. All the models recently proposed to explain Nafion morphology, such as lamellar and rod-like models, differ only in the geometry, but each considers the formation of ionic aggregates within the matrix to be crucial for efficient transport through the membrane.[149]

As a new alternative matrix material for IPT systems, EVAL shows a suitable chemical structure composed of hydrophobic ethylene units and hydrophilic vinyl alcohol units. In its dry state it shows inherent gas barrier properties while at high relative humidity it loses much of its barrier performance, due to its hygroscopicity and water absorbing characteristics. Thus, hydration of the hydrophilic vinyl alcohol component transforms EVAL from a barrier membrane to a potential transport membrane. Introduction of ionic functionalities can increase water uptake as well as open up a number of potential applications for EVAL based ionomers. In this direction, the ionic functionalities introduced on EVAL by sulfonation, together with the possibility of controlling the sulfonation degree, are factors that make EVALS an interesting candidate for IPMC matrices.

For the desired application, the polyanion must be subjected to cross-linking reaction to prevent dissolution of the membrane while retaining a highly swollen state. For example, a work reports the characterization of an EVAL-based IPMC in which introduction of ionic functionalities and cross-linking of the material are achieved simultaneously by using sulfosuccinic acid [150], similarly to the procedure used for sulfosuccinic acid modified poly(vinyl alcohol) membranes.[151]

Subsequently, this chapter is dedicated to the cross-linking of EVALS in correspondence of residual hydroxyl groups that are present in the partially sulfonated polymer. This was tested as a feasible way to obtain electro-active membranes, followed by their modification and functionalization towards the realization of an IPMC actuator system. In this case, the introduction of ionic functionalities, through prior sulfonation of EVAL, and following cross-linking of the membrane, can be realized as two distinct steps, allowing better tuning of composition and final properties of the material.

In order to construct electrodes on the external surfaces of EVAL membrane, layers with enhanced conductivity respect to the inner layer should be obtained. Manly two different methods for surface coverage could be applied: the diffusion of a metal salt and its reduction or the formation of a conducting polymer network, that is the formation of a semi-interpenetrating polymer network (semi-IPN). In all the cases, one has to take into account that:

- first of all, electrical conductivity of the layered electrodes should be high enough to maintain the electric field necessary to activate the ion migration along all the area of the membrane;

- the extension of diffusion of the conducting layers into the inner part of the electro-active membrane should be limited to a certain depth in order to avoid short-circuit phenomena between the two membrane faces;

- it should be possible to realize the surface coverage when the membrane is in its swollen state. Otherwise, a subsequent swelling process can involve the destruction of the surface conducting layers due to dimensional changes;

- the surface conducting layers should not alter the mechanical flexibility of the membrane composite.

A convenient way to obtain an electro-active composite based on EVALS, while considering all the previously reported conditions, would be the realization of surface electrodes consisting of PEDOT synthesized by vapor phase polymerization. In fact, use of PEDOT for surface electrodes formation allows in principle to obtain an all-organic device, thus ensuring flexibility of the composite and high conductivity of the electrodes at the same time. Moreover, VPP technique, allowing the control of EDOT monomer diffusion into the membrane matrix, would imply the feasible formation of suitable polymer surface electrodes free from unwanted short-circuit phenomena and characterized by geometries also complex.
Unfortunately, this strategy failed because of the low conductivity of the PEDOT layer achieved on the membrane faces. Therefore, in order to exploit all the preliminary experimental work carried out to find the optimal condition to obtain a self-standing, highly water swellable EVALS membrane, an alternative method to make conductive the membrane surface was investigated. In particular, the controlled reduction of silver ion from Tollens reactant in presence of glucose as reducing agent on the cross-linked EVALS surface was tested. The obtained membrane showed actuation when an electrical field was applied.

5.2 MATERIALS AND METHODS

5.2.1 General methods and instruments

- Attenuated Total Reflection Fourier Transform Infrared Spectroscopy (ATR FT-IR) analyses were performed by using a Nicolet 6700 FT-IR Spectrophotometer (Thermo Scientific) operating within the 4000-400 cm^{-1} spectral range and with a resolution of 2 $cm^{-}1$, equipped with an ATR Goldengate (Specac) single reflection accessory employing a synthetic diamond and an angle of incidence of 45°. Each spectrum was acquired by co-adding 200 intereferograms and baseline corrected.
- Ionic conductivity measurements were carried out by Electrochemical Impedance Spectroscopy (EIS). All the measurements were carried out at CNR-ISMNT by using Autolab PGSTAT-12 instrument. The tests were performed under the supervision of the Dr. Zane.

5.2.2 Chemicals

All solvents used were acquired from Carlo Erba. All other chemicals were acquired from Aldrich, except for EVALS32 synthesized according to the procedure described in chapter 2.

5.2.3 EVALS cross-linking

Chemical cross-linking of EVALS32 was carried out in solution by using glutaraldehyde (GLU) as cross-linker in acidic environment. Cross-linking involves the reaction of GLU aldehyde groups with EVALS32 hydroxyl groups, with formation of emiacetales and then acetales, under acid catalysis conditions.

The reaction has been conducted by prior dissolution of EVALS32 samples in water. Different volumes of a GLU aqueous solution (25 % wt/V) were added to EVALS32 solutions, and the volume was adjusted to a constant value with distilled water. By this way, solutions with varying GLU/OH molar ratio were prepared. Finally, a constant amount of HCl solution (0.3 M) was added. The table 5.1 shows reactants amounts and volumes ratios used for cross-linking reaction. The samples were named $EVALS_{cl}X$ (cross-linked EVALS) where X is the GLU/OH molar ratio.

All solutions were poured into Teflon molds, thus cross-linking reaction was left to occur through a drying step at 60° C for 6 h.

Sample code	$GLU/OH_{EVALS32}$ molar ratio	EVALS32 (mg)	GLU (25%wt/V) (µl)	H_2O volume (µl)	HCl (0.3 M) (µl)
$EVALS_{cl}1.11$	1.11	75	235	515	25
$EVALS_{cl}1.16$	1.16	75	250	500	25
$EVALS_{cl}1.54$	1.54	75	330	420	25
$EVALS_{cl}2.33$	2.33	75	500	250	25

Tab. 5.1 Reactants amounts and volumes ratios used for cross-linking reaction of EVALS32 in solution.

After drying step, all membranes were carefully washed with distilled water in order to remove excess of unreacted GLU and left to dry until constant weight was reached.

5.2.4 Methods for cross-linked EVALS characterization

Cross-linked EVALS32 membranes, obtained starting from a varying GLU/OH molar ratio, were first analyzed by FT-IR ATR at the dry state. All samples were dried accurately before all measurements.

FT-IR analysis was used to control the cross-linking degree of the membranes obtained at various GLU/OH molar ratios.

Moreover, cross-linked EVALS32 membranes were characterized by swelling experiments. In particular, the membranes were immersed in distilled water and extracted at increasing times and excess surface water was carefully removed with filter paper. By simple weight determinations, the swelling degree in water (SwD %) was calculated by the following relation:

$$SwD(\%) = \frac{Ws - Wo}{Wo} \times 100 \qquad (5)$$

where *Ws* and *Wo* are the weights of the swollen and dried sample, respectively.

The ionic conductivity of the cross-linked membranes was measured by electrochemical impedance spectroscopy (EIS). The fully hydrated sample was placed in sealed cell composed

of two circular stainless steel electrodes. A potential of 10 mV was applied in the 10-0.01 KHz frequency range.

5.2.5 Preparation of EVALS-based actuators

For actuation experiments, the cross-linked EVALS membrane surfaces were covered by PEDOT or silver layers to increase the electric conductivity.

Surface PEDOT was formed through EDOT VPP on previously water swollen membranes. For the purpose, after selecting membranes with suitable properties and a dried state thickness of about 300 µm, they were water swelled for 30 minutes and immersed for few minutes in the EVALS32/PTS solution ([PTS] = 11.4 % wt/V) used for EDOT VPP. The oxidant solution excess was carefully removed by filter paper and the membranes inserted in the VPP reaction chamber for a reaction time of almost 6 h.

After VPP, the membranes were then washed in methanol and swelled in water.

Alternatively, the cross-linked EVALS membrane surface was coated by a silver layer by using as prepared Tollens reactant [$Ag(NH_3)_2OH$] and glucose as reducing agent. In particular, the membranes were swelled for 2 minutes in glucose solution before being put in contact with Tollens reactant. Excess of glucose solution was removed from the membranes surface and the swelled membranes were then put in contact with the reactant for further 2 minutes. During this time a first silver ions reduction occurred. This first formed silver layer constituted an obstacle to further silver ions diffusion during the second contact with Tollens reactant. Silver ions reduction was evidenced by darkening of the membranes. Hence, samples were dabbed and again immersed into glucose solution for 2 minutes. The samples, were then dabbed and subjected to a second coverage by putting them in contact with the reactant solution for 10 minutes. At the end the membranes were immersed for further 2 minutes in glucose solution and then washed with distilled water in order to remove possible residual components. After the second coverage the membranes surface showed a metallic appearance.

5.2.6 Methods for actuators characterization

Before actuation tests, the edges of the membranes were removed by a scalpel.

The conductivity of the surfaces was measured by four point probe on dried samples.

Actuation tests were performed on the swollen membranes by using a DC generator and rheostat system applying a voltage in direct and reverse biasing within the range of 2-9 Volts (Fig. 5.3).

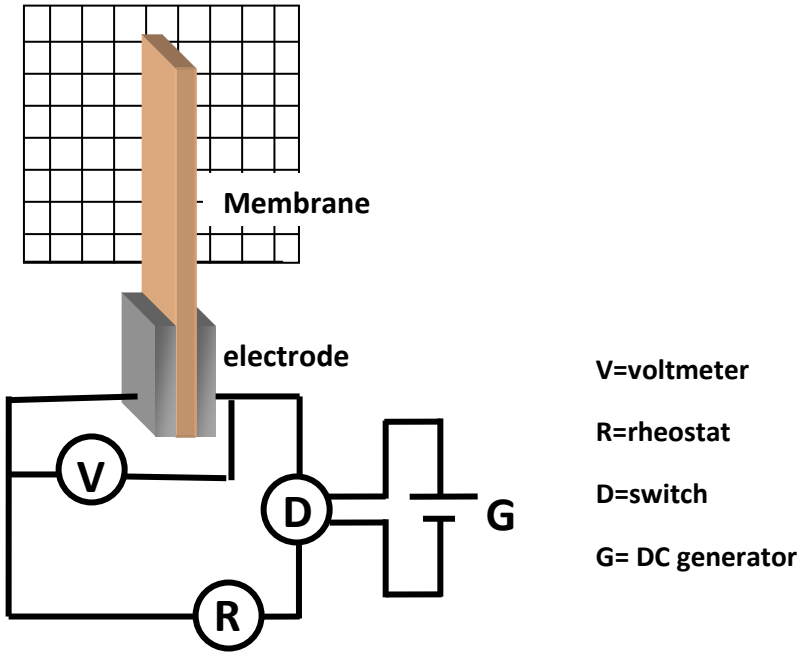

Fig. 5.3 Experimental setup for actuation experiments.

5.3 RESULTS AND DISCUSSION

5.3.1 Membranes based on cross-linked EVALS

Study of cross-linking of EVALS32 based membranes has been conducted preliminarily by infrared spectrophotometry and thermal calorimetry analyses.

First of all, ATR FT-IR spectra of an EVALS32 membrane obtained at a GLU/OH molar ratio of 1.16 is displayed in figure 5.4.

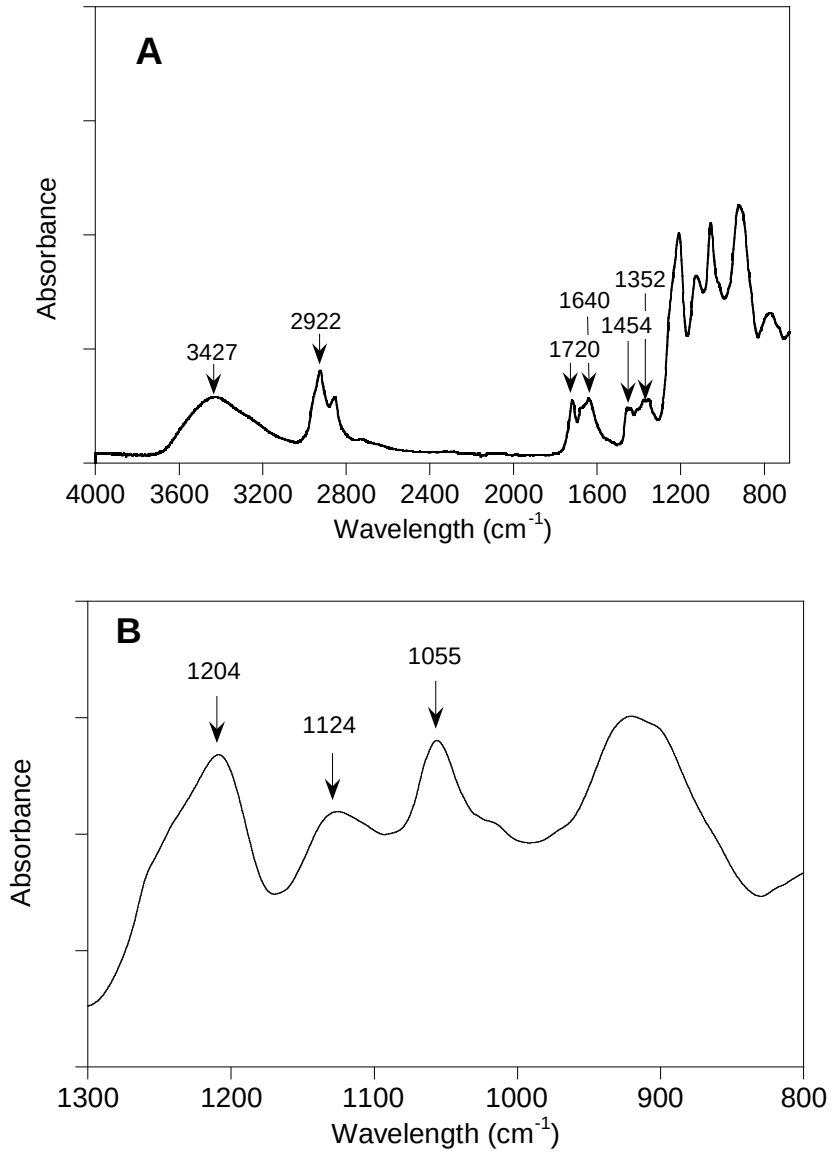

Fig. 5.4 (A) FT-IR ATR spectrum of an EVALS32 cross-linked membrane obtained at GLU/OH molar ratio of 1.16 ($EVALS_{cl}1.16$). (B) Spectrum in the 1300-800 cm^{-1} range.

Here, besides the absorptions already found in EVALS32 spectra with slight variations, such as those related to asymmetric stretching of CH_2, symmetric and asymmetric stretching of SO_3 at 2922, 1204 and 1055 cm^{-1} respectively, the absorptions related to the cross-linking reaction are evidenced. In particular, absorptions at 1720 and 1124 cm^{-1} were assigned to stretching of residual aldehyde C=O groups and of C-O-C stretching, respectively. Moreover, the spectral contribution due to bending of methylene groups of the whole membrane was related to the double peak found at 1454-1352 cm^{-1}.

In general, an increase of the GLU/OH ratio involves a decreasing of the intensity of the extended band at 3427 cm^{-1} due to OH stretching (Fig. 5.5) and a correspondent decrease of peaks of asymmetric stretching of CH_2.

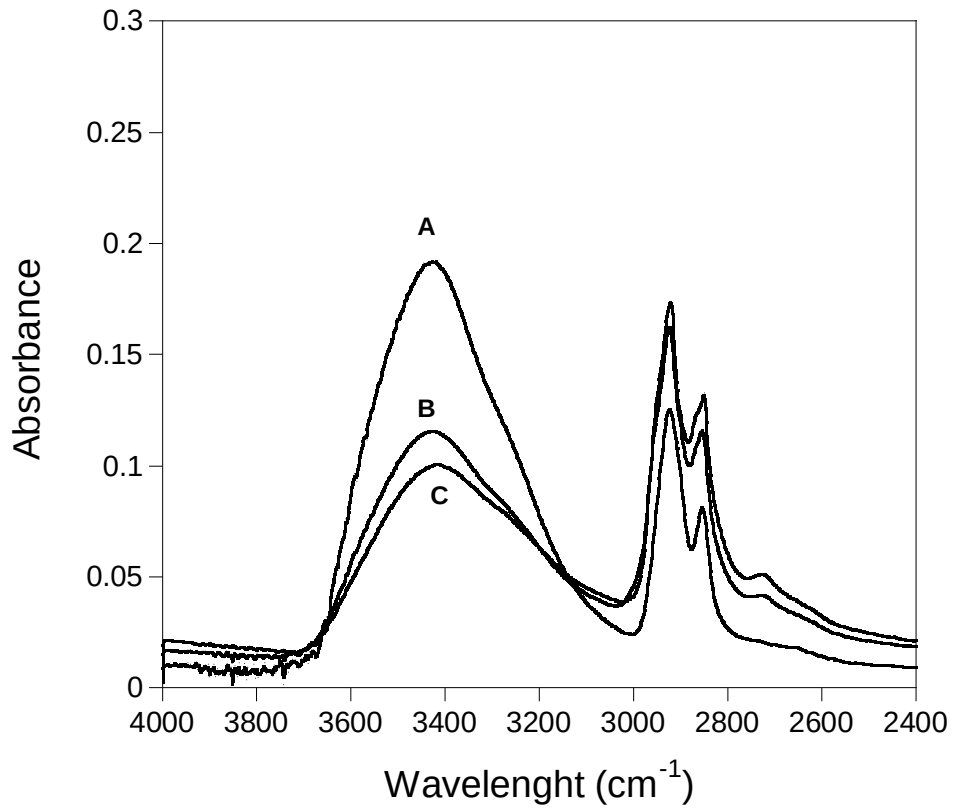

Fig. 5.5 FT-IR ATR spectra of EVALS32 (A) and cross-linked membranes $EVALS_c1.16$ (B) and $EVALS_{cl}2.33$ (C).

However, in order to investigate cross-linking degree, it was not possible to use intensity variation of the hydroxyls absorption band together with intensity variation of the peaks

related to CH_2, because of the presence of traces of water, as the water bending peak at 1640 cm^{-1} demonstrates. In fact samples easily absorb water due to polymer hygroscopicity and attention paid to preserve a complete dry state was not sufficient.

Then, in order to follow the cross-linking reaction, the intensity of peak at 1352 cm^{-1}, related to CH_2 bending, was normalized respect to intensity of the SO_3 peak at 1204 cm^{-1} and reported as a function of the of GLU/OH molar ratio in figure 5.6.

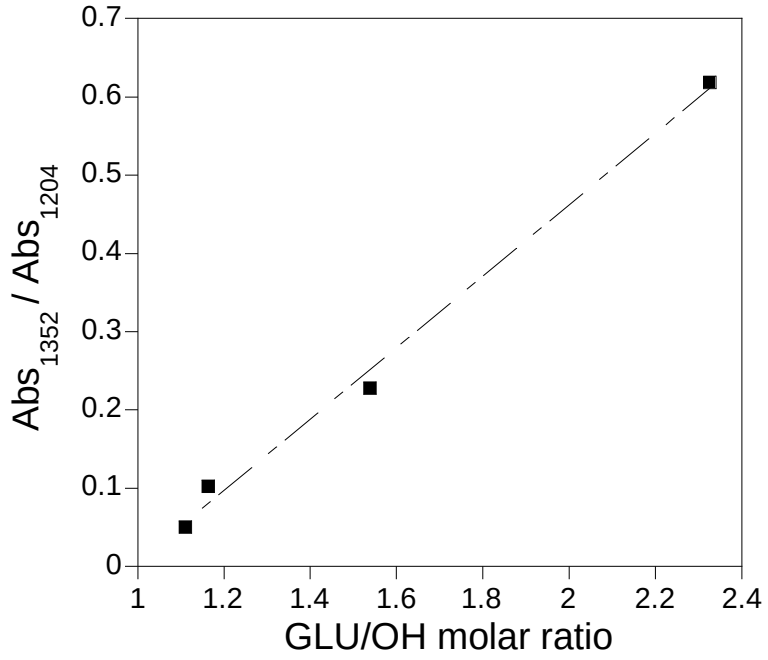

Fig. 5.6 Intensities of peak at 1352 cm^{-1} CH_2 bending, normalized respect to intensity of the SO_3 peak at 1204 cm^{-1}, as a function of GLU/OH molar ratio.

As expected, a good linear correlation was obtained.

Figure 5.7 shows the ratio between the intensities of C-O-C and C=O peaks at 1124 cm^{-1} and 1720 cm^{-1}, respectively, as a function of GLU/OH molar ratio. The intensity of the peak at 1720 cm^{-1} was obtained by subtracting the contribute at 1640 cm^{-1} of adsorbed water. These two absorptions can be related to reacted and non-reacted aldehyde groups, respectively. The trend could be easily explained taking into account that at lower GLU/OH molar ratio, most of the bifunctional aldehyde can react with the free hydroxyls of EVALS matrix. Differently, at the higher GLU/OH ratio, probably because of the restricted molecular mobility due to the

progressive cross-linking, the concentration of glutaraldehyde molecules that reacted with only one aldehyde group increased.

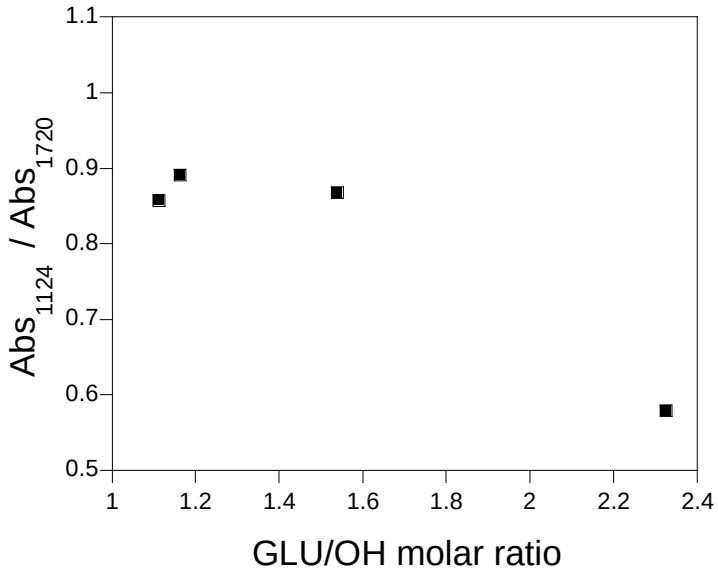

Fig. 5.7 Intensities ratio between the peaks at 1124 cm^{-1}(C-O-C stretching) and 1720 cm^{-1}(C=O stretching) as a function of GLU/OH molar ratio.

In order to test the possible use of these EVALS32 cross-linked membranes as actuator systems, it is important to have information about their swelling behavior, because the latter is strictly related to the their ionic conductivity, morphological and mechanical properties.

All the dried membranes at various cross-linking degree were swelled and the water uptake was determined after extraction from their aqueous medium at regular intervals of time. For each interval of swelling time the swelling degree, SwD (%), was calculated from water uptake as previously described. The kinetics obtained for the swelling process relative to all the samples is showed in figure5.8.

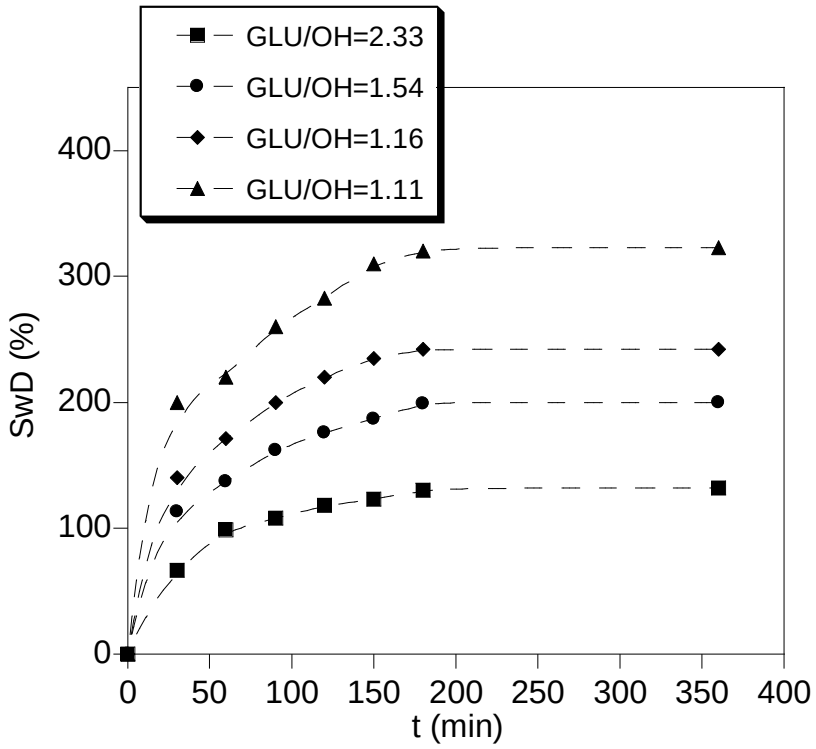

Fig. 5.8 Swelling degree, SwD (%), as a function of swelling time for cross-linked EVALS32 membranes with various GLU/OH molar ratio. All experiments was performed on dried samples with initial thickness of 300 μm.

The kinetic curves obtained for all the samples were fitted taking into account a general simplified diffusion Fick relation valid for moderate swelling (SwD < 60 %), by supposing that the swelling process would be determined by the diffusion of water within the membranes. The general Fick equation used for fitting is represented by:

$$\frac{SwD(t)}{SwD_{max}} = A\, t^{1/2} \qquad (6)$$

where SwD(t) and SwD_{max} are the swelling degree at the generic time *t* and the maximum swelling degree value, respectively, and *A* is kinetic constant dependent on sample geometry and diffusivity.

Figure 5.9 displays the parameters *A* and SwD_{max} found by fitting the swelling results by equation 6, as a function of GLU/OH molar ratio.

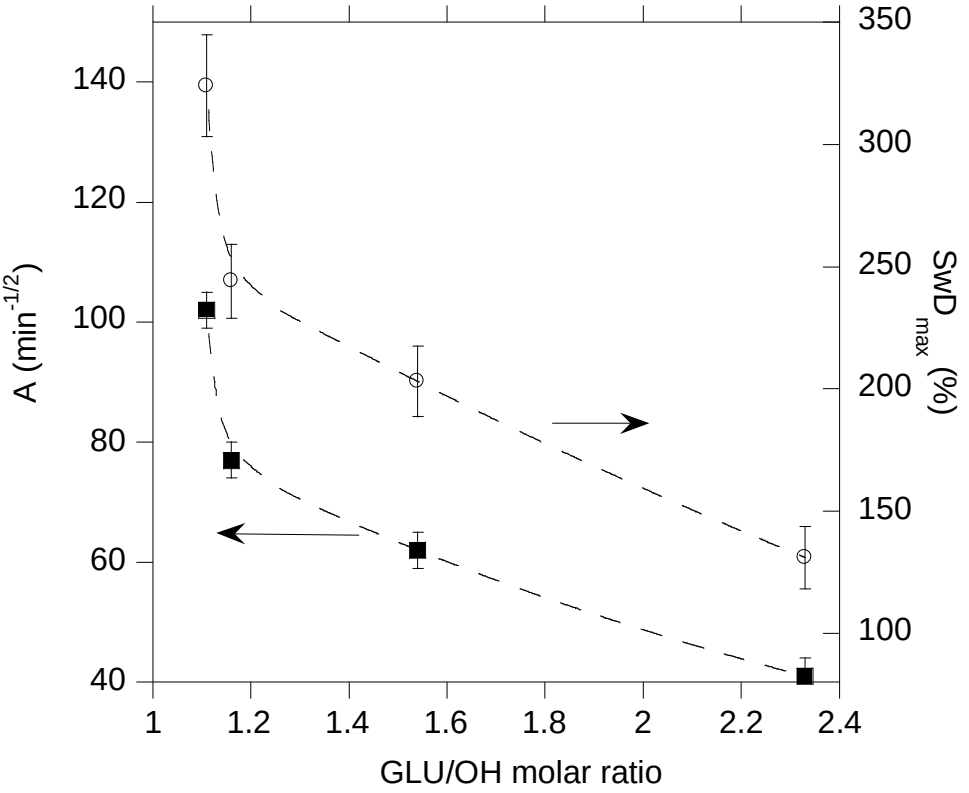

Fig. 5.9 Kinetic constant, *A*, and maximum swelling degree, SwD_{max} (%), as a function of GLU/OH molar ratio.

The general trend shows that both swelling kinetic and maximum swelling degree decreased as cross-linking degree increased. The attenuation of swelling rate and maximum swelling decrease at the higher GLU/OH molar ratio could be related to the fact that, as shown in figure 5.7, a fraction of GLU molecules couldn't participate to the formation of effective cross-linking points, a fraction of aldehyde groups remaining unreacted.

The mechanical properties and the dimensional stability of the membranes were strictly related to the swelling. The lowest cross-linking degrees lead to highly swollen gel-like membrane. On the other hand, $EVALS_{cl}2.33$ resulted to be stiff. However only the $EVALS_{cl}1.11$ sample was excluded for the further characterization.

The ionic conductivity of the selected fully hydrated membranes was measured by electrochemical impedance spectroscopy (EIS).

From the elaboration of the recorded current intensity and phase it was possible to determine the real (Z') and the imaginary (Z") components of the complex impedance (Z=Z'+iZ"). The obtained values were reported in a typical Nyquist plot of figure 5.10 ($EVALS_{cl}1.16$).

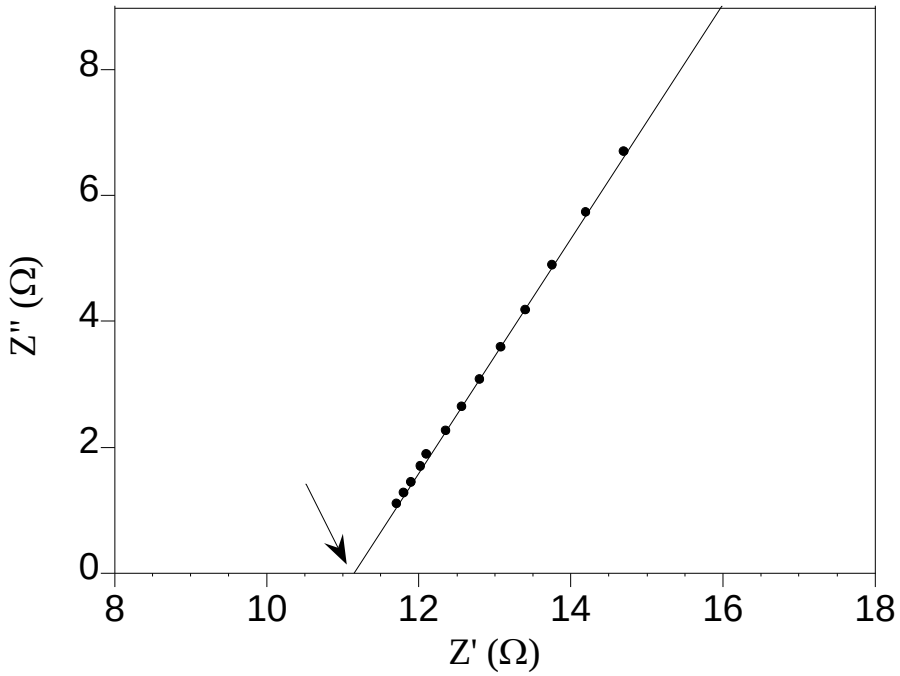

Fig. 5.10 Nyquist plot of the $EVALS_{cl}1.16$ recorded in the 10-0.01 KHz frequency range.

The ionic conductivity (σ_i) was evaluated as the reciprocal of the extrapolated value of Z' at Z''=0. The result was normalized respect to the electrodes surface and sample thickness (Tab. 5.2).

sample	$EVALS_{cl}1.16$	$EVALS_{cl}1.54$	$EVALS_{cl}2.33$	NAFION117
σ_i (S/cm)	$3x10^{-2}$	$2x10^{-2}$	$1x10^{-2}$	$3x10^{-3}$

Tab. 5.2 Ionic conductivity of the cross- inked swollen membranes.

For sake of comparison, in the table 5.2 was also reported the σ_i of NAFION117, which showed a lower conductivity respect the cross-linked EVALS32 sample. However, it must remarked that the NAFION membrane showed a maximum swelling of about 20 % and that the equivalent weight of the SO_3^- groups is about ten time higher than that of EVALS32.

The different values, σ_i, of cross-linked EVALS32 are probably related to the different swelling degree, being the same the concentration of ionic groups.

According to the recorded conductivity and qualitative evaluation of the mechanical properties, the membrane $EVALS_{cl}1.16$ was selected in order to prepare electro-active materials suitable for the preparation of an actuator system.

5.3.2 EVALS-based actuators

The membrane was subject to the described two coating processes, that is EDOT VPP and silver reduction, to increase the surface electronic conduction. Then the sample were dried and the conductivity of the surface (σ_s) and across the membrane (σ_{bulk}) was measured by four-point probe and two electrodes methods, respectively. This last test was carried out to exclude any possible electrical contact between the two conductive membrane surfaces. In table 5.3 the values were reported.

Coating method	σ_s (Ω^{-1})	σ_{bulk} (S/cm)
VPP PEDOT	$2x10^{-4}$	$1.8x10^{-8}$
Tollens 1 dep.	$2x10^{-4}$	$7x10^{-8}$
Tollens 2 dep.	0.2	$7x10^{-8}$

Tab. 5.3 Electronic conductivity of the dried cross-linked membranes.

The very low bulk conductivity showed by all the membranes evidences that no short-circuits exist between the two conducting faces. However, the method based on deposition of PEDOT by VPP on water swollen sample brought about a low surface conductivity, much lower than that observed in the previous experiment carried out on dried EVALS films (chapter 4). This effect was attributed to the low diffusivity of the hydrophobic EDOT into the hydrated membrane.

As for as the alternative coating methods base on the reduction of the silver ions by glucose (Tollens deposition), it can be observed that the surface conductivity after the first rapid immersion of the sample in the reducing and Tollens solutions (Tollens 1 dep. in table 5.3) was low. A drastic increase of σ_s was reached after the second deposition step (Tollens 2 dep. in table 5.3). If the membrane was left for long time in glucose and Tollens solution, that is by eliminating the first deposition step, the obtained membrane showed an high bulk conductivity. It means that the silver ions diffuse into the bulk of the sample and, after reduction, form conductive path between the two faces. A deeper analysis of the silver layer on the membrane with the highest conductivity was carried out by scanning electron

spectroscopy. In figure 5.11 A, B the images of the conductive surface at two magnifications are displayed.

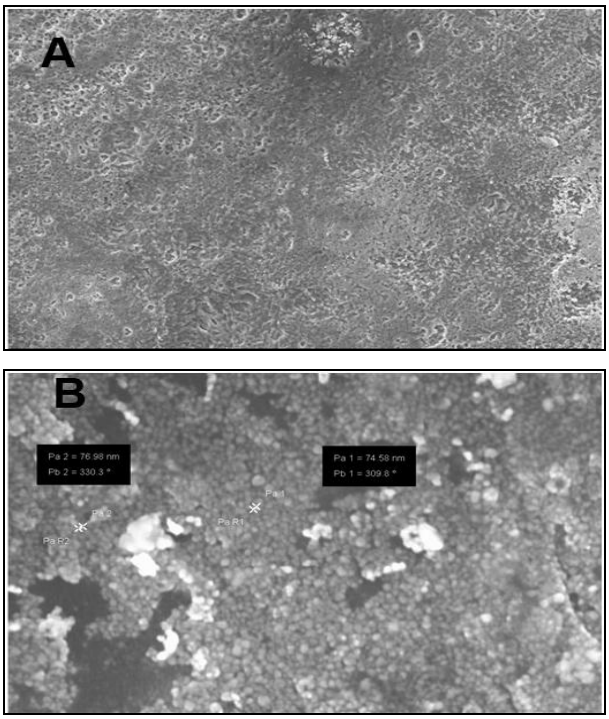

Fig. 5.11 A, B: SEM images of the EVALcl1.16 sample surface coated by silver.

From the SEM images it can be observed that, although the silver deposition was carried out on the swollen membrane, upon drying and dimensions reduction, the conducting layer was continuous, without fractures or cracks. This could be due to the silver nanoparticulate structure (particles diameter about 70-80 nm, Fig. 5.11 B) which confers a plastic behaviour to the metal layer.

In figure 5.12 A and B, the membrane fracture surface at two different magnification was reported respectively.

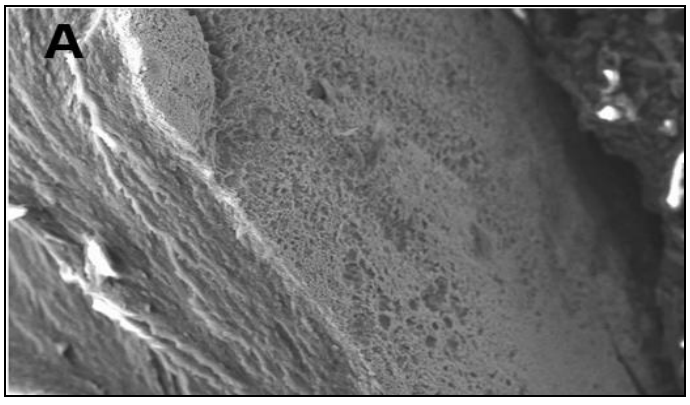

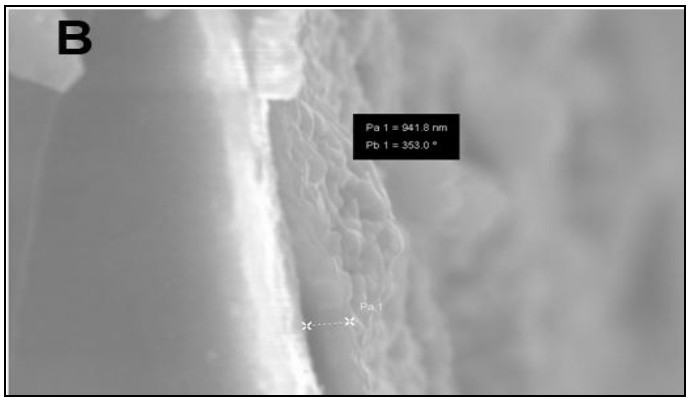

Fig. 5.12 A, B: SEM images of the fracture surface of EVALcl1.16 sample coated by silver.

The figure 5.12 A and B shows that the silver layer was well adherent to the EVALcl1.16 membrane and that its thickness is about 1 µm. Moreover no metallic particles can be observed into the membrane bulk.

The prepared conducting membranes were tested as actuator.

One end of the fully swollen sample was placed between two platinum electrodes and a variable potential was applied.

The following images (Fig. 5.13) show the bending process the EVALS32 based electro-active membrane coated with PEDOT under applying a low voltage of about 4.5 V in direct and reverse biasing.

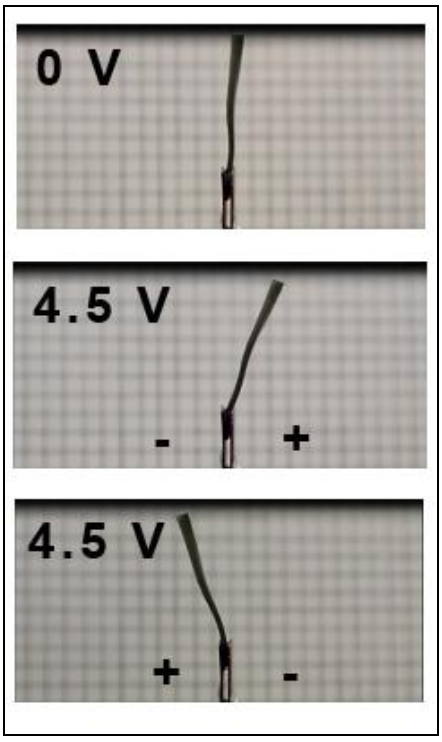

Fig. 5.13 Bending sequence of an electro-active EVALS32 based membrane coated by PEDOT layers under applying a 4.5 V electric potential (direct and reverse biasing).

At lower applied voltage the bending was negligible. The linear displacement of the free end of the device, normalized by its length, was about γ=0.35. However, it can be observed that the bending is essentially located in the device region close to the electrodes. This means that, because of the low surface conductivity, the electric field was not uniform along the membrane. Moreover, in the second biasing cycle a drastic reduction of γ was observed. Successively, the actuator did not respond to the applied stimuli. A visual inspection showed that the membrane region between the electrodes was rigid and degraded, probably because of redox reactions occurring at the interfaces.

The same experiments were carried out on the devices coated with silver. At a potential of 3 V the movement of the membrane was very slow and it reach the maximum displacement γ= 0.28 after about 1 h. During this period the membrane dried and the actuaction ceased.

At 6 V the movement is rapid, the displacement large (γ=0.6, Fig. 5.14) and it was possible to follow the actuaction in almost 6 biasing cycles.

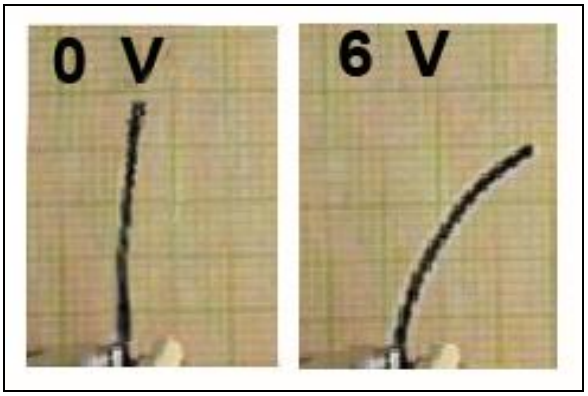

Fig. 5.14 Two frames of a movie recorded during the actuation of the EVALcl1.16 sample coated with silver. The second frame was taken after 30 s at a potential of 6 V.

In figure 5.15 is reported the γ values recorded in 6 successive cycles in which the polarity of the electrodes was changed every 30 s.

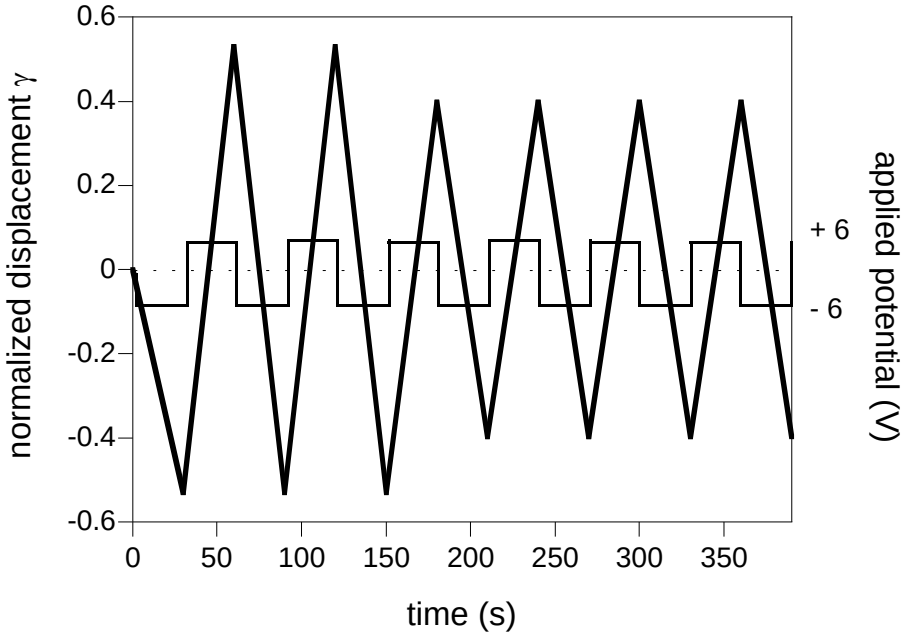

Fig. 5.15 Normalized displacement, γ, of the EVALcl1.16 sample coated with silver as a function of time under an applied potential of 6 V and 6 cycles of polarity inversion.

The graph in figure 5.15 shows that during the first 2 cycles of polarity inversion the maximum displacement reaches the value of 0.6, while during the following cycles the value decreases up to 0.4. Moreover, it is possible to observe that a symmetric displacement deformation arises when the polarity is inverted. Over 6 cycles of work the device starts to reveal an irregular response due to progressive loss of membrane hydration and degradation of the conducting films correspondent to the surface electrodes due to possible redox processes and hydrolysis of water.

Higher potentials than 6 Volts were not reached because of the rapid degradation shown by the device near the electrode contacts.

6

INTEGRATION OF A CONDUCTIVE CLICK-FUNCTIONALIZABLE PEDOT IN AN ETHYLENE VINYL ALCOHOL CO-POLYMER SUBSTRATE FOR MECHANICAL RESISTANCE IMPROVEMENT AND SURFACE PROPERTIES CONTROL

6.1 INTRODUCTION

6.1.1 PEDOT integration into non-conductive polymers

PEDOT, as their derivatives and the major part of conjugated conductive polymers, presents problems such as limited processability, lack of mechanical stability, poor surface adhesion properties on inorganic and polymeric substrates, that create problem such as surface delamination and limit its potentialities mostly in applicative field. A wide range of methods have been developed to reduce these unwanted features, such as formation of aqueous complex with polyanionic phases, PEDOT:PSS [23], vapor phase polymerization techniques into several kind of polymeric matrices[152,153], anchoring using plasma treatments.[154]

Those methods that allow to produce in situ polymerized PEDOT are advantageous for all those applications where the lowering of PEDOT electrical properties may become a limiting factor. Among these, a particular method is based on the integration of *in situ* polymerized PEDOT networks in non-conductive polymer substrates such as poly(methyl methacrylate) (PMMA), exploiting the PEDOT ability to be loaded by macromolecules and other polymers under swelling during washing steps and/or exposure to specific solvents.[155] A layer of PEDOT is polymerized using Fe(III) tosylate as oxidation agent and pyridine as acidity inhibitor on the non-conductive polymeric substrate, followed by washing with a solvent that partially dissolves the underlying substrate and swells PEDOT phase removing spent oxidant. In this way, an hybrid material, composed of the conducting polymer integrated in the top layer of the substrate bulk, is obtained acquiring some of the mechanical and chemical physical properties of the substrate, while still showing high conductivity as pristine PEDOT.

6.1.2 PEDOT "click" functionalization: PEDOT azide

In order to allow a specific application or tune its electronic properties, PEDOT has been chemically modified in several ways concerning, in general, modifications of the monomer and/or post-polymerization treatments. Usually these modifications consist of covalent bonding of a variety of chemical moieties to the ethylene group of the PEDOT monomeric unit, preserving the π-conjugation of the chain.

Several studies report the method to introduce functionalities on PEDOT using the well-known "click" reaction chemistry between the azide group and a molecule containing a terminal alkyne, the copper(I)-catalyzed azide-alkyne Huisgen 1,3-dipolar cycloaddition (CuACC).[156, 157] They are based on the synthesis of azide or alkyne modified PEDOT polymers and CuACC post-polymerization functionalization techniques.[158- 161]

In particular, the synthesis of 3,4-(1-azidomethylethylene)-dioxythiophene (EDOT-N_3) monomer has been previously developed. Using in-situ polymerization procedures, the monomer can be chemically oxidized to yield stable and insoluble tosylate p-doped PEDOT-N_3 films with high conductivity. These films can be functionalized by a range of alkynated reagents and, moreover, copolymers with EDOT can be obtained allowing to control the electrical properties simply varying the EDOT-N_3 unit percentage in the co-polymer .[159]

On these basis, further works showed the possibility to direct the click-functionalization at the surface or in the bulk of the polymer. This is achieved by tuning the degree and the depth of click-modification in dependence on the swelling properties of the polymer by proper solvents, such as DMSO and DMF, hence, on the specific solvent composition [162].

6.1.3 Aim of the work

Focusing on this context, it has been evaluated the possibility to combine the potentialities introduced by "click" functionalization of PEDOT-N_3, together with the use of a non-conducting polymeric substrate able to be integrated with the conducting phase and provided by the following general features: good mechanical properties, optical transparency, presence of basic chemical functions to be easily labeled for reactions at the surface. In this way, a following approach about orthogonal chemistry can be considered if functionalities, deriving from the conducting phase and substrate non-conducting phase respectively, are both available for surface heterogeneous phase reactions. For these reasons, as a first consideration, EVAL copolymer has been chosen and evaluated as supporting substrate for integration of a

PEDOT-PEDOT-N_3 conducting copolymer. Basically, the factors that have directed its choice are the possibility to introduce hydroxyl functionalities and its water insolubility and negligible solubility to major part of organic solvents at room temperature, especially those used in the CuAAC reactions conditions, such as DMF and DMSO.

The plasticization effect played by alcohol solvents on EVAL copolymers by effect of the increasing of fractional volume, has been exploited to promote the realization of a hybrid material through integration without the need of post-polymerization solvent washing procedures, as it is described in another work.[163]

Briefly, a layer of conducting polymer is polymerized onto an EVAL film by spin coating of an alcohol solution containing co-monomers and oxidant and subsequent drying on a hot plate, in accordance to a well-established *in situ* solution chemical oxidative reference method.[164]

A certain degree of surface integration is expected between EVAL substrate and the conducting copolymer phase. This may be hypothesized mostly by effect of moisture plasticization of EVAL, that arises when the EVAL substrate layer is left in contact with the alcoholic solution containing oxidant and co-monomers during deposition procedure. This would allow monomer and oxidant to permeate from the surface across the substrate matrix, while polymerization takes place during the following drying step.

However, aim of this work is to show the applicability of such a method, even if a more detailed understanding of the surface structure and a study of those parameters influencing integration and phase separation grade should be further considered.

First, surface availability both of azides and hydroxyls has been tested by mean of click reactions in water and organic phase and vapor phase fluorination treatment with trifluoroacetic anhydride (TFAA) to check the access of azide functions from one hand and of EVAL hydroxyl functions from the other. The possibility of reaction in organic phase has been tested through the clicking of an alkynated fluorophore, fluorescein methyl ester (ADT), while in water phase has been used an alkynated poly(ethylene glycol) (MPEG). The use of TFAA as derivatization agent of hydroxyl (Fig. 6.3), amine, thiol functions for XPS analysis of several kinds of polymeric surfaces is widely documented.[165- 168]

It has been also employed by vapor phase treatment for surface esterification of cellulose to enhance hydrophobicity and water repellency.[169] Beside the use as derivatization reactant for XPS analysis, vapor phase fluorination treatment with TFAA has been considered also as a feasible way to provide the hybrid conducting system with the typical properties of fluorine compounds, such as improvement of surface mechanical resistance and adherence to plastic

supports and the possibility to easily enhance the hydrophobicity of the surface without the use of solvent phase reactions.

6.2 MATERIALS AND METHODS

6.2.1 General methods

- Attenuated Total Reflection Fourier Transform Infrared spectrophotometry (ATR FT-IR) analysis was performed on a PerkinElmer Spectrum One model 2000 FT-IR with a universal attenuated total reflection (ATR) sampling accessory on a ZnSe/diamond composite.
- Water Contact Angle (WCA) measurements were obtained using a Data Physics OCA20 contact angle system and dedicated software. For each sample at least three different areas were measured using Milli-Q water as probe liquid. Prior to all measurements, any dust on samples was blown off by inert gas.
- Absorption UV-vis analysis was carried out using a multifunction Wallac Victor 1420 96-well plate reader (Perkin-Elmer).
- X-ray Photoelectron Spectroscopy (XPS) analysis was performed on a Thermo Fisher Scientific K Alpha (East Grinstead, UK) using monochromatized aluminum KR radiation in a 400 μm spot on the sample. Survey and high-resolution spectra were acquired and analyzed using the manufacturer's Avantage software package. In order to avoid the degradation of azides during the XPS analysis, the analyses were undertaken without electron charge compensation.
- Surface conductivity measurements were performed using a four-point probe (Jandel Engineering, Lindsdale, U.K.) connected to a Keithly 2400 source-meter (Cleveland OH). For each sample two measurements in perpendicular positions and for three different values of applied potential were done. Conductivity values were corrected taking into account the Valdes treatment for surface conductivity of thin films measured by four-point probe configuration. [137]
- Qualitative scratch hardness tests were carried out just moving the sample perpendicularly to a fixed stainless steel pin. A smooth and hemispherical pin was used (diameter = 4 mm) and it was charged on top by known weights (F=0.2-1.6 N). Several microscope slides were used as known weights.

6.2.2 Chemicals

All chemicals were acquired from Sigma-Aldrich and used as received unless otherwise specified. Baytron C was purchased from H.C. Starck. EVAL copolymer with 27/73 ethylene/vinyl alcohol weight ratio, corresponding to 40/60 repeating units molar ratio, was purchased from Monomer-Polymer&Dajac Laboratories. 3,4-(1-azidomethylethylene) dioxythiophene (EDOT-N_3) was synthesized in accordance to an earlier reported procedure[170] and methyl 2-(3-Oxo-6-(prop-2-ynyloxy)xanthen-9-yl)benzoate) (alkynated flourescein methyl ester) in accordance to Moore et al..[171]

6.2.3 Copolymerization method for poly(3,4-ethylenedioxythiophene-*co*-3,4-(1-azidomethylethylene) dioxythiophene (PEDOT-PEDOT-N_3) on EVAL substrate

The hybrid film was prepared starting from the deposition of EVAL substrate. A thin film of EVAL was deposited by spin-coating (deposition step: ω=500 rpm, t=30 s; drying step: ω=500 rpm, t=30 s) of an EVAL solution in hot DMF (6 % wt/V, T=90 °C, V=1 ml) on a thick cyclic olefin copolymer (COC) support. COC support was rinsed with acetone, isopropanol and ethanol and pre-heated on a hot plate (T=90 °C) before EVAL spin-coating. After spin-coating, EVAL film on COC was left to dry on the hot plate for 10 min at 90 °C.

The copolymerization method for 3,4-ethylenedioxythiophene (EDOT) and 3,4-(1-azidomethylethylene) dioxythiophene **(**EDOT-N_3) (Fig. 6.1) was based on earlier published methods.[172,173]

Two solutions were prepared. A solution of EDOT (0.15 M) was obtained mixing EDOT (0.22 ml), Baytron C (6.5 ml), butanol (6.5 ml) and pyridine (0.15 ml). While a solution of EDOT-N_3 (0.15 M) was obtained mixing EDOT-N_3 (40 mg), Baytron C (0.6 ml) and butanol (0.6 ml). The two solutions were mixed in equal volumes to yield a final solution containing 50 mol % of the two monomers. Then, the polymerization mixture (V=0.2 ml) was spin-coated onto the EVAL film on COC support (ω=500 rpm, t=15 s). The sample was placed on the hot plate at 90 °C for 20 min and subsequently washed with water, ethanol and dried with pressurized air.

6.2.4 Vapor phase treatment with trifluoroacetic anhydride (TFAA)

Vapor phase fluorination treatment (Fig. 6.3) was tested on EVAL/PEDOT-PEDOT-N_3 hybrid films both before and after clicking with alkynated reactants. Triflouroacetic anhydride (TFAA) (V=300 µl) was introduced into a small glass container previously placed into a flat-bottomed glass bottle with sealing lid. The samples were exposed to the TFAA vapors inside the sealed bottle on a hot plate at T=35 °C. The reaction was kept for 20 min. At the end the samples were removed and left under air suction for 30 min in order to remove volatile by-products.

6.2.5 Click reaction with alkynated ADT

The reaction mixture for the fluorophore clicking was prepared mixing 0.3 ml of alkynated fluorescein methyl ester (alkynated ADT) solution in DMF (16 mM) with 10 µl of $CuSO_4$ solution in water (0.1 M) and 20 µl of sodium ascorbate solution in water (0.1 M). The reaction mixture was used to click the fluorophore on EVAL/PEDOT-PEDOT-N_3 samples both before and after fluorination treatment. The mixture, like a drop, was left on the surface for 20 h. At the end the surface was rinsed with DMF and H_2O and dried. The PEDOT-PEDOT-N_3 phase in the sample was re-oxidized by washing the surface with a solution of Fe(III)Tosylate (PTS) in n-propanol (40 wt %) diluited with H_2O (1:3). Finally the surface was rinsed with H_2O and dried with pressurized air.

6.2.6 Synthesis of α-Methoxypoly(ethylene glycol)-ω-pent-4-ynoate (alkynated MPEG 2000)

Synthesis procedure follows a well-established method reported in supporting information of a reference work of Daugaard and colleagues.[174]

IR (cm-^{1}): 1737 (O-C=O stretch.); 1101 (C-O stretch.). ^{1}H NMR ($CDCl_3$, 250 MHz, δ_H, ppm): 1.92 (t, 1H, H-C≡); 2.4-2.6 (m, 4H, -OC-CH_2-CH_2-C≡); 3.31 (s, 3H, -OCH_3); 3.4-3.8 (m, O-CH_2-CH_2-O); 4.20 (t, 2H, -COO-CH_2-).

6.2.7 Click reaction with alkynated MPEG

In analogue conditions adopted for the click reaction with alkynated ADT, the reaction mixture for alkynated MPEG clicking was prepared mixing with the same ratios and concentrations a solution in H_2O of alkynated MPEG (2000) (16 mM) with $CuSO_4$ (0.1 M) and sodium ascorbate (0.1 M) solutions in H_2O. The reaction was conducted in similar way for 20 h. At the end the surface was rinsed with H_2O, and re-oxidized with the PTS solution, as previously described.

6.3 RESULTS AND DISCUSSION

6.3.1 Preliminary characterization

In order to realize a hybrid film composed of the two phases, EVAL and click-functionalizable PEDOT as a random PEDOT-PEDOT-N_3 copolymer, the copolymerization of EDOT and EDOT-N_3 was conducted on a previously deposited film of EVAL in accordance to the reaction in figure 6.1. EDOT-N_3 was co-polymerized with pure EDOT in order to limit the drop of conductivity of the resulting polymer. In fact, the functional polymers show a lower conductivity than pure PEDOT, that decreases with decreasing amount of EDOT in the copolymer.[175]

The general procedure followed to test this new hybrid is reported in figure 6.2. The click reaction was performed in organic and water phase with two alkynated reactants, ADT fluorophore and MPEG, respectively. Either way, the combination with the fluorination treatment was tested alternatively exchanging the sequence of click and fluorination reactions. The fluorination reaction (figure 6.3) was followed first by qualitative ATR FT-IR analysis.

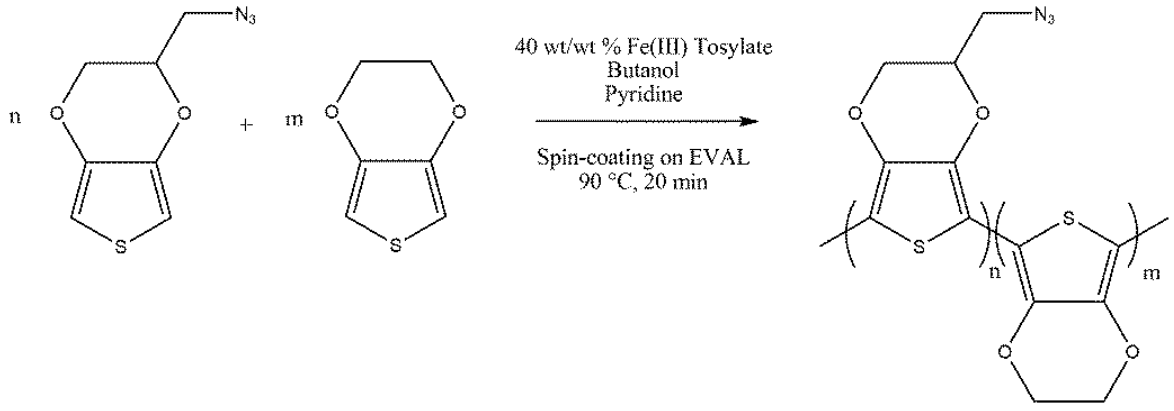

Fig. 6.1 Copolymerization of EDOT and EDOT-N_3 on EVAL substrate.

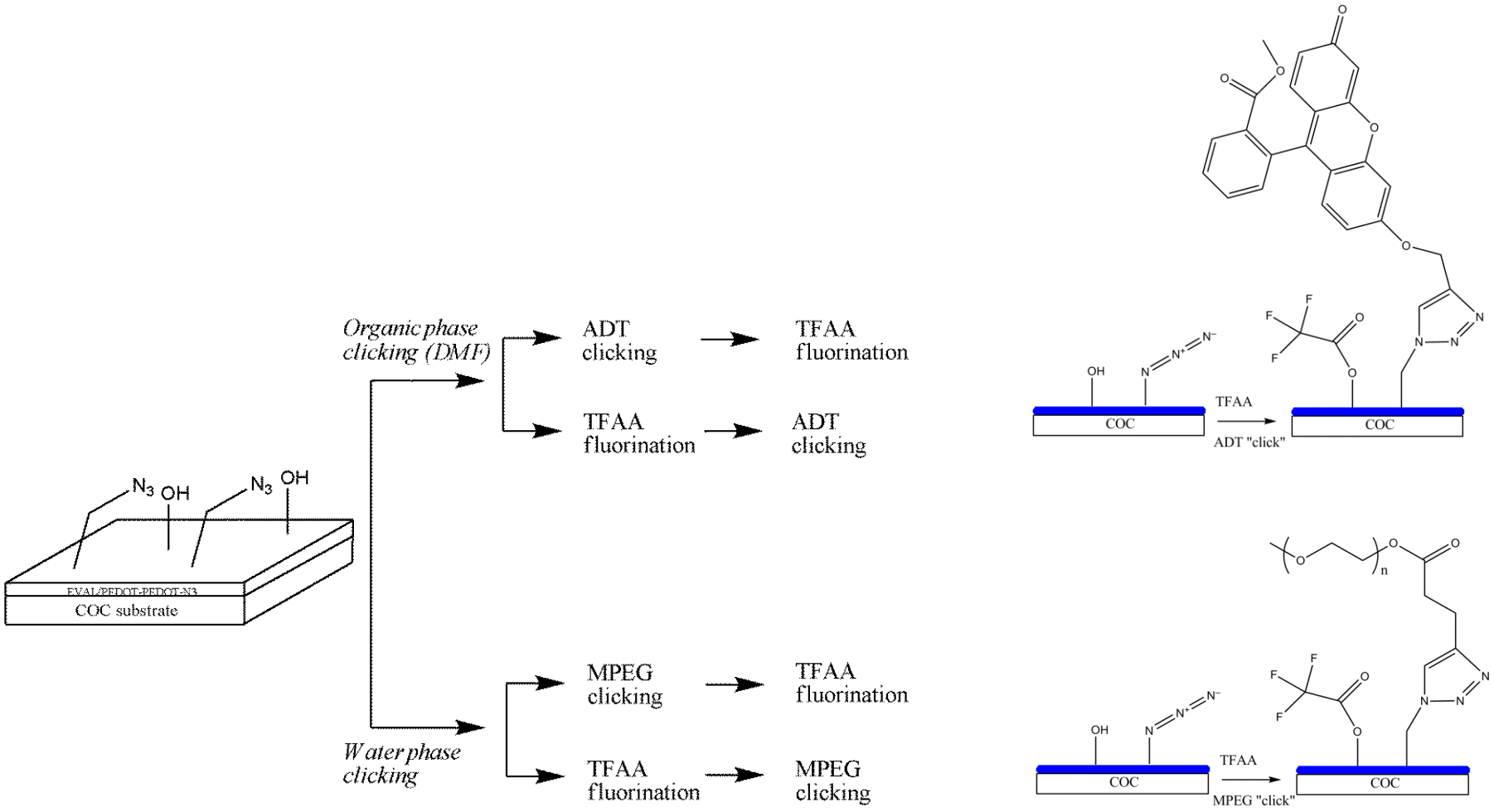

Fig. 6.2 General procedure adopted to test the applicability of EVAL/PEDOT-PEDOT-N_3 hybrid material for fluorination and click reactions.

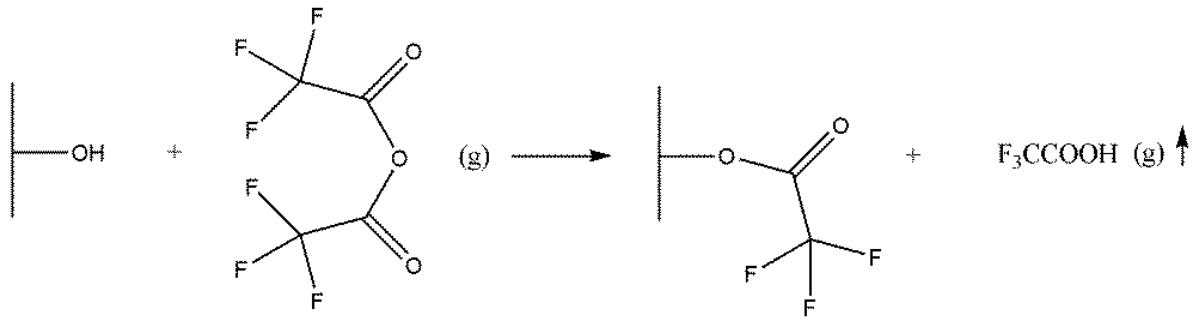

Fig. 6.3 Surface vapor phase fluorination reaction with TFAA on EVAL component of the EVAL/PEDOT-PEDOT-N_3 hybrid.

In figure 6.4 an indicative comparison of the ATR FT-IR spectra obtained on the surface of an EVAL film obtained in similar conditions and the EVAL/PEDOT-PEDOT-N_3 hybrid, before and after TFAA treatment, is reported. The insertion of trifluoroacetate group on EVAL surface produces clear modifications respect to EVAL spectrum, such as the C=O stretching mode at 1777 cm^{-1}, the overlapping of C-O stretching mode of ester group with the strong CF_3 stretching modes in the 1350-1120 cm^{-1} region (1347, 1217, 1145 cm^{-1}), the absorptions at 774 and 732 cm^{-1} in the fingerprint region. The spectrum of the hybrid surface is quite complex and it results as the combination of the two phases contributions. The characteristic azide peak of PEDOT phase is found at 2120 cm^{-1}. The fluorination reaction on the hybrid produces analogue spectral modifications as in pure EVAL sample.

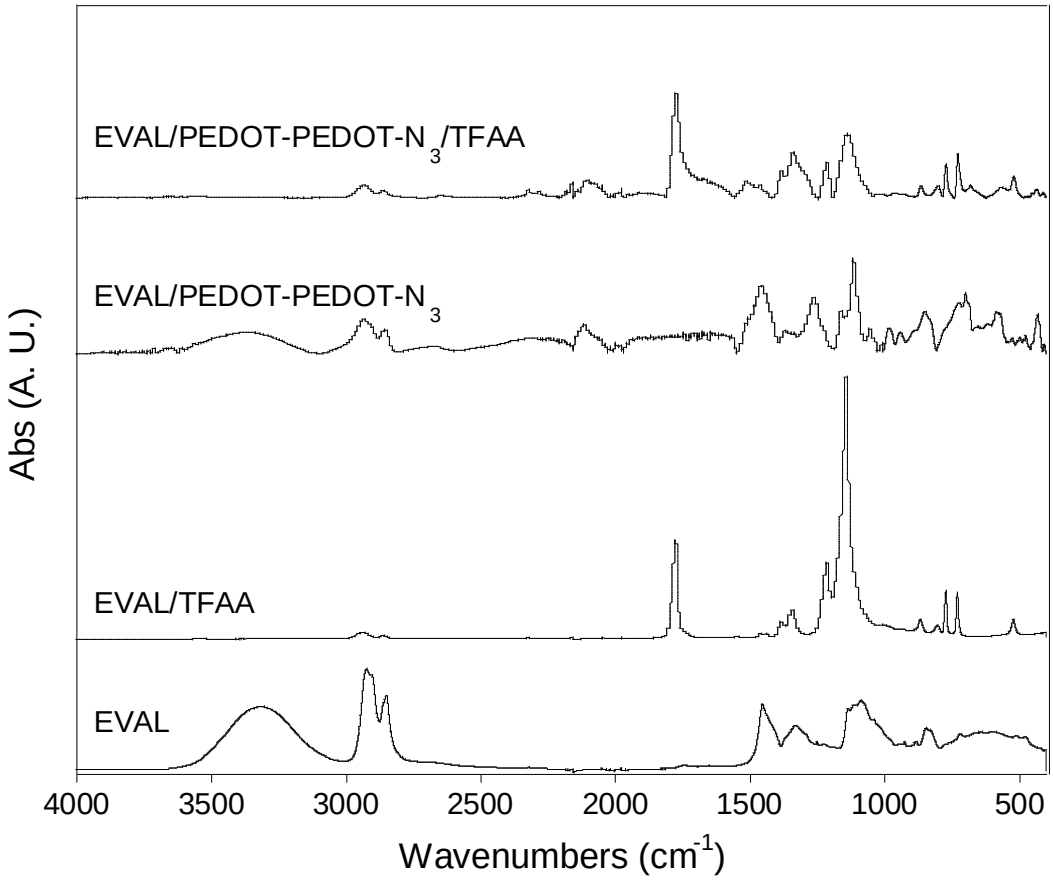

Fig. 6.4 ATR FT-IR spectra of EVAL substrate, TFAA treated EVAL substrate, EVAL/PEDOT-PEDOT-N_3 hybrid film and TFAA treated EVAL/PEDOT-PEDOT-N_3 hybrid film.

In table 6.1 results of water contact angle analysis in advancing mode are reported for the hybrid systems considering the order of treatments execution. Water contact angle for EVAL/PEDOT-PEDOT-N_3 hybrid was found at about 66° (Tab.6.1). This value is quite similar by those ones measured for pure EVAL and pure PEDOT-PEDOT-N_3 respectively (the latter is not showed in table 6.1). Measurements in advancing mode showed a strong increase in hydrophobicity of the hybrid material surface after fluorination, from about 66° to 105°.

reference sample	Adv. WCA (°)	Adv. WCA after TFAA (°)	Adv. WCA after ADT (°)	Adv. WCA after MPEG (°)
EVAL	67	110	-	-
EVAL/PEDOT	56	112	-	-
EVAL/PEDOT-PEDOT-N_3	66	**105**	**68**	**44**
EVAL/PEDOT-PEDOT-N_3/TFAA	**105**	-	no variation	no click reaction
EVAL/PEDOT-PEDOT-N_3/ADT	**68**	no variation	-	-
EVAL/PEDOT-PEDOT-N_3/MPEG	**44**	57	-	-

Tab. 6.1 Mean advancing water contact angles (advancing WCA) of the samples, indicated as reference, measured before and after TFAA treatment, ADT and MPEG clicking respectively (columns). Values for EVAL and EVAL/PEDOT samples before and after TFAA treatment are also reported for comparison. Data reported in bold are replicated.

From the other hand, the possibility to click ADT fluorophore on PEDOT-PEDOT-N_3 phase was first confirmed by absorption UV-vis analysis. In order to exclude any absorption effects of the fluorophore on the hybrid surface, a control reaction was conducted using inactivated ADT in analogue reaction conditions, giving no absorption. In figure 6.5 the absorption of the three peaks of ADT fluorophore clicked on EVAL-PEDOT-PEDOT-N_3 hybrid surface is reported.

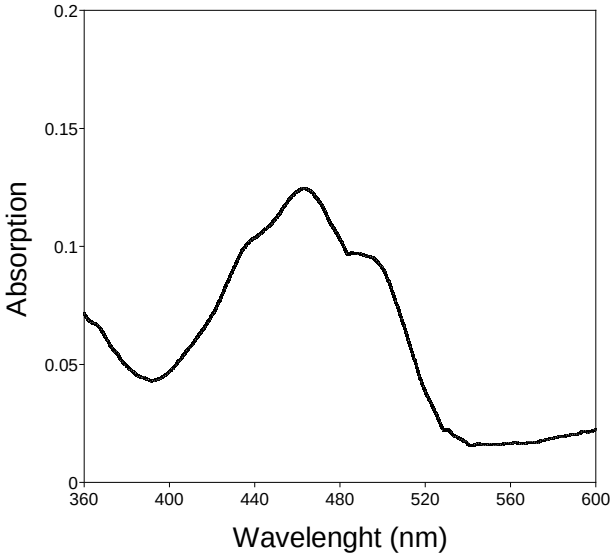

Fig. 6.5 Absorption Uv-vis spectrum of ADT fluorophore clicked on EVAL/PEDOT-PEDOT-N_3 hybrid surface.

As reported in table 6.1, after the fluorophore clicking, the hybrid sample doesn't show significant variation of the water contact angle. For this reason, one may serially combine ADT clicking with fluorination treatment, in order to check how the sequence of the two reactions can influence the final surface properties. In particular was found that when fluorination is conducted after clicking of ADT, no increasing of water contact angle is observed. In this way use of TFAA as a final treatment would be ineffective. This may be ascribed to occurring of modifications of surface structure due to the previous exposure to the organic solvent used for ADT click reaction. Otherwise, the click reaction may be carried out after fluorination step, as confirmed by UV-vis analysis, resulting in a still high hydrophobic clicked surface with no modification of the measured angle.

In table 6.2, surface conductivity measurements are reported. In particular, integration with EVAL matrix, for both PEDOT and PEDOT-PEDOT-N_3 copolymer, doesn't alter the final electrical properties of the hybrid system. The same was observed on the TFAA treated samples. In fact, fluorination involves only EVAL component of such a heterogeneous system, without influencing the total electrical properties, that are anyway dependant on the conducting phase. Differently, after fluorophore clicking a slight decrease in conductivity was found. The click reaction and hence the fluorophore loading, especially if conducted in organic solvent, produces structural modifications of the conducting phase that may affect the overall electrical response of the heterogeneous system.[174]

sample	$1/R_s$ mean (Ω^{-1})	σ_s (S x sq)
PEDOT	1.5e-03	3.3e-04
PEDOT-PEDOT-N_3	1.0e-03	2.2e-04
EVAL/PEDOT	1.0e-03	2.2e-04
EVAL/PEDOT/TFAA	1.5e-03	3.3e-04
EVAL/PEDOT-PEDOT-N_3	4.2e-04	9.3e-05
EVAL/PEDOT-PEDOT-N_3/ADT	1.3e-04	2.9e-05
EVAL/PEDOT-PEDOT-N_3/TFAA	4.7e-04	1.0e-04
EVAL/PEDOT-PEDOT-N_3/ADT/TFAA	1.0e-04	2.2e-05
EVAL/PEDOT-PEDOT-N_3/TFAA/ADT	3.9e-04	8.6e-05

Tab. 6.2 Electrical properties of the samples before and after ADT clicking and TFAA treatment and respective combinations. The table reports the mean surface conductance ($1/R_s$) as measured by four-point probe method. The surface conductivity (σ_s) is calculated according to Valdes correction.

As an alternative way, the possibility to click an alkynated MPEG was evaluated in order to use water phase milder reaction conditions. As early demonstrated [174], a water phase click reaction on PEDOT-N_3 produces a coverage limited to the surface and the absence of intense structural modifications of the conducting PEDOT phase. As it is shown in figure 6.6, after the MPEG clicking, a decreasing of about 22° in advancing water contact angle was found. Subsequently, TFAA reaction was tested after the MPEG functionalization, giving an increase of 13°, reaching a value that represents a balance between the hydrophobic contribution of fluorinated EVAL phase and the more hydrophilic MPEG functionalized PEDOT phase. In this case, a fast and solvent-free fluorination treatment with TFAA can be thought as a final step for surface properties control, especially if one considers the low selectivity of the reactant.

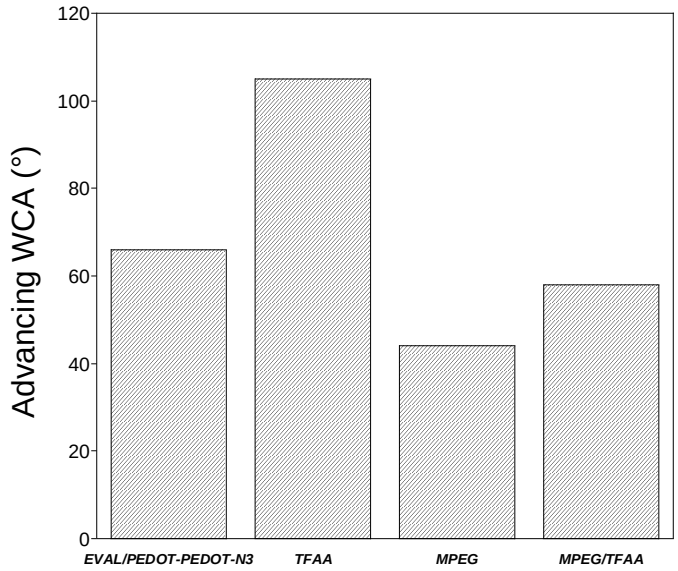

Fig. 6.6 Advancing water contact angle of pristine EVAL-PEDOT-PEDOT-N_3 compared to TFAA treated, MPEG clicked and the combination MPEG clicked followed by TFAA treatment.

6.3.2 X-ray photoelectron spectroscopy (XPS) analysis results

In order to investigate the clicked surfaces, X-ray photoelectron spectroscopy (XPS) analysis was conducted on the surface of the EVAL/PEDOT-PEDOT-N_3 hybrid sample and after every reaction step showed in scheme 6.2. An indication of the click reaction degree was obtained by evaluation of the N (1s) doublet peak related to the azide group (the azide nitrogens exist in two different oxidation states). This doublet peak is assigned in literature around 405 and 400 eV. Accordingly to this, in this case the peak was found at 404 and 401 eV, respectively (Fig. 6.7).

The peak ratio of this nitrogen doublet peak for azides, calculated as the ratio between peak intensity at 404 and 401 eV, should be found equal to 1:2. A deviation from this ratio towards lower values resulted in literature when the analyses were undertaken with electron charge compensation to avoid charging of the less conductive film samples. This was confirmed as the result of degradation of the azides during the XPS analysis under such conditions[176]. In order to avoid this degradation and because of the good conductivity showed by all samples, the analysis was conducted without electron charge compensation.

When the click reaction takes place and azide reacts to form a triazole, the smaller peak at higher energy disappears. Hence, for a complete click reaction spectra shouldn't show the

presence of the peak at 404 eV. From the expected ratio of the two peaks of 0.5 for the unreacted azide, smaller ratios are expected as the degree of reaction increases.

Figure 6.7 shows the modification of the N (1s) doublet peak after the click reaction with ADT in DMF and with MPEG in water respectively. The degree of reaction of azides is higher for the reaction in organic solvent than in water, although the reaction is never complete. Accordingly to a previous detailed study[174] about the effect of type of solvent and solvent composition on surface click-functionalization of PEDOT-N_3, the reaction performed in organic phase leads to a higher reaction degree due to the fact that it is less surface-limited respect to the case of reaction performed in water phase. In fact, it has been proved that polar solvents such as DMSO and DMF, induce swelling of the PEDOT phase that allows the reactants to better penetrate deep into the PEDOT layer and react with the more accessible azide groups.

Hence, the indication of the amount of click reaction degree was obtained evaluating the influence of the solvent used for the click reaction and, in combination, the effect of modification of the pristine hybrid surface through previous fluorination treatment with TFAA.

For this purpose, in figure 6.8 the resulting doublet N(1s) peak ratio is compared for the clicked samples with and without previous fluorination treatment. From this comparison it is possible to note that the loading of ADT in DMF is also feasible if the surface is pre-treated with TFAA, even though it leads to a lower reaction degree compared to the case of untreated sample. This indicates that changes of surface energy, induced by fluorination of EVAL phase, limit to a certain extent the following click reactions conducted on PEDOT phase using polar solvents.

From the other side, in the case of MPEG loaded samples in water, the reaction degree is inferior respect to the ADT loaded samples in DMF, for the reason previously explained.

In addition, if the sample is pre-fluorinated the click reaction in water doesn't occur. In fact, in this case the limiting effect induced by the fluorination pre-treatment, together with the milder adopted conditions, clearly represent factors that cause the complete inefficacy of the following click reaction.

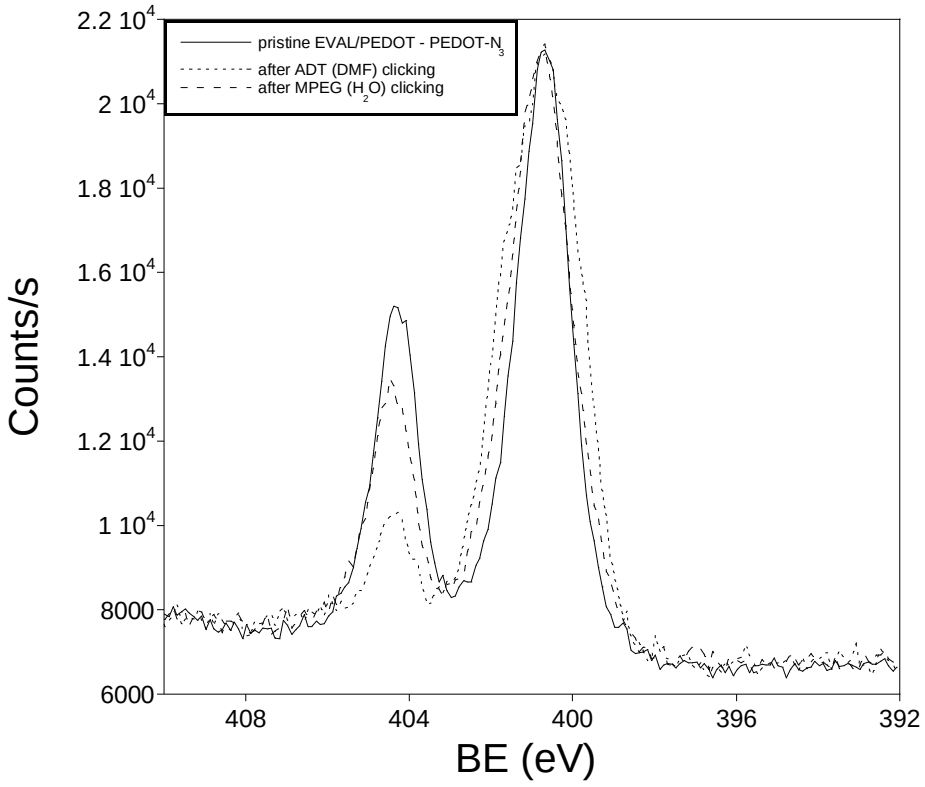

Fig. 6.7 XPS N (1s) doublet peak at 404 and 401 eV of pristine EVAL/PEDOT-PEDOT-N_3, after the click reaction with ADT in DMF and with MPEG in water, respectively.

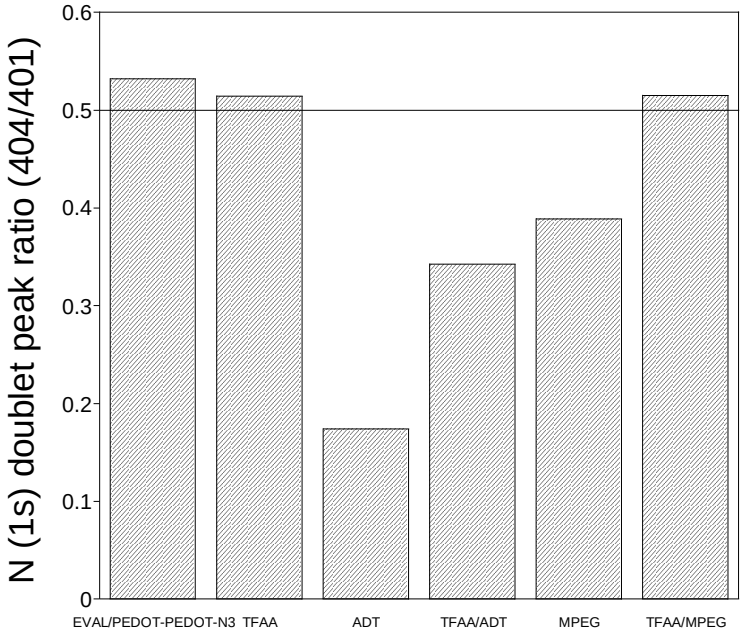

Fig. 6.8 Comparison of XPS N (1s) doublet peak ratio between intensity at 404 and 401 eV for different samples.

6.3.3 Scratch hardness test results

An indication of the enhanced hydrophobicity and scratch resistance after fluorination treatment has been yielded by a qualitative scratch hardness test made on an EVAL/PEDOT composite film.

Simply by visual inspection, it has been noted that at the lowest applied load (0.2 N) visible scratches are produced both on EVAL/PEDOT and pure PEDOT samples. While for the TFAA treated EVAL/PEDOT sample, scratches become visible in the range between 0.7 and 1 N. Digital pictures showed in figure 6.9 are a comparison of the scratch effect when the same sample, before and after fluorination, is moved away from a 1.6 N loaded pin. Moreover, by effect of enhanced hydrophobicity, TFAA treated sample seems to show better adherence to the underlying hydrophobic COC support.

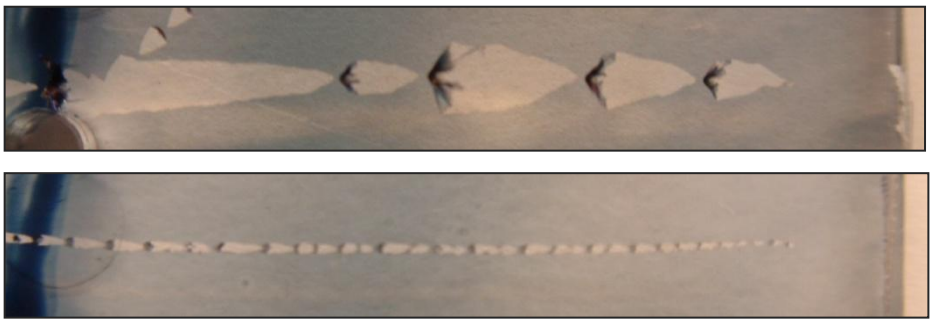

Fig. 6.9 Digital pictures comparing the scratches obtained on the surface of pristine EVAL/PEDOT (top) and TFAA treated EVAL/PEDOT (bottom) by moving away the samples under a loaded pin (1.6 N).

7
CONCLUSIONS

7.1 CHAPTER III CONCLUSIONS

Water phase polymerization of EDOT in presence of EVALS brings about EVALS/PEDOT suspensions characterized in general by poor stability that is however dependent on EVALS amount in formulation. Also electrical properties of such EVALS/PEDOT systems seems to depend on starting formulation. Even though conductivity reaches quite high values (2×10^1 S cm^{-1}), the formation of inhomogeneous suspensions, characterized by intense micrometric particles aggregation, doesn't allow a good processability of such systems. Thus, in order to obtain smooth, transparent and homogeneous films, vapor phase polymerization was conveniently tested and studied in deep.

7.2 CHAPTER IV CONCLUSIONS

The use of EVALS as new supporting matrix for EDOT vapor phase polymerization allowed the facile synthesis of a transparent conducting film. The possibility to homogeneously disperse the polymerization initiator (iron (III) tosylate) into the polyanion matrix, which obstacles its crystallization without requiring the use of specific additives, allows the formation of an homogeneous conducting film surface if the right initiator concentration is selected. The experimental results collected during the VPP showed that, during the polymerization, the film conductivity increases with PEDOT concentration according to the hypothesis of a percolation mechanism.

After a VPP time of 20 h, a water and alcohol insoluble EVALS32/PEDOT film is obtained, characterized by a conductivity of 1.6×10^2 S cm^{-1}, high optical transparency (>90 %) and surface smoothness. From an applicative point of view, the obtained EVALS32/PEDOT system may be subjected to further study and adapted to be used as possible hole injection layer (HIL) for electronic applications.

Mainly other two characteristics of such a system may allow to extend its use to other applicative targets. In fact, the matrix and oxidant simultaneous deposition opens the possibility of testing a facile VPP-mediated ink-jet printing application. Moreover, the partial sulfonation of EVAL, leaving residual hydroxyl groups along the co-polymer backbone, provides the possibility of further chemical modification of EVALS32/PEDOT film,

including grafting or cross-linking reactions, suitable for the preparation of all-organic devices applicable in electronics, sensor or actuation technology.

7.3 CHAPTER V CONCLUSIONS

In chapter 5 it has been showed that it is possible to cross-link EVALS32 samples by using reactions and procedures similar to those used in the chemistry of PVA. In fact, EVALS32 has been subjected to solution cross-linking in controlled conditions by using glutaraldehyde as cross-linker to give highly swollen cationic exchange membranes. In general, by varying cross-linker/hydroxyl groups molar ratio, it is possible to obtain EVALS32 based membranes with different swelling properties and mechanical strength.

These materials show electro-active properties under application of low electric potentials (2-9 Volts) and this possibility has been evaluated for the preparation of electro-active systems that, for example, in combination with the method applied for EDOT VPP, could be used for the realization of all-organic actuator systems.

It is worth to note that further characterization could directly follow the results reported in this chapter. For example, variations of EVALS sulfonation degree or use of different methods and conditions for cross-linking reaction could be in principle evaluated.

Moreover, regarding to realization of surface layered electrodes on such membranes for actuator assembling, other methods alternative or integrative respect to EDOT VPP and surface chemical reduction of metal salts, such as surface trapping of metal nanoparticles, could be taken into account.

Then, a promising scenario is in store for realization of novel EVALS based actuator systems and deeper study of their applicative electromechanical properties.

7.4 CHAPTER VI CONCLUSIONS

The method described in chapter 6 allows the integration of a conductive click-functionalizable PEDOT into an ethylene an EVAL co-polymer substrate for mechanical resistance improvement and surface property control. The preparation of these novel substrates has been optimized. Furthermore a method for detection of available hydroxyl groups on the optimized surfaces by use of fluorination have been developed. Similarly

surface available azide groups have been clicked by suitable marker molecules. The variation of surface characteristics has been proved by XPS, ATR FTIR and water contact angle (WCA) measurements.

REFERENCES

(1) C. K. Chiang, C. R. Fincher, Y. W. Park, A. J. Heeger, H. Shirakawa, E. J. Louis, S. C. Gau, A. G. McDiarmind *Phys. Rev. Lett.* (1977) 39, 1098

(2) H. Shirakawa, E. J. Louis, A. G. McDiarmind, C. K. Chiang, A. J. Heeger *J. Chem. Soc., Chem. Commun.* (1977), 16, 578

(3) H. Shirakawa, T. Ito, S. Ikeda, *Macromol. Chem.* (1978) 179, 1565

(4) H. Naarmann, N. Theophilou, *Synth. Met.* (1987) 22, 1

(5) G. Daust, M. Leclerc *Macromol.* (1991) 24, 455

(6) M. Feldhues, T. Mecklenburg, P. Wegener, G. Kämpf, EP 257 573 (Hoechst AG), Prior: 1986-08-26

(7) G. Kämpf, M. Feldhues, EP 292 905 (Hoechst AG), Prior: 1987-05-26

(8) M. Feldhues, G. Kämpf, H. Litterer, T. Mecklenburg, P. Wegener *Synth. Met.*(1999) 28, C487]

(9) F. Jonas, G. Heywang, W. Schmidtberg, J. Heinze, M. Dietrich, EP 339 340 (Bayer AG), Prior: 1988-04-22

(10) G. Heywang, F. Jonas *Adv. Mater.* (1992) 4, 117 ; F. Jonas, W. Krafft, EP 440 957 (Bayer AG), Prior: 1990-02-08

(11) J. Cornil, D. A. dos Santos, D. Beljonne, J. L. Brédas *J. Phys. Chem.* (1995) 99, 5604

(12) A. Dkhissi, F. Louwet, L. Groenendaal, D. Beljonne, R. Lazzaroni, J. L. Brédas *Chem. Phys. Lett* (2002) 359, 456

(13) C. Kvarnström, H. Neugebauer, S. Blomquist, H. J. Ahonen, J. Kankare, A. Ivaska *Elactrochim. Acta* (1999) 44, 2739

(14) C. Kvarnström, H. Neugebauer, A. Ivaska, N. S. Sariciftci *J. Mol. Struct.* (2000) 521, 271

(15) G. Heywang, F. Jonas *Adv. Mater.* (1992) 4, 116

(16) H. J. Ahonen, J. Lukkari, J. Kankare *Macromol.* (2000) 33, 6787

(17) M. Granström, O. Inganäs *Polymer* (1995) 36, 2867

(18) K. E. Aasmundtveit, E. J. Samuelsen, L. A. A. Petterson, O. Inganäs, T. Johansson, R. Feidenhans'l *Synth. Met*. (1999) 101, 561

(19) L. Niu, C. Kvarnström, K. Fröberg, A. Ivaska *Synth. Met.* (2001) 122, 425

(20) L. A. A. Petterson, T. Johansson, F. Carlsson *Synth. Met.* (1999), 101, 198

(21) K. E. Aasmundtveit, E. J. Samuelsen, L. A. A. Pettersson, O. Inganäs, T. Johansson, R. Feidenhans *Synth. Met.* (1999), 101, 561

(22) K. E. Aasmundtveit, E. J. Samuelsen, O. Inganäs, L. A. A. Pettersson, T. Johansson, S. Ferrer *Synth. Met.* (2000), 113, 93

(23) S. Kirchmeyer, K. Reuter *J. Mater. Chem.* (2005) 15, 2077

(24) J. P. Travers, B. Sixou, D. Berner, A. Wolter, P. Rannou, B. Beau, B. Pépin-Donat, C. Barthet, M. Guglielmi, N. Mermilliod, B. Gilles, D. Djurado, A. J. Attias, M. Vautrin *Synth Met.* (1999) 101, 359

(25) Q.Pei, G. Zuccarello, M. Ahlskog, O. Inganäs *Polymer* (1994) 35, 1347

(26) H. Randriamahazaka, C. Noël, C. Chevrot *J. Electroanal. Chem.* (1999) 472, 103

(27) T. Yamamoto *Bull. Chem. Soc. Jpn.* (1999) 72, 621

(28) T. Yamamoto, M. Abla *Synth. Met.* (1999) 100, 227

(29) T. Yamamoto, M. Abla, T. Shimizu, D. Komarudin, B. L. Lee, E. Kurokawa *Polym. Bull.* (1999) 42, 321

(30) S. Kirchmeyer, 5th International Symposium on Functional π-electrons system, 2002, Ulm, Germany

(31) L. Groenendaal, F. Louwet, P. Adriaensen, R. Carlreer, D. Vanderzande, J. Gelan, *Polym. Mater. Sci. Eng.* (2002) 86, 52

(32) K. Reuter, V. A. Nikanorov, V. M. Bazhenov, EP 1 375 560 (H. C. Starck GmbH), Prior: 2002-06-28

(33) D. M. de Leeuw, P. A. Kraakman, P. F. G. Bongaerts, C. M. J. Mutsaers, D. B. M. Klaassen *Synth. Met.* (1994) 66, 263

(34) L. A. A. Pettersson, T. Johansson, F. Carlsson, H. Arwin, O. Inganäs *Synth. Met.* (1999) 101, 198

(35) Bayer AG *Eur. Patent* (1991) 440 957

(36) F. Jonas, W. Krafft, B. Muys *Macromol. Symp.*(1995) 100, 169

(37) Bayer AG *Eur. Patent* (1993) 553 671

(38) F. Jonas, G. Heywang *Electrochim. Acta* (1994) 39, 1345

(39) L. Groenendaal, G. Zotti, F. Jonas, *Synth. Met.* (2001) 118, 105-109

(40) S. C. Ng, H. S. O. Chan, W. L. Yu *J. Mater. Sci. Lett.* (1997), 16, 809

(41) O. Stéphan, P. Schottland, P. Y. Le Gall, C. Chevrot, C. Mariet, M. J. Carrier *Electroanal. Chem.* (1998) 443, 217

(42) P. Schottland, O. Stéphan, P. Y. Le Gall, C. Chevrot *J. Chim. Phys.* (1998) 95, 1258

(43) M. L. Blohm, J. E. Pickett, P. C. VanDort (General Electric Company) *US Patent* (1992) 5 III 327

(44) D. M. Welsh, A. Kumar, M. C. Morvant, J. R. Reynolds *Synth. Met.* (1999) 102, 967

(45) L. J. Kloeppner, D. M. Welsh, J. R. Reynolds *Polym. Prepr.* (1999), 40, 792

(46) L. Groenendaal, G. Zotti, P. H. Aubert, S. M. Waybright, J. R. Reynolds *Adv. Mater.* (2003) 15, 855

(47) C. Wang, J. L. Schindler, C. R. Kannewurf, M. G. Kanatzidis *Chem. Mater.* (1995) 7, 58

(48) J. L. Reddinger, J. R. Reynolds *J. Org. Chem.* (1996) 61, 4833

(49) D. J. Irvin, C. J. DuBois, J. R. Reynolds *Chem. Commun.* (1999) 2121

(50) Y. Fu, H. Cheng, R. L. Elsenbaumer *Chem. Mater.* (1997) 9, 1720

(51) E. Yildiz, P. Camurlu, C. Tanyeli, I. Akhmedov, L. Toppare *J. Electroanal. Chem.* (2008) 612, 247

(52) B. Yigitsoy, S. Varis, C. Tanyeli, I. M. Akhmedov, L. Toppare *Electrochim. Acta* (2007) 52, 6561

(53) P. Camurlu, S. Tarkuç, E. Şahmetlioğlu, I. M. Akhmedov, L. Toppare *Sol. Energy Mater.Sol. Cells* (2008) 92, 154

(54) J. Mathiyarasu, S. Senthil Kumar, K. L. N. Phani, V. Yegnaraman *Mater. Lett.* (2008) 62, 571

(55) A. V. Murugan, C. S. Gopinath, K. Vijayamohanan *Electrochem. Commun.* (2005) 7, 213

(56) R. Kiebooms, A. Aleshin, K. Hutchison, F. Wudl, A. J. Heeger *Synth. Met.* (1999) 101, 436

(57) A. Aleshin, R. Kiebooms, A. J. Heeger *Synth. Met.* (1999) 101, 369

(58) N. Sakmeche, S. Aeiyach, J.-J. Aaron, M. Jouini, J. C. Lacroix, P.-C. Lacaze, *Langmuir* (1999) 15, 2566

(59) S. Shinkai, M. Takeuchi, A. -H. Bae *Supramol. Chem.* (2005) 17, 181-186

(60) F. Jonas, W. Krafft, EP 440 957 (Bayer AG), Prior: 1990-02-08

(61) K. Reuter, A. Karbach, H. Ritter, N. Wrubbel, EP 1 440 974 A2 (Bayer AG), Prior: 2003-01-21

(62) S. Ghosh, O. Inganäs *Synth. Met.* (1999) 101, 413

(63) A. Mantovani Nardes, M. Kemerink, R. A. J. Janssen, J. A. M. Bastiaansen, N. M. M Kiggen, B. M. W. Langeveld, A. J. J. M. van Breemen, M. M. de Kok *Adv. Mater.* (2007) 19, 1196

(64) L. A. A. Pettersson, S. Ghosh, O. Inganäs, *Org. Electr.* (2002) 3, 143

(65) J. Y. Kim, J. H. Jung, D. E. Lee, J. Joo, *Synth. Met.*(2002) 126, 311

(66) S. K. M. Jönsson, J. Birgerson, X. Crispin, J. Greczynski, W. Osikowicz, A. W. D van der Gon, W. R. Salaneck, M. Fahlman, *Synth. Met.* (2003), 139, 1

(67) S. Ghosh, J. Rasmusson, O. Inganäs *Adv. Mater.* (1998) 10, 1097

(68) A. R. Hopkins, J. R. Reynolds *Macromolecules* (2000) 33, 5221

(69) J. Drummond, S. J. Clarson, J. S. Zetts, F. K. Hopkins, S. J. Caracci *Appl. Phys. Lett.* (1999) 74, 368

(70) A. Thiess *Deutsche Gebrauchsmusterschrift* (2001) DE 20021226 U1, Prior: 2001-04-19

(71) T. Kawashima, T. Sekiya, JP 2002 241613 A2 (Sony Chemical Corp.), Prior: 2002-08-28

(72) Y. Morinoto, JP 2000 026817 A2 (Teijin Ltd.), Prior: 1998-07-14

(73) F. Nittel, H. Randolph, W. Himmelmann, EP 554 588 (Agfa AG), Prior: 1993-12-23

(74) H. Shinohara, JP 2003 246874 A2 (HS Planning Y. K.), Prior: 2002-02-26

(75) E. Enz, WO 2003 037039 A1 (Lumitec AG), Prior: 2001-10-24

(76) J. S. Kim, M. Granström, R. H. Friend, N. Johansson, W. R. Salaneck, R. Daik, J. F. Feast, F. Cacialli, *J. Appl. Phys.* (1998) 84, 6859

(77) M. P. De Jong, L. J. Van Ijzendoorn, M. J. A. De Voigt *Appl. Phys. Lett.* (2000) 77, 2255

(78) F. Zhang, M. Johansson, M. R. Andersson, J. C. Hummelen, O. Inganäs *Adv. Mater.* (2002) 14, 662

(79) T. Aemouts, P. Vanlaeke, W. Geens, J. Poortmans, P. Heremans, S. Borghs, R. Mertens, R. Andriessen, L. Leenders *Thin Solid Films* (2004) 451-452, 22

(80) M. Halik, H. Klauk, U. Zschieschang, T. Kriem, G. Schmid, W. Radlik, K. Wussow *Appl. Phys. Lett.* (2002) 81, 289

(81) P. Lin, F. Yan *Adv. Mater.* (2012) 24, 34

(82) M. Richardson-Burns, J. L. Hendricks, B. Foster, L. K. Povlich, D. H. Kim, D. C. Martin, *Biomaterials* (2007) 28, 1539–1552

(83) A. Kros, S. W. F. M. van Hövell, N. A. J. M. Sommerdijk, R. J. M. Nolte, *Adv. Mater.* (2001) 13, 1555-1557

(84) A. Blau, A. Murr, S. Wolff, E. Sernagor, P. Medini, G. Iurilli, C. Ziegler, F. Benfenati *Biomaterials* (2011) 32, 1778-1786

(85) R. Ravichandran, S. Sundarrajan, J. R.Venugopal, S. Mukherjee, S. Ramakrishna, *J. R. Soc. Interface* (2010**)** 7, S559-S579

(86) A. Kros, W. F. M. van Hovell, N. A. J. M. Sommerdijk, R. J. M. Nolte, *Adv. Mater.* (2001**)** 13, 1555-1557

(87) E. Smela, *Adv. Mater.* (2003) 15, 481-4

(88) R. A. Green, N. H. Lovell, L. A. Poole-Warren, *Biomaterials* (2009) 30, 3637–3644

(89) J. Che, Y. Xiao, X. Zhu, X. Sun, *Polym. Int.* (2008**)** 57, 750–755

(90) S-C. Luo, E. M. Ali, N. C. Tansil, H-h. Yu, S. Gao, E. A. B. Kantchev, J. Y. Ying, *Langmuir* (2008**)** 24, 8071-8077

(91) L. H. Jimison, A. Hama, X. Strakosas, V. Armel, D. Khodagholy, E. Ismailova, G. G. Malliaras, B. Winther-Jensen, R. M. Owens, *J. Mater. Chem.* (2012) 22, 19498-19505

(92) B. Somboonsub, S. Srisuwan, M. A. Invernale, S. Thongyai, P. Praserthdam, D. A. Scola, G. A. Sotzing *Polymer* (2010) 51, 1231

(93) B. Somboonsub, S. Srisuwan, M. A. Invernale, S. Thongyai, P. Praserthdam, D. A. Scola, G. A. Sotzing *Polymer* (2010) 51, 4472

(94) G. Sonmeza, P. Schottland, J. R. Reynolds, *Synth. Met.* (2005) 155, 130–137

(95) R. Kishi, K. Hiroki, T. Tominaga, K-I. Sano, H. Okuzaki, J. G. Martinez, T. F. Otero, Y. Osada, *J. Polym. Sci. Part B: Polym. Phys.* (2012**)** 50, 790–796

(96) T. Kim, J. Kim, Y. Kim, T. Lee, W. Kim, K. S. Suh *Curr. Appl. Phys.* (2009) 9, 120

(97) C. Dai, C. Chang, H. Chi, H. Chien, W. Su, W. Chiu *J. Polym. Sci.: Part A: Polym. Chem.* (2008) 46, 2536

(98) T. Iwanami, Y. Hirai *Tappi Journal* (1983) 66, 85

(99) R. H. Foster *Modern Plastics Mid-October Encyclopedia Issue*, McGraw-Hill: New York (1990) 67, 73

(100) T. Nishino, K. Takano, K. Nakamae *Polymer* (1995) 36, 959

(101) M. Takahashi, K. Tashiro, S. Amiya *Macromol.* (1999) 32, 5860

(102) Z. Zhang, I. J. Britt, M. A. Tung *J. Polym Sci.: Part B: Polym. Phys.* (1999) 37, 691

(103) S. Aucejo, C. Marco, R. Gavara, *J. Appl. Polym. Sci.* (1999) 74, 1201

(104) M. A. Samus, G. Rossi, *Macromol.* (1996) 29, 2275

(105) J. M. Lagaron, A. K. Powell, G. Bonner, *Polymer Testing* (2001) 20, 569

(106) W. Marconi, R. Marcone, A. Piozzi, *Macromol Chem. Phys.* (2000) 201, 715

(107) F. Louwet, L. Groenendaal, J. Dhaen, J. Manca, J. Van Luppen, E. Verdonck, L. Leenders, *Synth. Met.* (2003) 135-136, 115-117

(108) S. Timpanaro, M. Kemerink, F.J. Touwslager, M.M. De Kok, S. Schrader *Chem. Phys. Lett.* (2004) 394, 339

(109) F. Jonas, G. Heywang *Electrochim. Acta* (1994) 39, 1345

(110) A. Mohammadi, M. Hasan, B. Liedberg, I. Lundstrom, W. Salaneck *Synth. Met*. (1986) 14, 189

(111) A. Nannini, G. Serra *J. Mol. Electron.* (1990) 6, 81

(112) T. Ueno, H. D. Arntz, S. Flesch, J. Bargon *J. Macromol. Sci. Chem.* (1988) A25, 1557

(113) Y. Fu, R. A. Weiss, *Polym. Eng. Sci.* (1998) 38, 857

(114) J. Kim, E. Kim, Y. Won, H Lee, K. Suh *Synth. Met*. (2003) 139, 485

(115) D. M. de Leeuw, P. A. Kraakman, P. F. G. Bongaerts, C. M. J. Mutsaers, D. B. M. Klaassen, *Synth. Met*. (1994) 66, 263

(116) B. Winther-Jensen, J. Chen, K. West, G. Wallace *Macromolecules* (2004) 37, 5930

(117) M. A. Ali, H. Kim, C. Lee, H. Nam, J. Lee *Synth. Met.* (2011) 161, 1347

(118) B. Winther-Jensen, K. West *Macromolecules* (2004) 37, 4538

(119) B. Winther-Jensen, D. W. Breiby, K. West *Synth. Met.* (2005) 152, 1

(120) J. Chen, C.-A. Dai, W-Y. Chiu *J. Polym. Sci.: Part A: Polym. Chem.* (2008) 46, 1662

(121) M. Fabretto, K. Zuber, C. Hall, P. Murphy Macromolecular Rapid Communication (2008) 29, 1403

(122) K. Zuber, M. Fabretto, C. Hall, P. Murphy *Macromol. Rapid Commun.* (2008) 29, 1503

(123) X. Crispin, F. L. E. Jakobsson, A. Crispin, P. C. M. Grim, P. Andersson, A. Volodin, C. van Haesendonck, M. Van der Auweraer, W. R. Salaneck, M. Berggren *Chem. Mater*. (2006) 18, 4354

(124) J.P. Lock, S. G. Im, K. K. Gleason Macromolecules (2006) 39, 5326 ; S. G. Im, K. K. Gleason *Macromolecules* (2007) 40, 6552

(125) B. Winther-Jensen, F. C. Krebs *Solar Energy Materials & Solar Cells* (2006) 90, 123

(126) T. L. Truong, D.-O. Kim, Y. Lee, T.-W. Lee, J. J. Park, L. Pu, J.-D. Nam *Thin Solid Films* (2008) 516, 6020

(127) C. M. Madl, P. N. Kariuki, J. Gendron, L. F. J. Piper, W. E. Jones *Synth. Met*. (2011) 161, 1159

(128) M. Bongo, O. Winther-Jensen, S. Himmelberger, X. Strakosas, M. Ramuz, A. Hama, E. Stavrinidou, G. G. Malliaras, A. Salleo, B. Winther-Jensen, R. M. Owens, *J. Mater. Chem. Part B* (2013) 1, 3860-3867

(129) A. Uhlir, *Bell Syst. Tech. J.* (1954), 34, 105

(130) M. Fabretto, K. Zuber, C. Jariego-Moncunill, P. Murphy *Macromol. Chem. Phys*. (2011), 212, 2173

(131) C. M. Madl, P. N. Kariuki, J. Gendron, L. F. J. Piper, W. E. Jones Jr. *Synth. Met*. (2011) 161, 1159

(132) M. Lapkowski, A. Pron, *Synth. Met*. (2000) 110, 79–83

(133) D. M. DeLongchamp, B. D. Vogt, C. M. Brooks, K. Kano, J. Obrzut, C.A. Richter, O. A. Kirillov, E. K. Lin, *Langmuir* (2005) 21, 11480-11483

(134) C. Kvarnström, H. Neugebauer, S. Blomquist, H. J. Ahonen, J. Kankare, A. Ivaska *Electrochimica Acta* (1999) 44, 2739

(135) C. Kvarnström, H. Neugebauer, S. Blomquist, H. J. Ahonen, J. Kankare, A. Ivaska, N. F. Saricifteci *Synth. Met.* (1999) 101, 66

(136) J. P. Lock, S. G. Im, K. K. Gleason *Macromolecules* (2006) 39, 5326

(137) A. R. Blythe, *Polym. Test.* (1984) 4, 195-209

(138) J. Metsik, K. Saal, U. Maeorg, R. Lohmus, S. Leinberg, H. Mandar, M. Kodu, M. Timusk, J. *Polym. Sci. Part B: Polym. Phys.*, (2014**)** 52, 561-571

(139) A. Bunde, J. W. Kantelhardt *Diffusion in Condensed Matter Workshop*, Vieweg Verlag, Wiesbaden, 1998

(140) J. K. W. Sandler, J. E. Kirk, I. A. Kinloch, M.S.P. Shaffer1, A.H. Windle, *Polymer* (2003) 44, 5893–5899

(141) J.-S. Plante, S. Dubowsky, *Sensors and Actuators Part A: Phys.* (2007) 137, 96-109

(142) N. A. Shoenfeld, A. J. Grodzinsky, *Biopolymer* (1980) 19, 241-262

(143) Y. Osada, J. Gong, *J. Prog. in Polym. Sci.* (1993) 18, 187-26

(144) A. Eisenberg, M. Rinaudo, *Polymer Bulletin* (1990) 24, 671

(145) K. Asaka, K. Oguro, Y. Nishimura, M. Mizuhata, H. Takenaka, *Polymer J.* (1995) 27, 436-440

(146) M. Shahinpoor, *Smart Materials and Structures* (1992) 1, 91-94

(147) K. Sadeghipour, R. Salomom, S. Neogi, *Smart Materials and Structures* (1992) 1, 172-179

(148) P. G. de Gennes, K. Okumura, M. Shahinpoor, K. J. Kim, *Europhysics Letters* (2000) 50, 513-518

(149) K. A. Mauritz, R. B. Moore, *Chemical Reviews* (2004) 104, 4535-4596

(150) A. K. Phillips, R. B. Moore, *Polymer* (2005) 46, 7788-7802

(151) D. S. Kim, H. B. Park, J. -W. Rhim, Y. M. Lee, *J. Membr. Sci.* (2004) 240, 37-48

(152) S. L. Shenoy, I. Kaya, C. Erkey, R.A. Weiss, *Synth. Met.* (2001) 123, 509-514

(153) Y. Fu, R. H. Weiss, P. P. Gan, M. D. Bessette, *Polym. Eng. Sci.* (1998) 38, 857-862

(154) B. Winther-Jensen, K. Norrman, P. Kingshott, K. West, *Plasma Proc. Pol.* (2005) 2, 319-327

(155) T. S. Hansen, K. West, O. Hassager, N. B. Larsen, *Synth. Met.* (2006) 156, 1203-1207

(156) V. Rostovtsev, L. G. Green, V. V. Fokin, K. B. Sharpless, *Angew. Chem. Int. Ed.* (2002) 41, 2596-2599

(157) C. W. Tornoe, C. Christensen, M. Meldal, *J. Org. Chem.* (2002) 67, 3057-3064

(158) J. Sinha, R. Sahoo, A. Kumar, *Macromol.* (2009) 42, 2015-2022

(159) A. E. Daugaard, S. Hvilsted, T. S. Hansen, Niels B. Larsen, *Macromol.* (2008) 41, 4321-4327

(160) H. Bu, G. Götz, E. Reinold, A. Vogt, S. Schmid, R. Blanco, J. L. Segura, P. Bäuerle, *Chem. Commun.* (2008) 11, 1320-1322

(161) J. Xu, Y. Tian, R. Peng, Y. Xian, Q. Ran, L. Jin, *Electrochem. Commun.* (2009) 10, 1972-1975

(162) J. U. Lind, T. S. Hansen, A. E. Daugaard, S. Hvilsted, T. L. Andresen, N. B. Larsen, *Macromol.* (2011) 44, 495-501

(163) T. S. Hansen, K. West, O. Hassager, N. B. Larsen, *Synth. Met.*, (2006) 156, 1203-1207

(164) B. Winther-Jensen, D. W. Breiby, K. West, *Synth. Met.* (2005) 152, 1-4

(165) R. A. Dickie, J. S. Hammond, J. E. de Vries, J. W. Holubka, *Anal. Chem.* (1982) 54, 2045-2049

(166) A. Holländer, F. Pippig, M. Dubreuil, D. Vangeneugden, *Plasma Proc. Polym.* (2008) 5, 345-349

(167) A. Holländer, S. Kröpke, F. Pippig, *Surf. Interface Anal.* (2008) 40, 379-385

(168) F. Pippig, S. Sarghini, A. Holländer, S. Paulussen, H. Terryn, *Surf. Interface Anal.* (2009) 41, 421-429

(169) Y. Huihong, N. Yoshihara, K. Shigenori, *Cellulose* (2005) 12, 543-549

(170) A. E. Daugaard, S. Hvilsted, *Macromolecules* (2008) 41, 4321-4327

(171) M. Adamczyk, J. Grote, J. A. Moore, *Bioconjugate Chem.* (1999) 10, 544-547

(172) B. Whinter-Jensen, D. W. Breiby, K. West, *Synth. Met.* (2005) 152, 1-4

(173) A. E. Daugaard, S. Hvilsted, *Macromolecules* (2008) 41, 4321-4327

(174) J. U. Lind, T. S. Hansen, A. E. Daugaard, S. Hvilsted, T. L. Andresen, N. B. Larsen, *Macromol.* (2011) 44, 495-501

(175) A. E. Daugaard, S. Hvilsted, T. S. Hansen, Niels B. Larsen, *Macromol.* (2008) 41, 4321-4327

(176) S. Prakash, T. M. Long, J. C. Selby, J. S. Moore, M. A. Shannon *Anal. Chem.* (2007) 79, 1661-1667